Photoemission Cross Sections for Atomic Transitions in the Extreme Ultraviolet due to Electron Collisions with Atoms and Molecules

Cite as: Journal of Physical and Chemical Reference Data **18**, 1757 (1989); https://doi.org/10.1063/1.555844
Submitted: 30 September 1988 . Published Online: 15 October 2009

P. J. M. van der Burgt, W. B. Westerveld, and J. S. Risley

Photoemission Cross Sections for Atomic Transitions in the Extreme Ultraviolet due to Electron Collisions with Atoms and Molecules

P. J. M. van der Burgt,[a] W. B. Westerveld,[b] and J. S. Risley

Atomic Collisions Laboratory, Department of Physics, North Carolina State University, Raleigh, North Carolina 27695-8202

Received September 30, 1988; revised manuscript received February 15, 1989

This article reviews experimental photoemission cross sections in the extreme ultraviolet, for transitions in excited atoms and atomic ions formed in electron collisions with atoms and molecules. A survey of the available experimental data for each investigated target gas reveals severe inconsistencies between cross sections reported by different laboratories. As almost all reported cross sections are based on relative measurements, a detailed discussion is given of the methods used for normalization of the cross sections.

Key words: atoms; atomic transitions; cross sections; electron impact; extreme ultraviolet; molecules; normalization methods; photoemission; polarization.

Contents

List of Tables

[a] Present address: Department of Physics, University of Windsor, Windsor, Ontario N9B 3P4, Canada
[b] Permanent address: Buys Ballotlaboratorium, Rijksuniversiteit Utrecht, 3584 CC Utrecht, The Netherlands

List of Figures

1. Introduction

Electron impact on atoms, molecules, and ions plays a fundamental role in the physics of many parts of the universe. In particular, the precise modeling of atmospheres, including the earth's, requires a detailed knowledge of excitation processes (Massey and Bates 1982, Zipf 1984). Photoemission is an important way in which these excitation processes become manifest. Unfortunately, we currently know only the gross features of many excitation processes, for example the total excitation cross sections (Heddle and Gallagher 1988). Our article reviews the recent measurements of photoemission cross sections. It is limited to the extreme ultraviolet (EUV) wavelength region (25–200 nm), where experimental difficulties in EUV radiometry have seriously hindered accurate absolute measurements (Samson 1967).

Over 500 photoemission cross sections in the EUV have been measured for a variety of atomic and molecular targets during the last 25 years. Most of these cross sections are based on relative measurements, and are either directly or indirectly normalized to the Bethe or Born approximations. An important part of this review is therefore devoted to a discussion of the various types of normalization that have been used and their related experimental methods. The reliance on normalization is not surprising considering the difficulty of performing absolute radiometric calibrations in the EUV. At present the only absolute EUV radiometric standard of high accuracy that is being used for radiometric calibrations of photoemission cross sections, is the well-parametrized electron storage ring SURF II at the National Institute of Standards and Technology (formerly named the National Bureau of Standards) in Gaithersburg, Maryland (Hughey and Schaefer 1982, Ott *et al.* 1986). In principle the electron storage ring BESSY of the Physikalisch-Technische Bundesanstalt in Berlin, Germany, can also be used for high accuracy calibration (Fischer *et al.* 1984). Our review of the available literature shows that severe inconsistencies exist between cross sections reported by different laboratories, sometimes extending far outside the reported uncertainties. This illustrates the difficulty of performing accurate measurements of photoemission cross sections in the EUV.

This review encompasses measurements of photoemission cross sections in the extreme ultraviolet for transitions in excited atoms and atomic ions formed in electron collisions with atoms and molecules. We do not consider photoemission of excited molecules, photoemission in the visible or infrared wavelength regions, differential electron scattering, and theoretical methods used to calculate photoemission cross sections.

Some review articles have already been written on related topics. Electron impact excitation of atoms has been extensively reviewed by Moiseiwitsch and Smith (1968), Heddle and Keesing (1968), Heddle (1979), and Bransden and McDowell (1978). Electron scattering by molecules has been reviewed by Trajmar *et al.* (1983) and Zipf (1984). A brief review on photoemission cross sections for electron collisions with atoms and molecules has been given by McConkey (1984). Kühne and Wende (1985) have reviewed vacuum ultraviolet radiometry. Heddle and Gallagher (1989) have written an extensive review on measurements of optical excitation functions for electron collisions with atoms and ions.

In Sec. 2, below, the photoemission cross section is defined, and related to the number of photons observed per second in the experiment. In Sec. 3, the various normalization methods are discussed. In Sec. 4, the reported measurements of photoemission cross sections for individual target gases are discussed and compared. In Sec. 5, a table of select-

ed cross sections is presented, based on presently available data, that can be used for calibration of spectrometer-detector systems. The review ends with conclusions and three appendices covering instrumental polarization and the detection of photons, a summary of experiments by different researchers, and a list of all reported EUV photoemission cross sections.

2. Cross sections

2.1 Photoemission and Excitation Cross Sections

Photoemission due to electron impact on individual atoms or molecules can be represented schematically as

$$e + A \rightarrow A^* + e_{sc}$$
$$\lambda_{ij}.$$

where A represents a gaseous atomic or molecular target in the ground state and A^* a collisionally produced atomic or ionic species radiating in the extreme ultraviolet (EUV) at a wavelength λ_{ij} from an initial state i to a final state j. The probability that an incident electron makes a collision that (eventually) gives rise to a photon of wavelength λ_{ij} is proportional to the distance l the electron travels through the gas, the number density n of the target gas, and the photoemission cross section $\sigma(\lambda_{ij})$. For an electron beam of i_e electrons per second passing through the target gas the rate of photon emission $I_{\text{tot}}(\lambda_{ij})$ is given by

$$I_{\text{tot}}(\lambda_{ij}) = i_e n l \sigma(\lambda_{ij}). \tag{2.1}$$

An absolute measurement of the emitted intensity therefore provides access to the fundamental photoemission cross section $\sigma(\lambda_{ij})$. In Eq. (2.1) it is assumed that the electron beam current density and the target gas number density are low enough to prevent multiple collisions between electrons and atoms, in order to preserve the linear relationship expressed in the equation.

In general the upper level i is populated either directly by electron impact to this level or indirectly through radiative cascade from higher lying levels to level i:

$$\sigma(\lambda_{ij}) = \gamma_{ij}\{\sigma_i + \sum_{n>1} \sigma_n A_{ni} \tau_n + \text{multiple cascade}\}$$
$$= \gamma_{ij}\{\sigma_i + \sum_{n>i} \sigma_n \gamma_{ni} + \text{multiple cascade}\}, \tag{2.2}$$

where σ_i and σ_n are cross sections for direct excitation by electron impact, A_{ni} is the Einstein coefficient for the transition $n \rightarrow i$, τ_n is the lifetime of the level n, and $\gamma_{ni} = A_{ni}\tau_n$ is the branching ratio. Thus, when excitation cross sections for direct electron-impact excitation of higher levels can be estimated, and branching ratios are known, the photoemission cross section $\sigma(\lambda_{ij})$ can be related to the excitation cross section σ_i. All these cross sections depend, of course, on the energy of the electrons incident on the target gas. A graph of a photoemission cross section as a function of energy is commonly called an optical excitation function.

The observed radiation can be affected by two pressure-dependent processes: the absorption of resonance radiation, and the transfer of excitation due to collisions between excited atoms and atoms (or molecules) in the ground state. Both processes have been discussed and reviewed by Heddle and Keesing (1968) and Heddle (1979). To eliminate these effects it is important to take measurements under conditions where the radiation intensity is linearly proportional to the target-gas density.

Usually it is assumed that no excited atoms formed within the detector viewing region escape from the viewing region before radiatively decaying, and, vice versa, no excited atoms formed outside the viewing region contribute to the optical signal. A careful analysis is needed in situations where the above assumptions are not valid, such as long-lived excited states (see Van Zyl *et al.* 1980), or fast excited fragments produced in a dissociative process.

Because the scattered electrons are not detected and the target atoms are assumed to be unpolarized (before excitation), the angular distribution of emitted photons is of cylindrical symmetry which can be completely described in terms of the polarization Π_{ij} of the light emitted at 90° with respect to the electron beam. Π_{ij} is defined as

$$\Pi_{ij} = \frac{I_{\parallel,90^\circ}(\lambda_{ij}) - I_{\perp,90^\circ}(\lambda_{ij})}{I_{\parallel,90^\circ}(\lambda_{ij}) + I_{\perp,90^\circ}(\lambda_{ij})} \tag{2.3}$$

where $I_{\parallel,90^\circ}(\lambda_{ij})$ and $I_{\perp,90^\circ}(\lambda_{ij})$ are the intensities of light observed at 90° with respect to the electron beam, with the electric vector parallel or perpendicular to the electron beam, respectively. The rate of photon emission $I_\theta(\lambda_{ij})$ at angle θ, in units of number of photons per steradian and per second is (Westerveld *et al.* 1979)

$$I_\theta(\lambda_{ij}) = \frac{I_{\text{tot}}(\lambda_{ij})}{4\pi} \frac{1 - \Pi_{ij}\cos^2\theta}{1 - \frac{1}{3}\Pi_{ij}}. \tag{2.4}$$

In a general situation Eqs. (2.1) and (2.4) can be written for a small volume-element $dV = dxdydz$ at position (x,y,z) within the intersection of the electron beam and the target gas (see Fig. 1)

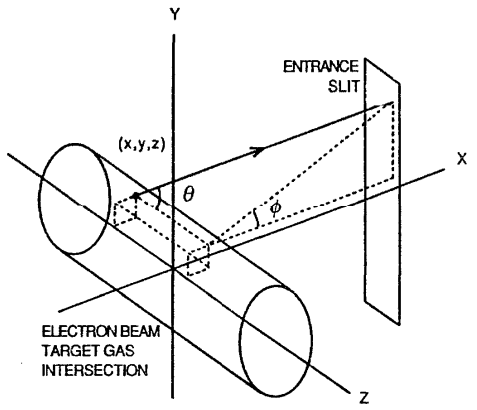

FIG. 1. Geometrical arrangement of the electron beam-target gas intersection and the entrance slit of the spectrometer. Photons emitted from a point (x,y,z) in the intersection enter the spectrometer in a direction characterized by the angles θ and ϕ. The x axis is the optic axis.

$$N_\theta dx\,dy\,dz\,d\Omega = J(x,y,z)n(x,y,z)dx\,dy\,dz \times \frac{\sigma(\lambda_{ij})}{4\pi}\frac{1-\Pi_{ij}\cos^2\theta}{1-\frac{1}{3}\Pi_{ij}}d\Omega. \quad (2.5)$$

Here N_θ is the rate of photon emission per steradian per unit of volume, $n(x,y,z)$ is the number density of the target gas, and $J(x,y,z)$ is the flux of electrons, the number of electrons per second crossing a unit area $dxdy$ located at (x,y,z). The photon count rate $S(\theta_0)$ integrated over the spectrometer line profile can now be written as

$$S(\theta_0) = \int N_\theta R(x,y,z,\theta,\phi,\lambda_{ij},\Lambda)d\Lambda\,dx\,dy\,dz\,d\Omega, \quad (2.6)$$

where θ_0 is the angle between the electron beam and the optic axis, Λ is the spectrometer wavelength setting, and R is the efficiency of the spectrometer-detector system. In practice, the efficiency R is nonzero only when $\Lambda \approx \lambda_{ij}$. For the moment we assume that the spectrometer has no polarization sensitivity.

At this point we must make a distinction between crossed-beams experiments and static-gas experiments. In a crossed-beams experiment, the experimenter produces a beam of atoms or molecules by flowing the target gas through a small diameter hole, a single capillary tube, or an array of tubes. A beam of mono-energetic electrons crosses the target beam at right angles, allowing the experimenter to detect photons emitted from the intersection of both beams, usually perpendicular to the plane containing both beams. The advantage of a crossed–beams experiment is its simple optical geometry. However, crossed-beams experiments are less suitable for accurate absolute measurements of photoemission cross sections, because it is difficult to model the nonuniform gas density accurately and absolutely. Even in relative measurements the shape of the intersection of both beams may depend on the electron energy. In a static–gas experiment the experimenter directs a beam of mono-energetic electrons through a collision chamber containing the target gas at a uniform density that needs to be accurately measured. A spectrometer-detector system, usually mounted perpendicular to the electron beam, detects photons emitted by excited atoms all along the electron beam intersecting the target gas. Equation (2.6) applies to either type of experiment:

1. Crossed-beams experiments: Usually the distance between the spectrometer and the emission volume (the intersection of the electron and gas beams) is large compared to the dimensions of the emission volume. If we replace the efficiency function $R(x,y,z,\theta,\phi,\lambda_{ij},\Lambda)$ in Eq. (2.6) with its average value $\bar{R}_c(\theta,\phi,\lambda_{ij},\Lambda)$ over the emission volume, where c denotes a crossed beams geometry, we find

$$S(\theta_0) = \frac{\sigma(\lambda_{ij})}{4\pi}\frac{1-\Pi_{ij}\cos^2\theta_0}{1-\frac{1}{3}\Pi_{ij}} \times k_c(\lambda_{ij})\int J(x,y,z)n(x,y,z)dx\,dy\,dz, \quad (2.7)$$

where

$$k_c(\lambda_{ij}) = \int \bar{R}_c(\theta,\phi,\lambda_{ij},\Lambda)d\Lambda\,d\Omega$$

is the efficiency integrated over the spectrometer line profile and over the acceptance angles of the spectrometer.

2. Static-gas experiments: The target density is assumed to be uniform i.e., $n(x,y,z) = n$, and the diameter of the electron beam is assumed to be small compared to the distance between the electron beam and the entrance slit of the spectrometer, so that $R(x,y,z,\theta,\phi,\lambda_{ij},\Lambda)$ may be replaced by its average value $\bar{R}_s(z,\theta,\phi,\lambda_{ij},\Lambda)$ over the cross-sectional area of the electron beam at position z, where s denotes a static gas geometry. Integration over x and y gives the electron beam current $i_e = \int J(x,y,z)dxdy$, and it follows that

$$S(\theta_0) = \frac{\sigma(\lambda_{ij})}{4\pi}\frac{1-\Pi_{ij}\cos^2\theta_0}{1-\frac{1}{3}\Pi_{ij}}k_s(\lambda_{ij})i_e nl, \quad (2.8)$$

where

$$k_s(\lambda_{ij}) = \frac{1}{l}\int \bar{R}_s(z,\theta,\phi,\lambda_{ij},\Lambda)dz\,d\Lambda\,d\Omega$$

is the efficiency integrated over the spectrometer line profile and over the acceptance angles of the spectrometer, and averaged over the length l of electron beam viewed by the spectrometer. For fixed values of θ the integration over z covers the width w of the entrance slit and leads to

$$k_s(\lambda_{ij}) = \frac{w}{l}\int \tilde{R}_s(\theta,\phi,\lambda_{ij},\Lambda)d\Lambda\,d\Omega,$$

where $\tilde{R}_s(\theta,\phi,\lambda_{ij},\Lambda)$ is the average value of $\bar{R}_s(z,\theta,\phi,\lambda_{ij},\Lambda)$ over the width of the entrance slit.

The efficiency of a particular spectrometer-detector system has been measured by McPherson *et al.* (1986) and Kendrick *et al.* (1987) as a function of wavelength and acceptance angles. They find great variation in the efficiency for different angles and different wavelengths, which underscores the strong dependency of the obtained photomultiplier count rate on the geometry of the light source.

2.2. Instrumental Polarization

The majority of photoemission cross sections have been measured using a spectrometer and a photomultiplier. The polarization properties of a spectrometer-photomultiplier system are conveniently described by an efficiency $k_\parallel(\lambda)$ for detection of light polarized parallel to the entrance slit and, similarly, an efficiency $k_\perp(\lambda)$ for light polarized perpendicular to the entrance slit (see Appendix A). The orientation of the electron beam with respect to the entrance slit of the spectrometer determines to what extent the instrumental polarization sensitivity affects the measured count rate for $\Pi_{ij} \neq 0$.

In a collision experiment with electron impact on unpolarized atoms, where the scattered electrons are not detected, the polarization of the light emitted at an angle θ_0 with respect to the electron beam can be described in terms of two independent components, one perpendicular and one parallel to the plane containing the electron beam and the emis-

sion direction (optic axis of the spectrometer), respectively. Assuming that the photon detector mounted behind the exit slit of the spectrometer has no significant polarization properties, it follows that instrumental polarization can be eliminated by mounting the spectrometer so that the entrance slit is at a 45° angle to the plane containing the electron beam and the optic axis.

The experimenter can also eliminate the effect of the anisotropy (associated with the polarization) of the photon emission on the measured photon count rate. Eq. (2.3) shows that in case photons are detected at the "magic angle" $\theta_0 = 54.74°$, so that $\cos^2\theta_0 = 1/3$, the photon count rate is directly proportional to the photoemission cross section $\sigma(\lambda_{ij})$, independent of the polarization Π_{ij}.

Appendix A gives a general derivation for the photon count rate obtained with the spectrometer at arbitrary angles. In practice, two different situations are encountered:

1. Measurements at the "magic angle": The experimenter can eliminate the effects of the instrumental polarization as well as the anisotropy of the emitted radiation on the measured count rate by orienting the electron beam at an angle of 54.74° (magic angle) to the optic axis of the spectrometer and setting the plane containing the electron beam and the optical axis at an angle of 45° to the entrance slit (method of Clout and Heddle 1969). The count rate of the photomultiplier in this case is given by (see Eq. A.11)

$$S(54.7°) = \frac{I_{\text{tot}}(\lambda_{ij})}{4\pi} k(\lambda_{ij}), \tag{2.9}$$

with

$$k(\lambda_{ij}) = \frac{1}{2}[(k_{\parallel}(\lambda_{ij}) + k_{\perp}(\lambda_{ij})] \tag{2.10}$$

independent of the polarization. Combination of Eqs. (2.1) and (2.9) gives

$$\sigma(\lambda_{ij}) = \frac{4\pi S(54.7°)}{i_e n l k(\lambda_{ij})}. \tag{2.11}$$

In some experiments the angle between the electron beam and the optic axis is 54.74° but the entrance slit is perpendicular to the plane containing the electron beam and the optic axis. In that case any instrumental polarization sensitivity gives rise to a polarization-dependent count rate:

$$S(54.7°) = \frac{I_{\text{tot}}(\lambda_{ij})}{4\pi(1 - \frac{1}{3}\Pi_{ij})} \frac{1}{2}\{(1 + \tfrac{1}{3}\Pi_{ij})k_{\perp}(\lambda_{ij}) + (1 - \Pi_{ij})k_{\parallel}(\lambda_{ij})\}. \tag{2.12}$$

Equation (2.9) now holds under the assumption that $k_{\perp}(\lambda) \cong k_{\parallel}(\lambda)$.

2. Measurements at 90°: In most experiments photons are detected at 90° with respect to the electron beam, and the plane of electron beam and optic axis is perpendicular to the entrance slit. The obtained count rate is (see Eq. A.12)

$$S(90°) = \frac{I_{\text{tot}}(\lambda_{ij})}{4\pi(1 - \frac{1}{3}\Pi_{ij})} \frac{1}{2}\{(1 + \Pi_{ij})k_{\perp}(\lambda_{ij}) + (1 - \Pi_{ij})k_{\parallel}(\lambda_{ij})\}, \tag{2.13}$$

which reduces to the form given in Eq. (2.9) when $\Pi_{ij} \cong 0$. Sometimes, assuming that $k_{\perp}(\lambda) \cong k_{\parallel}(\lambda)$, an apparent cross section is defined as

$$\sigma_{\perp} = \frac{4\pi S(90°)}{i_e n l k(\lambda_{ij})}. \tag{2.14}$$

with

$$\sigma(\lambda_{ij}) = \sigma_{\perp}(1 - \tfrac{1}{3}\Pi_{ij}). \tag{2.15}$$

Very few polarization measurements exist in the EUV. Measurements have been performed only for a few transitions in He, Ar, H_2, and N_2, see Sec. 4.

Van Brunt and Zare (1968) discuss the conditions for emission of polarized light by excited atomic fragments formed in molecular dissociation. The conditions are: (1) an anisotropic spatial distribution of dissociation products, and (2) a preferential population of the magnetic sublevels of the excited fragments. The first condition is satisfied, if preferred orientations for dissociation of the molecule exist with respect to the incident beam, because dissociation normally takes place in a time small compared to the rotational periods of the molecule (Dunn 1962). The second condition is satisfied only if a limited number of repulsive states contribute to the dissociation process. Since a very large number of repulsive channels exist for many molecules, EUV photoemission following dissociative excitation of molecules is generally unpolarized. In such cases photon detection at right angles to the electron beam is adequate to determine the photoemission cross section.

2.3. The radiometric problem

The formulae in the previous paragraph show that the basic experimental quantities needed to evaluate a photoemission cross section from a measured photon count rate are the efficiency $k(\lambda)$ of the spectrometer-detector system, the target-gas density, and the electron current. In the EUV, the most difficult experimental parameter to measure is the efficiency. Direct optical calibration of the spectrometer-detector system requires a radiometric standard. Although several radiometric standards exist for optical calibration in the vacuum ultraviolet (McPherson *et al.* 1986), below 115 nm the only absolute radiometric standard intrinsically accurate to a few percent is synchrotron radiation (attainable only when accurate parametrization is possible).

It is sometimes possible to measure a photoemission cross section for a transition in the EUV relative to a photoemission cross section for a transition in the visible, if the two transitions are in cascade or are branching from the same level. The calibration problem can then be transferred from the EUV to the visible, where standard calibration techniques are available. Lawrence (1970) measures the (O I 130.4 nm) photoemission cross sections for dissociative excitation of the O_2, CO, NO, and H_2O molecules relative to the (O I 844.7 nm) photoemission cross sections, by means of a cascade analysis of the 130.4 nm time decay curve. The (O I 844.7 nm) cross section is measured absolutely by using

a blackbody as a radiation intensity standard. Moustafa Moussa and de Heer (1967) obtain a calibration of their spectrometer at 53.7 nm by comparing the intensity of the 53.7 nm and 501.6 nm transitions from $He(3^1P)$ atoms formed in $He^+ + Ne$ collisions and using a theoretical value for the branching ratio. The intensity of the visible transition is measured with another spectrometer calibrated absolutely with a tungsten lamp.

Because of the radiometric problem most of the existing photoemission cross sections in the EUV are based on relative measurements, that are converted to an absolute scale by normalization. In Sec. 3 we consider the various normalization methods in more detail.

2.4. The Target-Gas Density

Absolute measurement of a photoemission cross section in a static-gas experiment requires an absolute measurement of the number density of the target gas. Absolute number densities are obtained by measuring absolute pressures and converting these to densities using the ideal gas law, provided that the gas temperature is known. Absolute pressures are usually measured with a capacitance manometer or (in older experiments) with a McLeod gauge. Below 10^{-4} Torr, an ionization gauge, calibrated against a capacitance manometer in the 10^{-4}–10^{-2} Torr range, can be used. Strictly speaking, the ionization-gauge signal is proportional to the number density rather than the pressure. The linearity of the ionization–gauge signal with the gas number density is usually assumed but is not always guaranteed, especially when reactive gases are used (see Tilford 1983 and references therein).

Conversion of absolute pressure to number density requires knowledge of the temperature. The definition of the temperature of the target gas is ambiguous if the target gas is exposed to steep temperature gradients such as cryogenic traps and heated cathodes. In addition, a difference in temperature between the interaction region and the measuring device requires a correction for thermal transpiration (see e.g. Poulter *et al.* 1983).

A number of additional methods is available to measure the density of the target gas. A very accurate method is the dynamic expansion technique used by Van Zyl *et al.* (1976). Another method is based on the absorption of resonance radiation. If the gas temperature and the oscillator strength of a particular transition are known, the relation between absorption and gas density can be computed from the formulae of Mitchell and Zemansky (1934). A novel and important new method is the spinning rotor gauge, (Fremeney 1985) which provides an accurate linear pressure scale in the 10^{-7}–10^{-2} Torr range. Although this device is now available commercially, it has not been used in any of the measurements reported in this review.

2.5. The Electron Current

The current of an electron beam passing through a target gas is commonly measured by collecting the electron beam in a Faraday cup and registering the current with an electrometer. Unless the experimenter applies a proper bias voltage to the Faraday cup his measurements will likely be incorrect. An incorrect current reading can result when secondary electrons are produced on the interior surface of the Faraday cup and escape through the entrance aperture. It is also possible that the current reading depends on the Faraday cup voltage, due to focusing of the electron beam by the electrostatic lens formed by the Faraday cup and the preceding electrode.

Apart from the inaccuracies in the electron current, the measurement of the cross section can be profoundly influenced by other effects related to the electron beam. Collisions with apertures can produce secondary electrons of relatively low energy in the beam. These secondary electrons could significantly influence the optical signal observed from the interaction region, particularly when the excitation cross sections peak at these lower energies. Surface charges or variations in contact potentials could influence both the geometry and the energy of the electron beam and thus have an effect on the shape of optical excitation functions. For low incident-electron energies, space-charge effects might lead to broadening of the electron beam. Such geometrical effects could easily lead to a change in the interaction volume and consequently affect the number of detected photons, especially in crossed-beams experiments. In experiments in which magnetic fields have been used to collimate the electron beam, effects may exist due to spiraling of the electrons or Larmor precession of the excited atoms.

3. Methods of Normalization

3.1 Introduction

Most of the reported photoemission cross sections in the EUV are based on relative measurements, which are either directly or indirectly normalized on the Bethe or Born approximations. In some cases the branching ratio method is used to measure a photoemission cross section in the EUV by relating it to a photoemission cross section in the visible, where absolute calibration is feasible using standard optical methods. Various types of normalization can be distinguished:

1. Normalization on a known photoemission cross section for the same transition of the same gas. This method can be used when an optical excitation function is measured on a relative scale. It requires accurate monitoring only of the relative pressure and current. The optical excitation function is put on an absolute scale by normalizing on another experimental cross section at a particular collision energy, on the Born approximation at sufficiently high energy, or on an optical oscillator strength by using the Bethe approximation.

2. Normalization on a known photoemission cross section for a transition of another gas at the same wavelength. This method requires either an absolute pressure measurement in a static-gas experiment, or the use of the relative gas-flow technique in a crossed-beams experiment. When a mix-

ture of gases is used, the experimenter must have accurate knowledge of the composition of the mixture. To measure a photoemission cross section for dissociative excitation of a molecule relative to the photoemission cross section for electron-impact excitation of one of the atomic fragments (for the corresponding transition), a partly dissociated beam of molecules, of which the dissocitative fraction is accurately determined, can be used.

3. Normalization on a known photoemission cross section for a transition of the same gas at another wavelength. This method requires a determination of the relative spectral response of the spectrometer-detector system used. The relative spectral response can be determined using the atomic or molecular branching-ratio technique or the double-monochromator technique. Sometimes photoemission cross sections are determined by interpolation between a number of known cross sections at different wavelengths, or by using cascade, when two cascade transitions are in different wavelength regions.

4. Normalization on a known photoemission cross section for a transition of another gas at another wavelength. This method requires a combination of techniques mentioned in 2 and 3.

It is important to note that all of the four cases mentioned involve a relative measurement. A photoemission cross section that is directly normalized on the Bethe approximation (method 1) by using a calculated oscillator strength for the transition concerned involves a relative measurement, but a photoemission cross section that is normalized on another cross section in another target gas (method 4) also involves a relative measurement, even though it involves an optical calibration of the spectrometer-detector system. This optical calibration is relative (e.g., when the molecular branching-ratio technique or the double monochromator technique is used), and the cross section used for normalization is usually obtained from a relative measurement, being either directly or indirectly normalized on the Bethe or Born approximations.

Only when the efficiency of the spectrometer-detector system is calibrated absolutely against an absolute radiometric standard, and the target-gas density and electron current are measured absolutely, one can speak of an absolute measurement.

In this context the term "absolute cross section" might be somewhat misleading. Both cross sections obtained in an absolute measurement, and cross sections obtained in a relative measurement and brought on an absolute scale by normalization, are called absolute cross sections.

3.2. The Bethe Approximation

Based on the Born approximation, Bethe (1930) shows that for electron-impact excitation of an atom via an optically allowed transition the excitation cross section behaves asymptotically for high electron energies as

$$\sigma_i = \frac{4\pi a_0^2}{E/R}\,\frac{f_i}{E_i/R}\ln(4c_i E/R). \tag{3.1}$$

Here E is the kinetic energy of the electrons, E_i is the excitation energy, f_i is the optical oscillator strength of the transition, c_i is a constant dependent on the transition, a_0 is the radius of the first Bohr orbit and R is the Rydberg constant. For optically forbidden transitions the excitation cross section behaves asymptotically as

$$\sigma_i = \frac{4\pi a_0^2}{E/R}\,b_i, \tag{3.2}$$

where b_i is a constant dependent on the considered transition. Inokuti (1971) and Inokuti *et al.* (1978) give an extensive review of the Bethe approximation. McFarlane (1974) develops a Bethe theory for the polarization of radiation emitted after excitation due to electron impact.

It follows directly from Eq. (3.1) that a plot of $\sigma_i E$ against ln E shows a straight line with a slope proportional to f_i/E_i and an intercept on the horizontal axis at $E = R/4c_i$ (Fano 1954). This is called a Fano plot.

When an optical excitation function (for an optically allowed transition) measured on a relative scale is multiplied by the energy E and plotted versus ln E, the high-energy part of the plot tends toward a straight line. The slope of this line can be normalized to the slope obtained from the optical oscillator strength, and the excitation cross section be put on an absolute scale, assuming that cascade is negligible or can be accurately corrected for. This method can be applied by using either experimental or theoretical values for the optical oscillator strength f_i. The photoemission cross section for the considered radiative transition $i \rightarrow j$ follows from Eq. (2.2), if the cascade contribution and the branching ratio γ_{ij} are known.

The underlying assumption in this method is that the Bethe approximation is valid at energies low enough to render relativistic effects negligible. For the heavier atoms this could restrict the applicability of the method.

The effect of polarization: The method described above can be applied only when the polarization of the emitted radiation is zero, or when the polarization of the emitted radiation and the instrumental polarization are eliminated from the measured photon count rate as described in Sec. 2.2. When photons are detected perpendicular to the electron beam, and cascade is negligible, the following Bethe approximation holds (Heddle 1979):

$$\sigma_\perp = \gamma_{ij}\,\frac{4\pi a_0^2}{E/R}\,\frac{f_i}{E_i/R} \times \frac{(1-\tfrac{1}{5}\Pi_{ij}^0)\ln(4c_i E/R) + \frac{1}{2}\Pi_{ij}^0}{(1-\tfrac{1}{3}\Pi_{ij}^0)}. \tag{3.3}$$

Here Π_{ij}^0 is the polarization at the excitation threshold. Π_{ij}^0 can be calculated exactly from conservation of angular momentum (Percival and Seaton 1958). In this case a plot of $\sigma_\perp E$ versus ln E also gives a straight line.

The effect of cascade: Cascade can greatly hamper the practical application of the Bethe approximation. Van Raan (1973) considers the cascade contribution to the population of resonance levels. He argues that all levels that radiatively decay to a particular resonance level are primarily populated

by electron-impact excitations corresponding to optically forbidden transitions. Therefore the Bethe approximation for the photoemission cross section for a resonance transition can be written as

$$\sigma(\lambda_{ij}) = \gamma_{ij}\frac{A}{E}\frac{f_i}{E_i}\ln(4c_iE/R) + \gamma_{ij}\frac{B}{E}$$

$$= \gamma_{ij}\frac{A}{E}\frac{f_i}{E_i}\ln\left[4c_iE/R\exp\left(\frac{BE_i}{Af_i}\right)\right], \qquad (3.4)$$

where A and B are proportionality constants (see Eqs. 3.1 and 3.2). A Fano plot shows a slope proportional to f_i/E_i. Van Raan (1973) uses this method for a few noble-gas resonance transitions. The method is also used by Tan *et al.* (1974) and (implicitly) by McConkey and Donaldson (1973) for noble-gas resonance transitions.

3.3. The Relative Gas-Flow Technique

In a crossed beams experiment the relative gas-flow technique provides a method of normalizing an unknown photoemission cross section to a known photoemission cross section for another atom or molecule. The technique has been developed at the Jet Propulsion Laboratory (Srivastava *et al.* 1975, Brinkman and Trajmar 1981, Trajmar and Register 1984, Khakoo and Trajmar 1986, Nickel *et al.* 1989) for measurements of elastic differential cross sections for scattering of electrons, but can readily be adapted for photoemission cross sections. In this technique, the experimenter compares the photon count rates obtained for each of the target gases, based on the known relative gas densities of the target gases. The target beam flux distribution, the electron beam current density, and the detector efficiency must be the same for both target gases during the two measurements. Under these conditions the following analysis applies.

In a crossed beams experiment the photon count rate for an unpolarized transition can be written as (Eq. 2.7)

$$S(\vartheta_0) = \frac{\sigma(\lambda_{ij})}{4\pi}k_c(\lambda_{ij})\int J(x,y,z)n(x,y,z)dxdydz \qquad (3.5)$$

For gas flow through a single capillary tube, Olander and Kruger (1970) show that

$$n(x,y,z) = \frac{\dot{N}}{v}\frac{j(\alpha)}{\pi r^2 K}, \qquad (3.6)$$

where $\dot{N}$ is the total flow rate (number of particles per second) through the tube, $v = \sqrt{(3kT/M)}$ is the average thermal velocity of the particles in the beam, $j(\alpha)$ is a normalized distribution function that depends on the flow conditions in the tube, α is the angle between the direction to (x,y,z) and the center line of the tube, r is the distance from the tube exit to the point (x,y,z), and K is the transmission probability (or Clausing factor) of the tube. Combination of Eqs. (3.5) and (3.6) gives

$$S(\vartheta) \sim \sigma(\lambda_{ij})k_c(\lambda_{ij})\dot{N}\sqrt{M/T}\beta, \qquad (3.7)$$

where

$$\beta = \int J(x,y,z)\frac{j(\alpha)}{\pi r^2 K}dxdydz.$$

The derivation of Eq. (3.7) can be generalized (Brinkman and Trajmar 1981, Nickel *et al.* 1989) for capillary arrays with the restriction that no significant interaction occurs among the beams originating from the different capillary tubes. This leads to a more general formula for the integral β.

We now compare the photon count rates $S(\theta)$ and $S_r(\theta)$ for two transitions of the same wavelength in two different gases at the same temperature, where the index r indicates the reference gas. If the conditions of the two gases are such that the Knudsen numbers behind the multicapillary array are the same, the distribution functions $j(\alpha)$ and $j_r(\alpha)$ are the same and $\beta/\beta_r = 1$. Therefore the ratio of the photon count rates in a relative gas-flow measurement can be written as

$$\frac{S(\theta)}{S_r(\theta)} = \frac{\sigma(\lambda)}{\sigma_r(\lambda)}\frac{\dot{N}}{\dot{N}_r}\sqrt{\frac{M}{M_r}}. \qquad (3.8)$$

The relative gas-flow technique is used by Ajello and co-workers (see Ajello and Franklin 1985, Shemansky *et al.* 1985) for measurements of cross sections in He, O_2, N_2, H_2O, CH_4, and C_2H_2, and by McConkey and co-workers (see Forand *et al.* 1986) for measurements of cross sections in SF_6, Ar, and N_2.

Under conditions of molecular (collisionless) flow in the capillary array, the pressure in the gas reservoir is directly related to the flow rate by $p \sim \dot{N}\sqrt{M}$, which leads to

$$\frac{S(\theta)}{S_r(\theta)} = \frac{\sigma(\lambda)}{\sigma_r(\lambda)}\frac{p}{p_r}. \qquad (3.9)$$

This formula shows that two photoemission cross sections can be related to each other by comparing the slopes of photon intensity versus pressure, a method that is used by McConkey and co-workers (see Tan and McConkey 1974).

3.4. A Partly Dissociated Molecular Target Gas

In a number of collision experiments the experimenter uses a partly dissociated molecular target gas, containing molecules and atomic fragments from dissociated molecules. This opens the possibility for the determination of a photoemission cross section for electron-impact excitation of one of the atomic fragments relative to a photoemission cross section for dissociative excitation of the molecule. Such a measurement requires accurate determination of the dissociative fraction.

Fite and Brackmann (1958), Kauppila *et al.* (1971) and Woolsey *et al.* (1986) use this method in crossed-beams experiments to determine the Lyman-alpha cross section ratio for the excitation of hydrogen atoms to the dissociative excitation of hydrogen molecules. Fite and Brackmann (1958) use a tungsten furnace to produce a partly dissociated beam of hydrogen molecules, and determine the dissociative fraction by monitoring the atomic and molecular ions formed in the collisions with a mass spectrometer. The disso-

ciative fraction follows from known ionization cross sections. Kauppila *et al.* (1971) use a tungsten furnace and a quadrupole mass filter. The dissociative fraction measured by the quadrupole mass filter is corrected for mass discrimination effects. Woolsey *et al.* (1986) use an RF discharge source and determine the dissociative fraction from the ratio of count rates obtained with the discharge on and off for groups of molecular bands in the vicinity of Lyman alpha.

Once the dissociative fraction is known, the ratio between atomic and dissociative photoemission cross sections can be determined in the following manner. Using Eq. (3.7) for the capillary tube of the molecular beam source it follows that

$$S_1 \sim \sigma_m(\lambda) F \frac{1}{\sqrt{T_1 M_m}} \tag{3.10}$$

and

$$S_2 \sim \frac{1}{\sqrt{T_2}} \left(\frac{\sigma_m(\lambda) F_m}{\sqrt{M_m}} + \frac{\sigma_a(\lambda) F_a}{\sqrt{M_a}} \right), \tag{3.11}$$

where the indices 1 and 2 stand for discharge off and on (or furnace off and on), respectively; a and m indicate the atom and molecule, respectively; and $F = M\dot{N}$ is the mass flow. If the mass flow into the source is constant, so that $F = F_a + F_m$, the dissociative fraction is $D = F_a/F = 1 - F_m/F$. From Eqs. (3.8) and (3.9) the relationship between $\sigma_a(\lambda)$ and $\sigma_m(\lambda)$ follows

$$\frac{\sigma_a(\lambda)}{\sigma_m(\lambda)} = \sqrt{\frac{M_a}{M_m}} \frac{1}{D} \left(\sqrt{\frac{T_2}{T_1}} \frac{S_2}{S_1} - (1 - D) \right). \tag{3.12}$$

Stone and Zipf (1974) and Zipf (1986) determine the ratio of atomic and dissociative cross sections for the 130.4 nm transition in oxygen. A static-gas configuration is used, where a microwave discharge in the gas delivery tube produces a partly dissociated mixture, which is led into a small collision chamber. It is assumed that metastable oxygen atoms formed in the discharge rapidly decay through numerous collisions with the wall of the flow tube, before entering the collision chamber. Stone and Zipf (1974) measure the density of oxygen atoms by observing the absorption of resonance radiation. Zipf (1986) measures the density of oxygen atoms and molecules by using a mass spectrometer. Photoemission cross sections for other oxygen transitions are determined by using the relative spectral response of the spectrometer-detector system.

3.5. The Relative Spectral Response

When two photoemission cross sections for transitions at different wavelengths are compared, the relative spectral response of the spectrometer-detector system used is an important quantity. There are various methods to determine the relative spectral response.

3.5. a. The Atomic Branching-Ratio Technique

The emission intensity in photons per second for an atomic transition from an upper level i to a lower level j is

$$I_{\text{tot}}(\lambda_{ij}) = n_i A_{ij} V, \tag{3.13}$$

where n_i is the population density of the upper level, A_{ij} is the Einstein transition coefficient, and V is the emission volume. The number of photons detected per second (at an angle θ_0 with respect to the electron beam) is

$$S(\lambda_{ij}) = k(\lambda_{ij}) \frac{I_{\text{tot}}(\lambda_{ij})}{4\pi} \frac{1 - \Pi_{ij} \cos^2 \theta_0}{1 - \frac{1}{3}\Pi_{ij}}. \tag{3.14}$$

When a branched radiative decay of level i through two or more transitions is possible, the experimenter can obtain the relative response of a spectrometer at the corresponding wavelengths. Consider two transitions $i \rightarrow j$ and $i \rightarrow n$ with the same polarization, i.e., $\Pi_{ij} = \Pi_{in}$. It follows that

$$\frac{k(\lambda_{ij})}{k(\lambda_{in})} = \frac{S(\lambda_{ij})}{S(\lambda_{in})} \frac{A_{in}}{A_{ij}}. \tag{3.15}$$

Thus, if the ratio of transition probabilities A_{in}/A_{ij} is known, the relative spectral response at one wavelength with respect to the other can be found by measuring the photon count rates $S(\lambda_{ij})$ and $S(\lambda_{in})$. Equation (3.15) is valid only if the polarization of both transitions is the same. In general, the polarization of the emitted radiation and the instrumental polarization have to be eliminated as described in Sec. 2.2.

The atomic branching-ratio technique is applied by Beyer *et al.* (1979) for some transitions of ionized neon.

3.5.b. The Molecular Branching-Ratio Technique

As is suggested by Aarts and de Heer (1968) and McConkey, (1969) the branching ratio technique can be extended to molecular emissions. For radiative transitions between a particular vibrational level v of an upper electronic state to different vibrational levels v' and v'' of the same lower electronic state, Eq. (3.15) can be written in the form

$$\frac{k(\lambda_{vv''})}{k(\lambda_{vv'})} = \frac{S(\lambda_{vv''})}{S(\lambda_{vv'})} \frac{A_{vv'}}{A_{vv''}}. \tag{3.16}$$

This equation can be applied only if transition probabilities are available.

Since the molecular transition proceeds through the electric dipole interaction in most cases, the Franck–Condon principle can be used to simplify Eq. (3.16). In the Born–Oppenheimer approximation, the transition probability for an electric dipole transition from a vibrational level v of an upper electronic state i to a vibrational level v' of a lower electronic state f can be written as

$$A_{vv'} = C E_{vv'}^3 |\langle v'|v\rangle|^2 |\langle \Phi_f|\mathbf{d}|\Phi_i\rangle|^2$$
$$\sim \lambda_{vv'}^{-3} q_{vv'} |M_e(R_{vv'})|^2, \tag{3.17}$$

where C is a constant, $|v\rangle$, $|v'\rangle$ are vibrational wavefunctions, $|\Phi_i\rangle$, $|\Phi_f\rangle$ are electronic wavefunctions, $\mathbf{d}$ is the electric dipole-moment operator, $q_{vv'} = |\langle v'|v\rangle|^2$ is the Franck–Condon factor for the transition, $M_e(R_{vv'})$ is the electronic transition moment, $R_{vv'}$ is the average internuclear distance (R-centroid), and $\lambda_{vv'}$ and $E_{vv'}$ are the wavelength and the energy of the transition, respectively. The transition moment $M_e(R_{vv'})$ usually varies slowly with $R_{vv'}$ within a given band system, because the electronic eigenfunctions depend

only weakly on the internuclear distance. Often $M_e(R_{vv'})$ is effectively constant and may be replaced by its average value $\overline{M_e(R)}$ (Franck–Condon principle), so Eq. (3.16) reduces to

$$\frac{k(\lambda_{vv''})}{k(\lambda_{vv'})} = \frac{S(\lambda_{vv''})}{S(\lambda_{vv'})} \frac{\lambda^3_{vv''}}{\lambda^3_{vv'}} \frac{q_{vv'}}{q_{vv''}}. \tag{3.18}$$

This formula can be used for a relative calibration of a spectrometer-detector system, by using transitions from a particular vibrational level v of an upper electronic state to a variety of vibrational levels v',v'' of a lower electronic state.

The molecular branching-ratio technique can also be used in a more general form, by considering the rate of direct excitation P_{0v} of a vibrational level v of the upper electronic state from the ground state, which may be written as

$$P_{0v} \sim i n_0 q_{0v} |G(0,v)|^2, \tag{3.19}$$

where i is the electron beam current, n_0 is the population density of molecules in the ground state (assuming negligible population of higher vibrational levels), and $G(0,v)$ is the electronic transition matrix element. If $|G(0,v)|^2$ varies only slowly with the internuclear distance, it follows that the population rates vary as q_{0v}. After substitution in Eq. (3.17) the intensity distribution as a function of v and v' follows:

$$I(\lambda_{vv'}) \sim i n_0 \frac{q_{0v} q_{vv'}}{\lambda^3_{vv'}}. \tag{3.20}$$

Under the assumptions mentioned above, this formula may likewise be used for relative calibration. In this case, however, one looks at transitions $v \rightarrow v'$, where v as well as v' are allowed to vary.

In applications of the molecular branching ratio technique, four different molecular band systems have been used. The details concerning these band systems are reviewed by Mumma (1972) and Ajello *et al.* (1988), and we will only give a brief discussion.

The $N_2(a^1\Pi_g - X^1\Sigma_g^+)$ Lyman-Birge-Hopfield (LBH) band system can be used for relative calibration between 127 and 260 nm (or extended to 116 nm if some NI multiplets are used in addition (see Mumma and Zipf 1971b). Ajello *et al.* (1988) summarize its advantages: (1) no measurable cascade ($<5\%$); (2) intense and regularly spaced ($\sim$every 2 nm) features from 127 to 230 nm; (3) minimal blending with NI features; (4) narrow (<0.05 nm FWHM) rotational structure at 300 K; and (5) variation in electronic transition moment smaller than 5%. Its disadvantages are that it requires: (1) a background pressure lower than 10^{-4} Torr; (2) a characteristic pathlength of several cm and a wide field of view due to the 80 μs lifetime of the transition; and (3) electron energies greater than 30 eV due to threshold effects. The N_2(LBH) band system is used by Ajello and co-workers (see Ajello *et al.* 1982) to measure photoemission cross sections in CS_2, N_2, CH_4, and C_2H_2; by de Heer and co-workers (see Aarts and de Heer 1971a, van Sprang *et al.* 1979) to measure cross sections in H_2, N_2; by Morgan and Mentall (see Mentall and Morgan 1972) to measure cross sections in NO, H_2O, NH_3, and CH_4; and by Zipf and co-workers (see Mumma and Zipf 1971c) to measure cross sections in H_2, O_2, N_2, CO_2, NO, N, and O.

The $H_2(C^1\Pi_u - X^1\Sigma_g^+)$ Werner band system can be used for relative calibration between 90 and 125 nm. Stone and Zipf (1972b) argue that a spectrometer resolution better than about 0.04 nm is required to resolve rotational lines and eliminate effects of rotational perturbations. When transitions of the $H_2(B^1\Sigma_u^+ - X^1\Sigma_g^+)$ Lyman band system and other Rydberg band systems are included, a model spectrum for relative calibration between 80 and 165 nm can be generated (Ajello *et al.* 1984, 1988), based on published values for the transition probabilities, oscillator strengths, Franck–Condon factors, and excitation cross sections. This method is used by Ajello and co-workers (in combination with the double monochromator technique to extend the calibration down to 40 nm, see Ajello *et al.* 1984) to measure cross sections in H_2O, He, O_2, CH_4, and C_2H_2. The H_2 Werner band system is used by de Heer and co-workers (de Heer and Carriére 1971) to measure cross sections in H_2 and N_2; by McConkey and co-workers (Forand *et al.* 1986, and in combination with other Rydberg band systems by Forand *et al.* 1988) to measure cross sections in SF_6, Ar, and N_2; by Mentall and Morgan (Mentall and Morgan 1974) to measure cross sections in H_2O, NH_3, and CH_4; and by Zipf and co-workers (Zipf *et al.* 1979) to measure cross sections in O_2 and CH_4.

Specific vibrational and rotational levels of the $H_2(B^1\Sigma_u - X^1\Sigma_g^+)$ and $HD(B^1\Sigma_u - X^1\Sigma_g^+)$ Lyman band systems can be excited by absorption of Ar I(106.7 nm) resonance radiation (Becker *et al.* 1971) resulting in a clear spectrum of 28 well-separated lines that can be used for relative calibration between 106 and 171 nm. These lines are used by Zipf and co-workers (in combination with the N_2 LBH bands, see Stone and Zipf 1972a) to measure cross sections in NO, N, and O.

The $CO(A^1\Pi - X^1\Sigma^+)$ fourth positive band system is used by Becker and McConkey (1984) for relative calibration between 133 and 173 nm, in combination with the H_2 Werner bands. They use this calibration to measure cross sections in D_2 and SF_6.

3.5.c. The Double-Monochromator Technique

In the double-monochromator technique essentially monochromatic light of variable wavelength is obtained by using a monochromator with an ultraviolet light source at its entrance slit. The experimenter uses a rotatable mirror to direct the ultraviolet light available at the exit slit of the monochromator either onto the entrance slit of the spectrometer-detector system to be calibrated, or onto a photomultiplier coated with sodium salicylate. Since the efficiency of sodium salicylate is essentially flat between 30 and 112 nm (Samson 1964, 1967), a relative calibration of the spectrometer can be established by comparing the signals.

The double-monochromator technique is based on several assumptions. The sensitivity of sodium salicylate is assumed to be independent of wavelength to a satisfactory level. Unless the same part of the grating in the spectrometer is used during the calibration and the actual measurement, it must be assumed that the efficiency of the grating as a function of wavelength does not vary appreciably across the grating. The reflection coefficients for light polarized parallel

and perpendicular to the grating grooves are assumed to have similar wavelength dependencies, and the polarization of the monochromatic light from the monochromator is assumed to be independent of wavelength.

Ajello and co-workers (see Ajello *et al.* 1984, Ajello and Franklin 1985) use the double-monochromator technique for a relative calibration between 40 and 130 nm in combination with the molecular branching ratio technique for H_2 Rydberg band systems (80–130 nm), with an estimated uncertainty of 15%. The geometry of their arrangement ensures that the same part of the grating is used in the experiment and the calibration. The monochromator of Ajello *et al.* (1984) produces radiation of rather high polarization. They use Fresnel equations for reflection to apply a correction. This calibration method is used for cross section measurements in H_2O, He, O_2, CH_4, and C_2H_2. Mentall and Morgan also use the double-monochromator technique (see Mentall and Morgan 1976) for a relative calibration between 50 and 130 nm with an estimated uncertainty of 13%. They use this calibration method for cross section measurements in N_2, O_2, and Ar.

3.5.d. Interpolation on Known Cross Sections

Relative calibration of a spectrometer-detector system is difficult for wavelengths shorter than 100 nm, because there are no suitable molecular band systems. Several authors use cross sections or oscillator strengths for some noble gas transitions to determine absolute efficiencies at some wavelengths and then interpolate between these wavelengths.

Aarts and de Heer (1971a, b) and van Raan (1973) use oscillator strengths as measured by de Jongh and van Eck (1971a) for the He I(52.2, 53.7, 54.8 nm), Ne I(73.4 nm), Ar I(104.8 nm), and Kr I(116.4 nm) resonance transitions. Becker *et al.*, (1983), Becker and McConkey, (1984) and Forand *et al.* (1986) use cross sections for Ar I(106.7 nm) and the resonance transitions listed above, and for the He II(30.4 nm), Ar II(92.0, 93.2 nm) transitions measured by various authors.

This method is only reliable if the cross sections for the above listed lines are accurate (see discussions in Sec. 4) and if the efficiency of the spectrometer-detector system varies monotonically between the sometimes widely spaced calibration lines. Extrapolation is even more risky. Van Raan (1973) deduces the photoemission cross sections for Ne II(46.1, 46.2 nm) based on extrapolation below 52.2 nm. This extrapolation apparently leads to a large error (see Dijkkamp and de Heer 1981).

3.5.e. Time-Domain Cascade Analysis

When two atomic transitions in a radiative cascade have significantly different lifetimes, a time-domain cascade analysis can be applied for absolute calibration. It is required that the lower transition is much faster than the upper transition. The experimenter uses a pulsed electron beam to measure the time delay curve for the lower transition. This provides a cascade ratio, which relates the photoemission cross sections for both transitions. Lawrence (1970) uses this method to measure the (O I 130.4 nm) photoemission cross sections for dissociative excitation of the O_2, CO, NO, and H_2O molecules relative to the (O I 844.7 nm) photoemission cross sections. He calibrates the (O I 844.7 nm) photoemission cross sections absolutely by using blackbody radiation. In this particular measurement polarization effects are negligible, since the 130.4 nm transition is unpolarized and the 844.7 nm transition has a polarization of less than 0.5%.

4. Photoemission Cross Sections

In this section measurements of photoemission cross sections for individual target gases are discussed and compared. To make the comparisons meaningful, we have renormalized most cross sections to the same value of 7.3×10^{-18} cm^2 for the H_2(H I Ly-α) cross section (Sec. 4.3). In the Tables 1 to 7, to be discussed in the next paragraphs, it is indicated which cross sections have been renormalized. However, no renormalizations have been applied to the cross sections shown in the figures, nor to the cross sections listed in Table C1. in Appendix C. The reported uncertainties listed in the Tables 1 to 7 are found in the papers and are root-square additions of limits of error estimated for one or more of the experimental measurements involved in the determination of the cross section. Most authors do not give detailed information to clarify the nature of their uncertainties. It is of dubious value to compare data based on these reported uncertainties.

4.1 Helium

Helium is an important target gas for EUV cross section measurements, because it is of fundamental theoretical interest, and its resonance transitions are important for normalization of other cross sections below 60 nm. Cross sections have been reported for the three most intense resonance lines and for a few ion lines:

1. The He I(58.4 nm), He I(53.7 nm), and He I(52.2 nm) photoemission cross sections. The five following measurements have been performed by normalization on the Bethe approximation using calculated oscillator strengths from Schiff and Pekeris (1964), Weiss (1967), and Schiff *et al.* (1971) By adding cascade corrections and multiplying by the branching ratios, the excitation cross sections obtained in the normalization can be converted to photoemission cross sections. Branching ratios for the 53.7 and 52.2 nm transitions are 0.976 and 0.965, respectively, calculated from transition probabilities listed by Wiese *et al.* (1966)

Moustafa Moussa *et al.* (1969) measure the He I(58.4 nm) excitation cross section in a static gas experiment in which a spectrometer is used to detect photons perpendicular to the electron beam. They make no correction for the effects of polarization of the radiation. Their published excitation cross sections can be converted to photoemission cross section using cascade corrections from de Jongh (1971).

Van Eck and de Jongh (1970) measure the excitation cross sections for all three transitions in a static gas experi-

Table 1. Comparison of helium photoemission cross sections in 10^{-18} cm^2 at 200 eV

Authors	He II 30.4	He I 52.2	He I 53.7	He I 58.4	He II 121.5	He II 164.0	Reported uncertainty
Moustafa Moussa and de Heer (1967)	0.38				0.027	0.080	30%[c]
Moustafa Moussa et al. (1969)[a]				7.58			–
van Eck and de Jongh (1970)[a]		0.85	2.28	9.42			–
de Jongh and van Eck (1971b)[a]		0.88	2.16	9.12			–
Donaldson et al. (1972)[a]		0.87	2.39	8.66			38, 10, 8%
Westerveld et al. (1979)[a]			2.11	8.78			5%
Bloemen et al. (1981)	0.56						25%
Forand et al. (1985)	0.62						28%
Shemansky et al. (1985b)[b]		0.79	1.89	7.44	0.020	0.040	22%

[a] Cascade corrections added and multiplied by branching ratios (see text).
[b] Data renormalized by 7.3/8.18 (see text).
[c] Uncertainty reported for 121.5 nm only.

ment. By combining two series of measurements of photons detected perpendicular to the electron beam, with the entrance slit of the spectrometer either parallel or perpendicular to the electron beam, they obtain a polarization-free excitation cross section. The measurements are repeated by de Jongh and van Eck (1971b) by placing the spectrometer at 54.7°, with the spectrometer entrance slit at 45° with respect to the electron beam. This setup eliminates polarization effects as described by Clout and Heddle (1969), see Sec. 2.2. The published excitation cross sections can be converted to photoemission cross sections using cascade corrections from de Jongh (1971).

Donaldson *et al.* (1972) measure the excitation cross sections for all three transitions in a crossed-beams experiment. They eliminate polarization effects by using the method of Clout and Heddle (1969). Cascade corrections are listed in the article.

Westerveld *et al.* (1979) measure the He I(58.4 nm) and He I(53.7 nm) excitation cross sections with an experimental setup similar to the one used by de Jongh and van Eck (1971b). Cascade corrections are listed in the article.

Shemansky *et al.* (1985b) use a different method to measure the He I(58.4 nm), He I(53.7 nm), and He I(52.2 nm) photoemission cross sections. They use a crossed-beams experiment with a spectrometer placed at 54.7° with respect to the electron beam, and correct their measurements for instrumental polarization. Their cross sections are based on a relative calibration of their spectrometer-detector system using the double-monochromator technique and the molecular branching-ratio technique for H_2 Rydberg band systems, and a normalization on the H_2(H I Ly-α) dissociative cross section measured by Shemansky *et al.* (1985a). The H_2(H I Ly-α) cross section is normalized on the Bethe approximation for H_2 Werner and Lyman band transitions.

In addition to measurements of photoemission cross sections, polarization measurements in the EUV have been performed by Mumma *et al.* (1974) and Westerveld *et al.* (1979). Mumma *et al.* (1974) extract the polarization of the unresolved $n^1P \rightarrow 1^1S$ transitions (58.4–50.6 nm) from a measurement of the angular intensity dependence of the emitted light. Westerveld *et al.* (1979) determine the polarization of the 58.4 and 53.7 nm transitions from intensity measurements at 90° and 54.7°. The graphs in their article show that the polarization decreases from 47% at 50 eV to less than 2% at 400 eV. Information on polarization has also been yielded by a number of electron-photon coincidence experiments (e.g. Standage 1977).

Table 1 provides a comparison of photoemission cross sections at a collision energy of 200 eV. Optical excitation functions for the 58.4 and 53.7 nm transitions, corrected for cascade, are found in Westerveld *et al.* (1979). We note good agreement regarding the cross sections published by de Jongh and van Eck, (1971b), Donaldson *et al.* (1972), Westerveld *et al.* (1979), and Shemansky *et al.* (1985). Among these authors Westerveld *et al.* (1979) claim the lowest experimental uncertainty of 5%. The 53.7 nm data from Donaldson *et al.* (1972) seem somewhat on the high side. We consider the data of van Eck and de Jongh (1970) less accurate than the data of de Jongh and van Eck (1971b) because of the complicated method they use for the correction of polarization in their earlier measurement. The He I(58.4 nm) cross sections of Moustafa Moussa *et al.* (1969) apparently are too low above 80 eV.

Comparing these EUV measurements with theory or with measurements for transitions branching in the visible is outside the scope of the present review, but a detailed discussion is given by Westerveld *et al.* (1979). We note here, however, that numerical integration of generalized oscillator strengths obtained from experimental differential electron-scattering experiments of the $1^1S \rightarrow 2^1P$ excitation (Dillon and Lassettre 1975) shows excellent agreement with the definitive Born calculations by Bell *et al.* (1969) for electron energies above 300 eV. (The results of Dillon and Lassettre (1975) and Bell *et al.* (1969) at 300 eV are 7.17×10^{-18} cm^2

and 7.40×10^{-18} cm^2, respectively.) Above 350 eV the optical excitation functions measured in the EUV (Westerveld *et al.* 1979) agree on a relative scale to within a few percent with the Bethe and Born approximations (Kim and Inokuti 1968, Bell *et al.* 1969). Cascade contributions are of the order of a few percent and can be accurately estimated. Thus the He I(58.4 nm) and He I(53.7 nm) photoemission cross sections should be considered the most accurately known photoemission cross sections in the EUV.

2. The He II(25.6 nm), He II(30.4 nm), He II(121.5 nm), and He II(164.0 nm) photoemission cross sections. Moustafa Mousssa and de Heer (1967) measure cross sections for all four transitions in a static gas experiment by using a spectrometer to detect photons emitted perpendicular to the electron beam. They normalize the spectral response of their detector at two wavelengths by using the H_2(H I Ly-α) dissociative cross section (CUV cross section, see Sec. 4.3) from Fite and Brackmann (1958), and the atomic branching-ratio technique for the 53.7 and 501.6 nm transitions for the He 3^1P level produced in He^+ + Ne collisions (the 501.6 nm visible radiation was detected using a calibrated Leiss spectrometer). They estimate the spectral response at other wavelengths by extrapolation.

Bloemen *et al.* (1981) measure the He II(30.4 nm) cross section in a static gas experiment. They detect photons with a neon-filled ionization chamber and a photomultiplier provided with a scintillator, with aluminum films in front of the ionization chamber and the photomultiplier, mounted perpendicular to the electron beam. They obtain the photoemission cross section from the proportionality of the ion current to the number of photons entering the ionization chamber per second, by using literature values for the photoabsorption cross sections.

Forand *et al.* (1985) measure the He II(30.4 nm) cross section by using a combination of two detector systems, both perpendicular to the plane containing the electron beam and the helium beam. They detect radiation from unresolved He I and He II EUV transitions by using a channel electron multiplier with an EUV filter in front. The other system is a spectrometer with a photomultiplier. The He II(30.4 nm) photoemission cross section is obtained from the transmission properties of the EUV filter, the spectral response of the channel electron multiplier, and cross sections for the He I transitions at 58.3, 53.7, and 52.2 nm averaged from van Eck and de Jongh (1970), Donaldson *et al.* (1972), and Westerveld *et al.* (1979).

Shemansky *et al.* (1985b) also measure the He II(121.5) and He II(164.0 nm) cross sections.

Table 1 lists photoemission cross sections measured by the various groups. The He II(25.6 nm) and He II(30.4 nm) cross sections measured by Moustafa Moussa and de Heer (1967) are probably inaccurate as they extrapolated the relative spectral response of their spectrometer. We note good agreement within the reported uncertainties between the cross sections of Bloemen *et al.* (1981) and Forand *et al.* (1985). The He II(30.4 nm) optical excitation functions of Forand *et al.* (1985) and Moustafa Moussa and de Heer (1967) are in satisfactory agreement on a relative scale. The He II(121.5 nm) and He II(164.0 nm) cross sections of Moustafa Moussa and de Heer (1967) and Shemansky *et al.* (1985b) are in disagreement (after renormalization of the He II(121.5 nm) cross section to the same value for the H_2(H I Ly-α) cross section). Moustafa Moussa and de Heer (1967) use a rather inaccurate method to determine the spectral response, so the values given by Shemansky *et al.* (1985b) should be more reliable. The 164.0 nm optical excitation functions of both groups are in reasonable agreement on a relative scale.

4.2 Neon, Argon, Krypton and Xenon

The heavier noble gases provide important ion lines of the type $nsnp^6 \rightarrow ns^2np^5$ and resonance lines of the type $np^5(n+1)s \rightarrow np^6$, where $n = 2$, 3, 4, and 5 for Ne, Ar, Kr and Xe. Wavelengths of the ion lines are Ne II(46.1, 46.2 nm), Ar II(92.0, 93.2 nm), Kr II(91.7, 96.5 nm), and Xe II(110.0, 124.5 nm). Wavelengths of the resonance lines are Ne I(73.6, 74.4 nm), Ar I(104.8, 106.7 nm), Kr I(116.5, 123.6 nm), and Xe I(129.6, 147.0 nm).

Hertz (1969) measures the Ne I(73.6, 74.4 nm) optical excitation functions. He normalizes on the He I(52.2, 53.7, 58.4 nm) cross sections from Jobe and St. John (1967) and Gabriel and Heddle (1960), and determines the relative spectral response of the spectrometer-detector system (see Sroka 1968) using literature data for the grating reflection and the quantum efficiency of the multiplier cathode.

De Jongh (1971) measures optical excitation functions of the Ne I(73.6 nm), Ar I(104.8 nm), and Kr I(116.5 nm) resonance transitions, normalized on the Bethe approximation. He uses a static gas arrangement with the spectrometer placed such that polarization effects are eliminated (Clout and Heddle 1969).

Lloyd *et al.* (1972) measure an optical excitation function of the Ar I(104.8 + 106.7 nm) transitions (the lines are not resolved), normalized to the Born approximation at 160 eV. The radiation is observed at 90° to the electron beam by using a channel electron multiplier with a LiF window in front.

Luyken *et al.* (1972) report cross sections for the noble gas ion lines: Ne II(46.1 + 46.2 nm) Ar II(92.0 + 93.2 nm), Kr II(91.7 + 96.5 nm) and Xe II(110.0 + 124.5 nm). They measure the intensity of the strongest component of each doublet as a function of the electron energy. Only in a limited energy range do they check that the other component has the same energy dependence. The cross sections are normalized on measurements at 300 eV of van Raan *et al.* (1971) and van Raan (1973). (Luyken *et al.* (1972) list their cross sections in a table; note that the graph in their Fig. 7 is not correct below 120 eV).

Van Raan *et al.* (1971) and van Raan (1973) measure cross sections for the Ne II(46.1, 46.2 nm), Ar II(92.0, 93.2 nm), Kr II(91.7, 96.5 nm) and Xe II(110.0 nm) transitions in a static gas experiment using a spectrometer and a photomultiplier. They calibrate their spectrometer absolutely at a number of discrete wavelengths by measuring the intensities

of the He I(52.2, 53.7, and 58.4 nm), Ne I(73.5 nm), Ar I(104.8 nm), and Kr I(116.4 nm) resonance lines normalized on the Bethe approximation with measured oscillator strengths from de Jongh and van Eck (1971a). The efficiency at other wavelengths is found through interpolation and extrapolation.

McConkey and Donaldson (1973) measure the Ar I(104.8 nm) and Ar I(106.7 nm) photoemission cross sections, normalized on the Bethe approximation for Ar I(104.8 nm) with a measured oscillator strength from de Jongh and van Eck (1971a). Tan *et al.* (1974) measure the Ne I(73.6 nm) photoemission cross section normalized on an average of experimental values for the oscillator strengths for this transition, and the Ar II(92.0 and 93.2 nm) cross sections, normalized at 300 eV on the cross sections of van Raan (1973). Tan and McConkey (1974) report photoemission cross sections for 48 Ar II transitions between 48.7 nm and 76.3 nm, based on an interpolation between absolute calibration points provided by cross sections for the He I(52.2, 53.7, 58.4 nm) and Ne(73.6 nm) transitions. All measurements are performed in a crossed beams arrangement, and the spectrometer is placed so that polarization effects are eliminated (Clout and Heddle 1969).

Dassen *et al.* (1977) measure the polarization of the Ar II(104.8 + 106.7 nm) resonance lines, using a crossed beams arrangement and a reflection polarizer followed by a LiF window and a channel electron multiplier. This measurement shows a maximum polarization of 13% at 45 eV, decreasing to − 5% at 300 eV. The measurement is weighted in favor of the 106.7 nm transition because of the cutoff of the LiF window. Accurate measurements of the polarization of some noble gas resonance transitions are in progress (Plessis *et al.* 1988).

Zapesochnyi *et al.* (1974) report optical excitation functions for the Ne II(46.1 + 46.2 nm), Ar II(92.0 + 93.2 nm), Kr II(91.7 + 96.5 nm), and Xe II(110.0 + 124.5 nm) transitions. They normalize on the first Born approximation, resulting in Ne II and Ar II cross sections that are almost ten times higher than other measurements. Papp *et al.* (1977) measure optical excitation functions for the Ne III(37.9, 49.0 nm), Ar III(76.9, 88.7 nm), Kr III(78.6, 83.8 nm), and Xe III(90.2, 101.8 nm) transitions. Their spectrometer is calibrated against the data of van Raan (1973).

Pavlov and Yakhontova (1975) measure the Kr I(116.5, 123.6 nm), and Xe I(129.6, 147.0 nm) cross sections. Their measurements are corrected for the absorption of resonance radiation, and are normalized based on an interpolation between calibration points provided by the He II(164.0 nm) cross section from Moustafa Moussa and de Heer (1967) and the H_2(H I Ly-α) cross section from Mumma and Zipf (1971a).

Mentall and Morgan (1976) measure cross sections for 13 Ar I, II transitions between 71.8 nm and 106.7 nm based on a relative calibration using the double-monochromator technique and a normalization on the N_2(N I 120.0 nm) cross section from Mumma and Zipf (1971b). Their measurements are taken in a static gas configuration with the spectrometer at 54.7° to the electron beam. They estimate that the effects of instrumental polarization are about 5%.

Dijkkamp and de Heer (1981) reanalyze the Ne II(46.1 + 46.2 nm) cross section from Luyken *et al.* (1972). Normalization on the Bethe approximation instead of van Raan's (1973) result leads to a cross section that is 3.7 times smaller.

Schartner and co-workers report photoemission cross sections for Ne II(46.1 + 46.2 nm) Ne II(49.0 nm), Ar II(54.3 nm) Ar II(54.7 nm), and Ar II(76.9 nm) (Beyer *et al.* 1979, Eckhardt and Schartner 1983, and Schartner *et al.* 1987). The Ne II cross sections are based on a determination of the absolute efficiency of their spectrometer at the discrete transitions He I(52.2, 53.7 and 58.4 nm) and Ne I(73.6 nm) by using the Bethe formula with experimental and theoretical values for the optical oscillator strengths from de Jongh and van Eck (1971a) and Kim and Inokuti (1968). Polarization effects are eliminated with the method of Clout and Heddle (1969). The Ar II cross sections are based on a relative calibration using synchrotron radiation and a normalization on the Ar II(92.0, 93.2 nm) cross sections from McPherson (1984) and the Ar II(72.3 nm) cross section from Tan *et al.* (1974).

McPherson (1984) uses synchrotron light for the absolute calibration of his spectrometer-detector system and measures the Ar II(92.0, 93.2 nm) photoemission cross sections. The method used is described in detail by McPherson *et al.* (1986) and Kendrick *et al.* (1987).

Forand *et al.* (1988) measure the Ar II(92.0, 93.2 nm) and Ar I(104.8, 106.7 nm) cross sections in a crossed beams arrangement, with a spectrometer perpendicular to both beams. They determine the relative spectral response of their spectrometer by using the relative intensities of the H_2 Rydberg band systems, and the relative intensities of the Lyman series of atomic hydrogen. The H_2(H I Ly-α) cross section from Woolsey *et al.* (1986) is used for normalization.

Li *et al.* (1988b) measure the Ar II(90.2, 93.2 nm) cross sections in a crossed beams arrangement, with the spectrometer placed such that the polarization effects are eliminated (Clout and Heddle 1969). They determine the relative spectral response of their spectrometer using relative intensities of the H_2 Werner and Lyman bands and normalize on the excitation cross section for the Ar I(106.7 nm) transition at 500 eV, measured by Li *et al.* (1988a) using electron energy-loss spectroscopy. Also, Suzuki *et al.* (1983) report measurements of the Kr III(90.6 nm), Xe III(90.2 nm), and Xe III(108.9 nm) cross sections, based on a determination of the relative spectral response using the relative intensities of the H I Lyman series in $e + NH_3$ scattering, and a normalization on excitation cross sections for some Xe I resonance transitions from Williams *et al.* (1975).

Several cross sections have been measured by more than one group and are therefore suitable for comparison, see Table 2. We only renormalize the cross sections of Mentall and Morgan (1976) and Forand *et al.* (1988). Mentall and Morgan (1976) normalize on the N_2(N I 120.0 nm) cross section of Mumma and Zipf (1971b), which is normalized on the H_2(H I Ly-α) cross section of Mumma and Zipf (1971a), suggesting a renormalization of 7.3/12. Forand *et al.* (1988) normalize on the H_2(H I Ly-α) cross section

Table 2. Comparison of neon and argon photoemission cross sections in 10^{-18} cm^2 at 200 eV

Authors	Ne II 46.1	Ne II 46.2	Ar II 92.0	Ar II 93.2	Ar I 104.8	Ar I 106.7	Reported uncertainty
de Jongh (1971)					14.		–
Luyken et al. (1972)	[8.29]		[6.15]				50, 25%
Lloyd et al. (1972) [a]					[23.]		–
van Raan (1973) [b]	5.21	2.61	3.19	1.80			20-25%
McConkey and Donaldson (1973)					16.0	6.34	–
Tan et al. (1974)			3.82	1.96			–
Mentall and Morgan (1976) [c]			2.15	1.22	14.6	6.0	20%
Dijkkamp and de Heer (1981)	[2.26]						26%
Eckhardt and Schartner (1983)	[3.05]						35%
McPherson (1984)			5.50	2.75			8%
Forand et al. (1988) [d]			3.89	2.01	13.1	5.4	15-19%
Li et al. (1988b)			2.89	1.50			21%

[a] 180 eV data.
[b] 300 eV data. The 200 eV cross sections are 5.52 and 2.77 for Ne II(46.1, 46.2 nm), and 3.76 and 2.27 for Ar II(92.0, 93.2 nm), based on the NeII optical excitation function from Luyken et al. (1972), and the Ar II cross sections from van Eck, private communication to Forand et al. (1988).
[c] Data renormalized by 7.3/12 (see text).
[d] Data renormalized by 7.3/7.13 (see text).

from Woolsey *et al.* (1986), leading to a small renormalization of 7.3/7.13. A comparison leads to the following comments and conclusions:

1. The Ne II(46.1 + 46.2 nm) photoemission cross section. Dijkkamp and de Heer (1981) note that their values are in agreement with the values of Eckhardt and Schartner (1983) within the reported uncertainties. The cross sections from van Raan (1973) and Luyken *et al.* (1972) are much higher. According to Dijkkamp and de Heer (1981) extrapolation of van Raan's (1973) calibration down to 46 nm leads to a significant error.

2. The Ar II(90.2, 93.2 nm) photoemission cross sections. The three most recent measurements by Forand *et al.*, (1988), Li *et al.* (1988b), and McPherson (1984) are in disagreement. The cross sections of Li *et al.* (1988b) are probably too small, because they normalize on the excitation cross section for the Ar I(106.7 nm) transition, without converting this cross section to a photoemission cross section by adding the cascade contribution. Correction of the measurements of Li *et al.* (1988b) for a 40% cascade contribution to the Ar I(106.7 nm) transition (as estimated above 200 eV by Forand *et al.* 1988) would result in agreement between the Ar II(90.2, 93.2 nm) cross sections of Li *et al.* (1988b) and Forand *et al.* (1988)Earlier measurements by van Raan (1973), and Luyken *et al.* (1972) and Tan *et al.* (1974) who normalize on van Raan's (1973) measurements, may suffer from inaccuracies due to van Raan's (1973) interpolation between absolute calibration at 73.6 and 104.8 nm. The (renormalized) results of Mentall and Morgan (1976) are significantly lower than any other measurements. Optical excitation functions for the 92.0 nm transition are shown in Fig. 2. Above 120 eV all measurements show the same trend, but the curves are clearly in disagreement between 40 and 120 eV. The curve of Mentall and Morgan (1976) shows a structure around 90 eV that is absent in the other measurements. The reason for this discrepancy is not clear. Possibly Mentall and Morgan (1976) have a difficulty with the measurement of the Faraday cup current. A similar discrepancy is observed near 100 eV in the O_2(O I 83.4 nm) excitation function from Morgan and Mentall (1983) (see Sec. 4.4). The data of Luyken *et al.* (1972) is obtained from their Table II and multiplied by 1.97/2.97 (Luyken (1972) calculates the 92.0 and 93.2 nm transition probabilities and finds a value of 1.97 for the ratio).

3. The Ar I(104.8, 106.7 nm) photoemission cross sections. Within error bars all measurements of the Ar I(104.8, 106.7 nm) cross sections in Table 2 are in agreement. The measurements of de Jongh (1971) and McConkey and Donaldson (1973) are normalized on the Bethe approximation, a procedure that is only correct when cascade is negligible or is primarily of an optically forbidden character (van Raan (1973); see Sec. 3.2). Forand *et al.* (1988) argue that the cascade contribution to the 104.8 nm transition is small or negligible, but estimate a 40% cascade contribution to the 106.7 nm transition. Optical excitation functions, see Fig. 2, show agreement above 100 eV regarding the shape of the curves, but there is some spread in the maximum of the 104.8 nm curve for several authors.

4. The Ar II(54.3 + 54.7 nm), Ar II(72.3 nm) photoemission cross sections. Graphs of these cross sections are shown by Tan and McConkey (1974) and Tan *et al.* (1974). The Ar II(54.3 + 54.7 nm) cross section from Schartner *et*

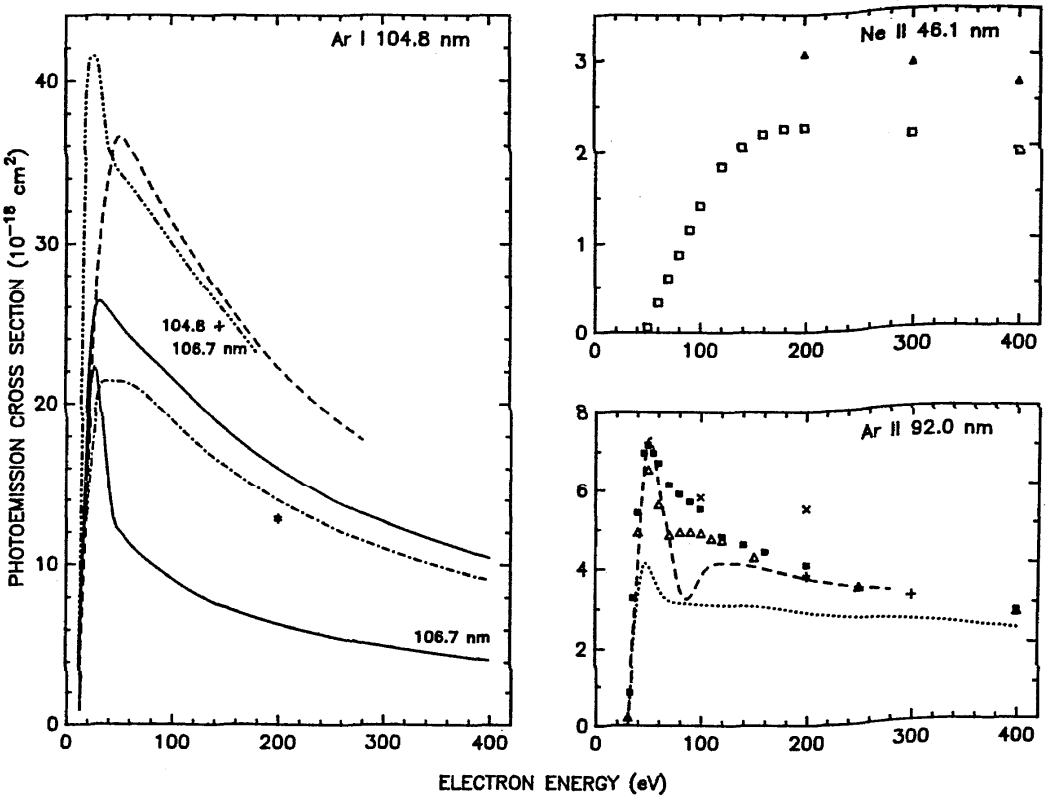

FIG. 2. Comparison of excitation functions for neon and argon transitions. All photoemission cross sections are in 10^{-18} cm^2. Measurements shown are:- de Jongh (1971), ■ Luyken *et al.* (1972), ···Lloyd *et al.* (1972), + van Raan (1973),— McConkey and Donaldson (1973), Δ Tan *et al.* (1974), ---Mental and Morgan (1976), □ Dijkkamp and de Heer (1981), ▲ Eckhardt and Schartner (1983), × McPherson (1984), * Forand *et al.* (1988), and ····Li *et al.* (1988b). In addition to the Ar I(104.8 nm) optical excitation functions, Ar I(106.7 nm) and Ar I(104.8 + 106.7 nm) curves are shown as indicated.

al. (1987) at 500 eV is within error bars in agreement with these measurements. The renormalized Ar II(72.3 nm) cross section at 200 eV from Mentall and Morgan (1976) is significantly lower than the value from Tan *et al.* (1974).

5. Other comparisons. The Ne III(49.0 nm) cross sections at 200 eV from Papp *et al.* (1977) and Schartner *et al.* (1987) are in agreement within error bars. The Kr I(116.5 nm) cross sections at 150 eV from de Jongh (1971) and Pavlov and Yakhontova (1975) are in agreement within error bars. The Xe III(90.2 nm) optical excitation functions from Papp *et al.* (1977) and Suzuki *et al.* (1983) are in agreement on a relative scale, but the photoemission cross sections disagree. Somewhat outside the scope of this review are the Ne I(73.6, 74.4 nm) cross sections, measured by Phillips *et al.* (1985) by detecting laser-induced fluorescence in the visible. They normalize on the Born approximation and determine the cascade condition by direct measurement, and find a Ne I(73.6 nm) photoemission cross section that is 50% higher than the result of Tan *et al.* (1974). The Ne I(73.6 nm) cross section from Hertz (1969) is in disagreement with these results, but Hertz (1969) uses an unreliable method to determine the relative spectral response.

4.3 Hydrogen

The H_2(H I Ly-α) cross section is the most commonly used for the normalization of other photoemission cross sections in the EUV. Table 3 summarizes the different measurements that have been performed so far.

In addition to the atomic cross section, H I(Ly-α), several authors make a distinction between the dissociative cross section, H_2(H I Ly-α), and the so called countable ultraviolet (CUV) cross section, which was introduced by Fite and Brackmann (1958). The CUV cross section is based on detection of ultraviolet radiation by using a LiF-O_2 gaseous filter, consisting of a small cell with two LiF windows filled with oxygen gas, and an iodine-vapor-filled Geiger–Müller counter. This method allows detection of photons only in a small wavelength region, as LiF does not transmit below 105 nm and the counter does not detect photons at wavelengths longer than 133 nm. Within this wavelength region the oxygen filter transmits radiation only within seven narrow windows (Watanabe *et al.* 1953), one of which occurs at about Ly-α. Later measurements by Lee (1955), Ogawa (1968), and Gaily (1969) map the window around Ly-α in much

Table 3. Comparison of hydrogen Lyman-alpha photoemission cross sections in 10^{-18} cm^2 for 100 eV electrons on atomic and molecular hydrogen

Authors	Cross section[a]		Reported uncertainty	Normalization
Fite and Brackmann (1958)	σ_a	62.	12%	Born approximation
	σ_{cuv}	14.0	30%	σ_a at 100 eV
Dunn et al. (1962)	σ_{cuv}	14.0		Fite and Brackmann (1958)
Long et al. (1968)	σ_a	60.0	3%	Born approximation
Vroom and de Heer (1969b)	σ_d	13.1	32%	Fite and Brackmann (1958) at 250 eV
McGowan et al. (1969)	σ_d	11.		$\sigma_d/\sigma_{cuv} = 0.75$; Fite and Brackmann (1958)
de Heer and Carrière (1971)	σ_d	10.3	20%	Bethe approximation for Werner bands
Mumma and Zipf (1971a)	σ_d	12.0	11%	$(\sigma_d/\sigma_{cuv})\,\sigma_a/(\sigma_d/\sigma_{cuv})$; Long et al. (1968)
Kauppila et al. (1971)	σ_{cuv}	14.8	3.4%	$\sigma_d/\sigma_{cuv} = 4.05 \pm 0.07$; Long et al. (1968)
Carrière and de Heer (1972)	σ_d	11.0		$\sigma_{cuv}/\sigma_d = 1.26$; Fite and Brackmann (1958)
McConkey and Donaldson (1972)	σ_d	12.1		Mumma and Zipf (1971a)
Möhlmann et al. (1978)	σ_d	12.0		Mumma and Zipf (1971a)
Zipf (1984)	σ_d	14.4		Born approximation underestimates σ_a?
Van Zyl et al. (1985)	σ_d	7.22	18.8%	Ly-α radiation from H+Ne collisions
Ligtenberg et al. (1985)	σ_d	6.57	8.0%	synchrotron radiation
Shemansky et al. (1985a)	σ_d	8.18	14.7%	Bethe approximation for Werner bands
Woolsey et al. (1986)	σ_d	7.13	8.3%	Long et al. (1968)

[a] σ_a is the H I(Ly-α) photoemission cross section for excitation of atomic hydrogen, σ_d is the H_2(H I Ly-α) photoemission cross section for dissociative excitation of hydrogen molecules, and σ_{cuv} is the countable ultraviolet cross section as discussed in Paragraph 4.3.

more detail. Thus, in dissociative excitation of hydrogen molecules by electrons, part of the radiation detected by using an oxygen filter is radiation from molecular transitions. Unfortunately, the definition of the CUV cross section is not rigid. The spectral intensity distribution of light traversing through a gas depends strongly on the gas density and the path length through the gas. Since some of the transmission windows of oxygen are very narrow (e.g., ~0.2 nm around Ly-α), the ratio of molecular radiation versus atomic radiation for dissociative excitation of hydrogen is subject to change depending on the thickness of the filter and the gas pressure. It must also be noted that any MgF_2 components in the optical system will affect this ratio due to the cutoff of MgF_2 around 114 nm.

Fite and Brackmann (1958) measure the CUV cross section by detection of ultraviolet radiation with a LiF-O_2 filter and an iodine-filled Geiger–Müller counter. Their cross section is measured relative to the H I(Ly-α) cross section for electron impact on atomic hydrogen (see Sec. 3.4), which in turn is normalized on the Born approximation (Massey 1956) from 200 to 700 eV.

Dunn *et al.* (1962) measure the CUV cross section from threshold to 400 eV, normalized on the cross section of Fite and Brackmann (1958).

Long *et al.* (1968) measure the H I(Ly-α) cross section for electrons on atomic hydrogen in a crossed beams experiment in which photons emitted at 90° to the electron beam are detected with an ionization chamber. They normalize on the Born approximation taking cascade into account, but they apply no correction for the polarization of the emitted radiation. Cox and Smith (1972) measure an optical excitation function of the CUV cross section on a relative scale.

Vroom and de Heer (1969b) (see also de Heer *et al.* 1967) measure the H_2(H I Ly-α) dissociative cross section, by detecting photons at 90° to the electron beam with a spectrometer and a photomultiplier. They normalize their cross section on the CUV cross section of Fite and Brackmann (1958) at 250 eV.

McGowan *et al.* (1969) measure the fraction of the radiation of molecular origin passing through the LiF-O_2 filter to be between 25% and 30% (numbers are given by McGowan and Williams 1969). Using this number they correct their CUV cross section measurement, which is normalized on the CUV cross section of Fite and Brackmann (1958).

De Heer and Carrière (1971) measure the H_2(H I Ly-α) cross section by detecting light perpendicular to the electron beam with a spectrometer. The cross section is measured relative to photoemission cross sections for the H_2 Werner bands, which are brought on an absolute scale by using the Bethe and Born approximations. Carrière and de Heer (1972) measure the contribution of radiation of molecular origin transmitted through a LiF-O_2 filter and use this number to obtain the H_2(H I Ly-α) cross section based on the CUV cross section of Fite and Brackmann (1958) and Dunn *et al.* (1962).

Kauppila *et al.* (1971) measure a ratio of 4.05 ± 0.07

between the CUV cross section and the H I(Ly-α) photoemission cross section for 100 eV electrons on atomic hydrogen. Using this number and the H I(Ly-α) cross section from Long *et al.* (1968) they calculate the CUV cross section at 100 eV.

Mumma and Zipf (1971a) use the ratio between the CUV and the atomic cross section from Kauppila *et al.* (1971), the ratio between the dissociative and the CUV cross section from McGowan and Williams (1969) and Carrière and de Heer (1972), and the atomic cross section from Long *et al.* (1968) to find the H_2(H I Ly-α) dissociative cross section. They use this number to absolutely calibrate their H_2(H I Ly-α) optical excitation function.

McConkey and Donaldson (1972) make a polarization free measurement (method of Clout and Heddle 1969), corrected for the amount of molecular radiation observed by the spectrometer and normalized at 100 eV on the cross section from Mumma and Zipf (1971a).

Möhlmann *et al.* (1978) measure the CUV cross section using a LiF-O_2 filter at 90° to the electron beam. They use the ratio between the dissociative and the CUV cross section from Carrière and de Heer (1972) to find the H_2(H I Ly-α) dissociative cross section and normalize to Mumma and Zipf (1971a) at 100 eV.

Zipf (1984) suggests that the Born approximation may underestimate the Ly-α cross section for electrons on atomic hydrogen by as much as 20%. Based on this suggestion the H_2(H I Ly-α) dissociative cross section from Mumma and Zipf (1971a) should be scaled upward 20%.

Ligtenberg *et al.* (1985) report a preliminary measurement of the H_2(H I Ly-α) cross section, that takes polarization fully into account. They absolutely calibrate their spectrometer-detector system by using synchrotron radiation. The cross section measured by Ligtenberg *et al.* (1985) is not yet definite; more accurate measurements are in progress.

Shemansky *et al.* (1985a) measure the H_2(H I Ly-α) cross section relative to the total cross section for excitation of the H_2 Lyman and Werner band systems. These cross sections are brought on an absolute scale using the Bethe approximation.

Van Zyl *et al.* (1985) use a combination of an interference filter, a LiF-O_2 gaseous filter and a solar blind photomultiplier with a MgF_2 window to detect Ly-α photons. They calibrate their detector in the following way. A beam of hydrogen atoms is directed into a collision area filled with Ne gas. Ly-α radiation from H + Ne collisions is measured as a function of the detector position in the collision area, and fitted to a model for the population of H($2p$) by direct excitation and cascade. The cascade contributions, predominantly from long-lived *ns* states, are deduced from the absolute measurements of the Balmer line photoemission cross sections for the reaction. By filling the collision area with hydrogen gas and directing an electron beam through the gas, the H_2(H I Ly-α) cross section is measured and corrected for the H_2 molecular emissions observed by the Ly-α detector.

Woolsey *et al.* (1986) measure the H_2(H I Ly-α) cross section relative to the atomic cross section by using a partly dissociated beam of H_2 molecules (see Sec. 3.4) and normalizing to the atomic cross section of Long *et al.* (1968).

We find good agreement within the reported uncertainties for the four most recent measurements. This agreement is remarkable since entirely different methods are used in the measurements. Thus, the H_2(H I Ly-α) cross section should be regarded as reliable. The unweighted average of the four most recent measurements is 7.3×10^{-18} cm^2.

Most of the measurements before 1980 are normalized to either Fite and Brackmann's (1958) result or to Mumma and Zipf's (1971) result. Only four independent measurements exist. Fite and Brackmann (1958) and Kauppila *et al.* (1971) measure the ratio between the CUV cross section and the atomic cross section and use the atomic cross section (Born approximation and the measurement of Long *et al.* (1968), respectively) to extract the CUV cross section. The two ratios are in agreement but Kauppila *et al.* (1971) claim a smaller uncertainty. De Heer and Carrière (1971) and Mumma and Zipf (1971a) determine the dissociative cross section. De Heer and Carrière (1971) normalize their cross section on the Bethe approximation for H_2 Werner bands and Mumma and Zipf (1971a) normalize their cross section on the atomic cross section of Long *et al.* (1968). The spectral response of de Heer and Carrière (1971) shows a pronounced structure near Ly-α that is attributed by Stone and Zipf (1972b) to the insufficient spectral resolution in the experiment of de Heer and Carrière. Therefore, their H_2(H I Ly-α) cross section should be considered unreliable.

The discrepancy between the H_2(H I Ly-α) cross section determined by Mumma and Zipf (1971a) and the four most recently measured cross sections is most likely due to an error in the ratio between the dissociative and the CUV cross section, that Mumma and Zipf used in their determination. McGowan *et al.* (1969) determine this ratio to be between 0.70 and 0.75 (numbers are given by McGowan and Williams 1969), but they do not give any information concerning the method they use. By placing a spectrometer behind a LiF-O_2 filter, Carrière and de Heer (1972) measure this ratio to be $0.79 \pm 10\%$. Their number is likely inaccurate, because they determine the relative spectral response with insufficient resolution. Shemansky *et al.* (1985a) attempt to determine the ratio between the dissociative and CUV cross sections based on a theoretical model for the H_2 Werner band emissions and the measurements of Ogawa (1968) for the O_2 transmission near Ly-α, and find a ratio of 0.66. Combining the average of the four most recent measurements of the dissociative cross section and the CUV cross section of Kauppila *et al.* (1971) suggests that this ratio might be close to 0.50.

Optical excitation functions or tabulated cross sections are found in most of the papers published before 1980. We note good agreement on a relative scale. (The measurements of Vroom and de Heer (1969b) below 80 eV are too high.)

Fite and Brackmann (1958) measure the polarization of Ly-α radiation due to electron collisions with hydrogen atoms by combining intensity measurements at 45° and 90° with respect to the electron beam. Ott *et al.* (1967, 1970) repeat this measurement by using a reflection polarizer in front of a LiF-O_2 filter and an iodine filled Geiger counter.

Ott *et al.* (1970) also measure the polarization of Ly-α radiation due to dissociative excitation of hydrogen molecules. This measurement is also performed by Malcolm *et al.* (1979) who use a reflection polarizer mounted behind the exit slit of their spectrometer. Both measurements are in good agreement. Arai *et al.* (1985) obtain the polarization from a measurement of the angular distribution of the emitted Ly-α radiation. Their results show a large discrepancy with the results of Ott *et al.* (1970) and Malcolm *et al.* (1979). The reason for this discrepancy is not clear.

The following cross sections are also reported in the literature. Ajello *et al.* (1984) measure the H_2(H I Ly-β) cross section. Vroom and de Heer (1969b), Möhlmann *et al.* (1978), and Becker and McConkey (1984) measure the D_2(D I Ly-α) cross section. Möhlmann *et al.* (1978) also measure the HD(H I, D I Ly-α) cross section. Becker and McConkey (1984) use a cross beams experiment with a spectrometer-detector system perpendicular to both beams. Their cross section is normalized at 100 eV to the H_2(H I-Ly-α) cross section of Mumma and Zipf (1971a). The D_2(D I Ly-α) cross sections measured by these groups are in agreement. Renormalization to 7.3×10^{-18} cm^2 for the H_2(H I Ly-α) cross section suggests that the D_2(D I Ly-α) cross section should be about 6.1×10^{-18} cm^2.

4.4 Oxygen

Radiation of molecular oxygen in the EUV proceeds through dissociative processes, because oxygen does not display molecular emission features between 40 and 185 nm. The region 40–85 nm shows main O II features, and the region 85–140 nm shows mainly O I features.

The first reported measurements of photoemission cross sections were made by Sroka (1967, 1968) for four transitions between 70 and 100 nm. Sroka (1968) determines the relative spectral response of his spectrometer-detector system based on literature data for the grating reflection and the quantum efficiency of the tungsten cathode of the multiplier, and normalizes on the He I(58.4 nm) cross section. Considering the large discrepancy between his cross sections and more recently measured cross sections this is apparently an inaccurate method.

Then followed some determinations of the O_2(O I 130.4 nm) photoemission cross section by Lawrence (1970), Mumma and Zipf (1971a), Ajello (1971a), and Aarts and de Heer (1971b). By a cascade analysis of the 130.4 nm time-decay curve (see Sec. 3.5) Lawrence (1970) measures the O_2(O I 130.4 nm) cross section relative to the O_2(O I 884.7 nm) cross section, which he measures absolutely by using a blackbody radiator. Mumma and Zipf (1971a) measure the O_2(O I 130.4 nm) cross section based on a relative spectral response by using the molecular branching-ratio technique for N_2LBH bands and a normalization on the H_2(H I Ly-α) cross section reported in the same article. Ajello (1971a) measures the relative spectral response using the molecular branching-ratio technique for N_2 LBH bands and normalizes on the CO(159.7 nm band) photoemission cross section from Aarts and de Heer (1970). Aarts and de Heer (1971b) determine the relative spectral response using the molecular branching-ratio technique for H_2 Werner bands and N_2 LBH bands with a normalization on the CO(159.7 nm band) photoemission cross section from Aarts and de Heer (1970) and photoemission cross sections for some Ar and Kr multiplets below 100 nm from de Jongh and van Eck (1971a).

Efforts in recent years have led to photoemission cross sections for many transitions, measured in three different laboratories.

Zipf and co-workers report cross sections for the O_2(O I 98.9, 102.7, 104.0 nm) transitions (Zipf *et al.* 1979), normalized on the N_2(N I 120.0 nm) cross section from Mumma and Zipf (1971b), and the O_2(O II, O III 83.4 nm) transition (Zipf *et al.* 1985), normalized on the O_2(O I 130.4 nm) cross section from a reanalysis of older data by Zipf (1986). The relative spectral response of their monochromator is determined by using the molecular branching-ratio technique for H_2 Werner bands, and extended below 90 nm by using cross sections for O II and N II multiplets. Zipf (1986) renormalizes the O_2(O I 130.4 nm) cross section from Mumma and Zipf (1971a) to a value of 7.5×10^{-18} cm^2 for the H_2(H I Ly-α) cross section (Risley, private communication to Zipf 1986), and finds a value of 2.16×10^{-18} cm^2 at 100 eV. In addition Zipf (1984) lists a number of cross sections without giving any additional experimental details.

Morgan and Mentall (1983) measure cross sections for eleven transitions between 53.9 and 115.2 nm, based on a relative calibration using the double-monochromator technique, and a normalization on the N_2(N I 120.0 nm) photoemission cross section from Mumma and Zipf (1971b).

Ajello and Franklin (1985) report an extensive list of cross sections for thirty transitions between 42.9 and 130.4 nm. They determine the relative spectral response of their spectrometer-detector system by using both the double-monochromator technique (40–130 nm) and the relative intensities of the H_2 Rydberg band systems (80–130 nm; predominantly Werner and Lyman band systems), and normalize on the H_2(H I Ly-α) cross section from Shemansky *et al.* (1985a).

In order to make a meaningful comparison of the various cross sections we renormalize all cross sections to the same value 7.3×10^{-18} cm^2 for the H_2(H I Ly-α) cross section. Table 4 shows renormalized results for some important oxygen transitions. Note that the cross sections of Zipf *et al.* (1979) and Morgan and Mentall (1981) are normalized on the N_2(N I 120.0 nm) cross section from Mumma and Zipf (1971b), which is normalized on the H_2(H I Ly-α) cross section from Mumma and Zipf (1971a), leading to a renormalization by 7.3/12. A comparison leads to the following comments and conclusions.

1. The O I 130.4 nm transition. The measurement of Lawrence (1970) is in excellent agreement with Ajello and Franklin's (1985) measurement. Lawrence (1970) gives a detailed estimate of the uncertainties involved in his measurement. The shapes of the optical excitation functions as shown in Fig. 3 (no renormalization applied) are in good agreement. The deviation of Ajello's (1971a) curve, not shown in Fig. 3, is due to problems with the efficiency of

Table 4. Comparison of photoemission cross sections for dissociative excitation of oxygen molecules in 10^{-18} cm^2 at 200 eV

Authors	O II 53.9	O II 61.6	O II 71.8	O II 83.4	O I 87.9	O I 98.9	O I 102.7	O I 115.2	O I 130.4	Reported uncertainty	Renormalization
Lawrence (1970)									2.2	14%	–
Mumma and Zipf (1971a)									1.7	17%	7.3/12
Aarts and de Heer (1971b)				1.36					2.76	50, 30%	–
Zipf et al. (1979)						0.91	0.73			–	7.3/12
Morgan end Mentall (1983)	0.43	0.13	0.09	0.78	0.23	0.86	0.64	0.42		13%	7.3/12
Zipf (1984)						1.96	1.46			–	–
Ajello and Franklin (1985)	0.61	0.36	0.35	1.92	0.41	0.89	0.63	0.27	2.11	22%	7.3/8.18
Zipf et al. (1985)				2.09						–	7.3/7.5
Zipf (1986)									2.10	15%	7.3/7.5

their electron-beam collection in the Faraday cup (Ajello and Shemansky 1985). Zipf's (1986) result, obtained by renormalizing the O_2(O I 130.4 nm) cross section of Mumma and Zipf (1971a) to the updated H_2(H I Ly-α) cross section, is also in good agreement; however, we performed a similar calculation and obtained a different result (1.7×10^{-18} cm^2 instead of 2.1×10^{-18} cm^2, see Table 4).

2. The O I transitions between 85 nm and 122 nm. After renormalization we find good agreement between the cross sections of Ajello and Franklin (1985), Morgan and Mentall (1983), and Zipf *et al.* (1979). The cross sections from McLaughlin's thesis (1977, unpublished, quoted by Ajello and Franklin 1985) are also in agreement, but the cross sections given by Zipf (1984) deviate significantly from the cross sections of Ajello and Franklin (1985) and Morgan and Mentall (1983). The shapes of the optical excitation functions for the 98.9 nm and 102.7 nm transitions from Ajello and Franklin (1985) and Zipf *et al.* (1979) are in good agreement as can be seen in Fig. 3. The 98.9 nm optical excitation function of Sroka (1968) is not shown, because it deviates significantly from the other two optical excitation functions. Also not shown are the 87.9 nm optical excitation functions of Sroka (1968) and Morgan and Mentall (1983) which are in serious disagreement.

3. The O II transitions between 40 nm and 85 nm. Unlike the results for the O I transitions, there is a discrepancy between the O II cross sections from Ajello and Franklin (1985) and the (renormalized) cross sections of Morgan and Mentall (1983). Ajello and Franklin (1985) note that the O II features are strongly pressure dependent and suggest that the measurements of Morgan and Mentall (1983) were taken at too high a pressure. The optical excitation functions of the 83.4 nm transition also show a discrepancy: the curve of Morgan and Mentall (1983) has a structure near 100 eV that is absent in the curves of Ajello and Franklin (1985) and Zipf *et al.* (1979) (see Fig. 3). The disagreement between the O_2(O I 83.4 nm) cross section of Aarts and de Heer (1971b) and the cross section of Ajello and Franklin (1985) is likely due to problems with the determination of the relative spectral response by Aarts and de Heer (1971b) as indicated by Stone and Zipf (1972b). The 53.9 nm optical excitation function of Ajello and Franklin (1985) and the 71.7 nm optical excitation function of Sroka (1968) are not shown in Fig. 3.

4.5. Nitrogen

Molecular nitrogen is one of the most important molecular gases for obtaining photoemission cross sections in the EUV. The EUV spectrum exhibits many molecular features, e.g., the LBH band system, interspaced with a number of atomic features. Related to the review of photoemission cross sections presented here are the review and data compilation by Itikawa *et al.* (1986) on cross sections for collisions of electrons and protons with nitrogen molecules, and the work by Filipelli *et al.* (1982) and Rall *et al.* (1987) on emission in the visible after dissociative excitation of nitrogen molecules due to electron impact.

Sroka (1969a) measures cross sections for eleven transitions and bases the relative calibration of his spectrometer on literature data for the grating reflection and the quantum efficiency of the multiplier cathode, a method that apparently leads to serious errors since his cross sections are on average a factor of 10 higher than cross sections reported by other groups. Ajello (1970) measures cross sections for three transitions, but these are inaccurate above 30 eV due to Faraday cup problems (Ajello and Shemansky 1985). We therefore omit the cross sections measured by these authors from the following comparison.

Aarts and de Heer (1971a) measure cross sections for twelve transitions between 74.6 and 174.3 nm. They measure the relative spectral response of their spectrometer by using the molecular branching-ratio technique for N_2 LBH bands (127–180 nm) and for H_2 Werner bands (103–124 nm). The relative spectral response is normalized at 159.7 nm by using the CO(159.7 nm band) photoemission cross section from Aarts and de Heer (1970). Calibration below 100 nm is based on photoemission cross sections for some Ar and Kr multiplets from de Jongh and van Eck (1971a). Stone and Zipf (1972b) suggest that the H_2 Werner bands in the experiment of Aarts and de Heer (1971a) are measured with in-

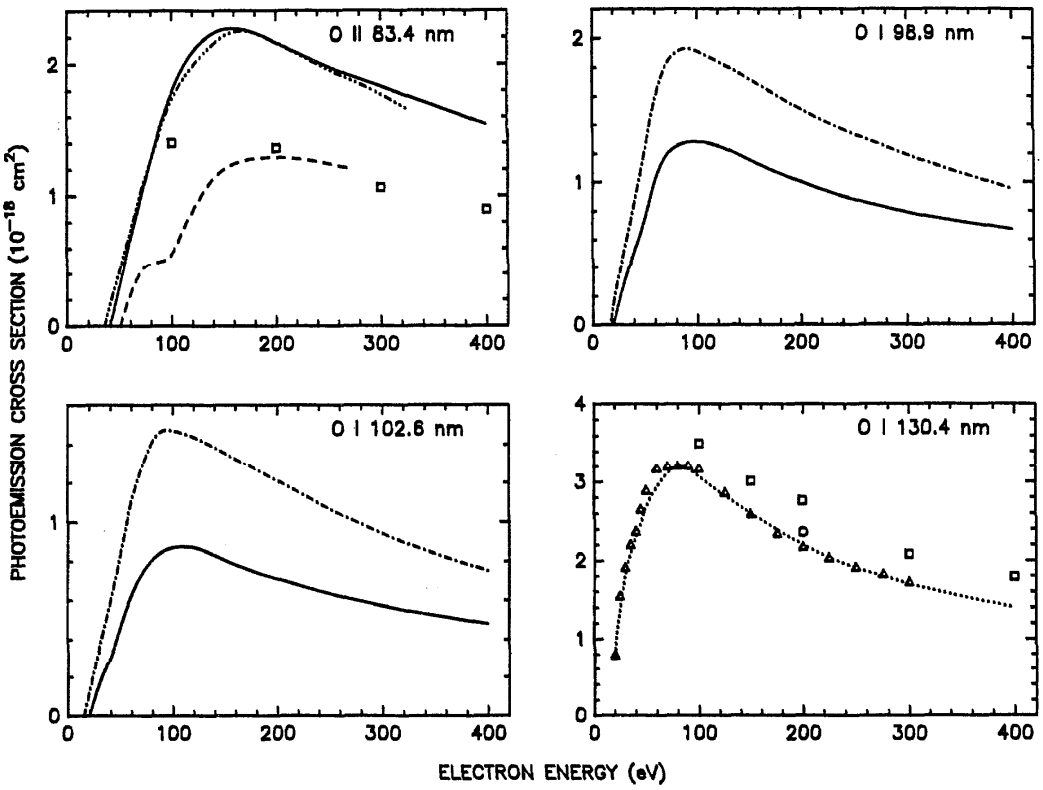

FIG. 3. Comparison of excitation functions for oxygen transitions. All photoemission cross sections are in 10^{-18} cm^2. Measurements shown are: ····Lawrence (1970), □ Aarts and de Heer (1971b), -· Zipf *et al.* (1979), ---Morgan and Mentall (1983), —and ○ Ajello and Franklin (1985), -···Zipf *et al.* (1985) and Δ Zipf (1986).

sufficient resolution, making the calibration unreliable between 103 and 124 nm.

Mumma and Zipf (1971b) measure cross sections for nine transitions between 116.4 and 174.3 nm. They determine the relative spectral response by using N_2 LBH bands and normalize on the H_2(H I Ly-α) cross section from Mumma and Zipf (1971a). In addition Stone and Zipf (1973) report cross sections for three transitions.

Huschilt *et al.* (1981) measure the N_2(N I 120.0 nm) cross section on a relative scale and normalize on the same cross section from Mumma and Zipf (1971b). This cross section is measured again by Forand *et al.* (1988), based on a relative calibration with H_2 Rydberg band systems and a normalization on the H_2(H I Ly-α) cross section from Woolsey *et al.* (1986). They also measure the polarization of the N_2(N II 108.4 nm), N_2(N I 120.0 nm), and N_2(N I 124.3 nm) transitions by mounting a reflection polarizer behind the exit slit of their spectrometer (McConkey *et al.* 1981).

Morgan and Mentall (1983) measure cross sections for eight transitions between 67.1 and 117.7 nm, based on a relative calibration using the double-monochromator technique and a normalization on the N_2(N I 120.0 nm) cross section from Mumma and Zipf (1971b).

Ajello and Shemansky (1985) measure cross sections for ten transitions between 116.4 and 174.3 nm, based on a relative calibration using the molecular branching-ratio technique for the N_2 LBH bands (127–260 nm) and H_2 Rydberg band systems (80–170 nm) and a normalization on the H_2(H I Ly-α) cross section from Shemansky *et al.* (1985a).

Table 5 lists some results from the various authors after renormalization to the same value of 7.3×10^{-18} cm^2 for the H_2(H I Ly-α) photoemission cross section. Note that the cross sections of Morgan and Mentall (1983) are normalized on the N_2(N I 120.0 nm) cross section from Mumma and Zipf (1971b) which in turn is normalized on the H_2(H I Ly-α) cross section from Mumma and Zipf (1971a), leading to a renormalization by 7.3/12.

We find good agreement between the normalized N I cross sections from Mumma and Zipf (1971b), Stone and Zipf (1973),Ajello and Shemansky (1985), and Forand *et al.* (1988). The N I cross sections of Aarts and de Heer (1971a) are somewhat higher, but—within the reported uncertainties—in agreement with these authors (with the exception of the N_2(N I 116.4 nm) cross section). The N II cross sections of Aarts and de Heer (1971a) are somewhat higher than those of Morgan and Mentall (1983) but agree within the reported uncertainties.

Relative cross sections for the N_2(N I 120.0 nm) tran-

Table 5. Comparison of photoemission cross sections for dissociative excitation of nitrogen molecules in 10^{-18} cm^2 at 200 eV

Authors	N II 74.6	N II 91.6	N II 108.4	N I 113.4	N I 120.0	N I 124.3	N I 131.1	N I 149.3	N I 174.3	Reported uncertainty	Renormalization
Aarts and de Heer (1971a)	0.15	0.44	2.42	0.78	3.47	1.01	0.23	1.43	0.59	30-50%	–
Mumma and Zipf (1971b)					3.11	0.60		1.20	0.43	18-25%	7.3/12
Stone and Zipf (1973)				0.52			0.17[a]			25, 30%	7.3/12
Morgan and Mentall (1983)	0.10	0.29	1.37	0.59						13%	7.3/12
Ajello and Shemansky (1985)					3.11	0.79	0.16	1.17	0.45	16-20%	7.3/8.18
Forand et al. (1988)					3.05					12%	7.3/7.13

[a] Scaled to 200 eV using σ(200 eV) / σ(100 eV) from Ajello and Shemansky (1985).

sition are in good agreement (see Fig. 4). We also note good agreement between Aarts and de Heer (1971a) and Mumma and Zipf (1971b) regarding the 124.3 and 149.4 nm optical excitation functions (although data below 80 eV from Aarts and de Heer (1971a) are too high).

4.6. Carbon Dioxide

Three different groups have reported cross sections for dissociative excitation of CO_2. Sroka (1970) measures cross sections for CO_2(O I 130.4 nm) and CO_2(C II 133.5 nm) and in addition for fourteen transitions between 68.7 and 115.2 nm. Ajello (1971c) measures cross sections for twelve transitions between 126.1 and 193.1 nm. Mumma *et al.* (1972) measure cross sections for six transitions between 130.4 and 165.7 nm. Zipf (1984) lists cross sections for six transitions between 95.3 and 115.2 nm but does not give experimental details.

Sroka (1970) bases the relative calibration of his spectrometer on literature data for the grating reflection and the quantum efficiency of the multiplier cathode, and normalizes on the He I(58.4 nm) cross section from Jobe and St. John (1967)and Gabriel and Heddle (1960) and the H_2(H I Ly-α) cross section from Vroom and de Heer (1969b) (7.4×10^{-18} cm^2, a correction of unclear origin, of the cross section of Vroom and de Heer 1969b). Ajello (1971c) uses the molecular branching-ratio technique for N_2 LBH bands for relative calibration and normalizes on the cross section for the CO(159.7 nm) band from Aarts and de Heer (1970). Mumma *et al.* (1972) also use N_2 LBH bands and N I multiplets for relative calibration and normalize on the H_2(H I Ly-α) cross section from Mumma and Zipf (1971a).

Comparison of cross sections at 100 eV for transitions below 116 nm shows disagreement between Sroka (1970) and Zipf (1984), which is at least partly due to the inaccuracy of the relative spectral response determined by Sroka (1970). Concerning transitions above 116 nm, we focus on the CO_2(O I 130.4 nm) and CO_2(C II 133.5 nm) photoemission cross sections. For comparison we renormalize the cross sections of Mumma *et al.* (1972) by a factor of 7.3/12 due to the update of the H_2(H I Ly-α) cross section. The differences in the CO_2(O I 130.4 nm) cross sections of Sroka, (1970) Ajello (1971c) and Mumma *et al.* (1972) are just within the reported uncertainties but there is a clear discrepancy between the CO_2(C II 133.5 nm) cross sections. Comparison of optical excitation functions for both transitions shows disagreements; only the 133.5 nm curves of Sroka (1970) and Mumma *et al.* (1972) agree on a relative scale.

4.7. Carbon Monoxide

The CO(O I 130.4 nm) cross section has been measured by Aarts and de Heer (1970), Lawrence (1970), and Ajello (1971b). Aarts and de Heer (1970) determine the relative spectral response of their spectrometer by using the molecular branching-ratio technique for H_2 Werner bands and CO bands of the fourth positive system and normalize on the CO(159.7 nm band) cross section evaluated from inelastic differential scattering cross sections from Lassettre and Silverman (1964), and Lassettre and Skerbele (1971). Lawrence (1970) bases his measurement on a cascade analysis of the 130.4 nm time decay curve (see Sec. 3.5). Ajello (1971b) uses the molecular branching-ratio technique for N_2 LBH bands for relative calibration and normalizes on the CO(159.7 nm band) cross section from Aarts and de Heer (1970).

We find good agreement among these authors regarding both the photoemission cross sections at 100 eV and the shape of the optical excitation functions. However, for the CO(C I 127.9 nm) and CO(C II 133.5 nm) cross sections the agreement between Aarts and de Heer (1970) and Ajello (1971b) is not as good. Ajello's (1971b) values may be unreliable due to Faraday cup problems (Ajello and Shemansky 1985), but Aarts and de Heer (1970) note that the error in their relative spectral response might be 100% at some wavelengths. Zipf (1984) quotes cross sections for seven transitions between 95 and 131 nm but does not give experimental information; his CO(O I 130.4 nm) cross section is about twice as large as measurements by the other authors.

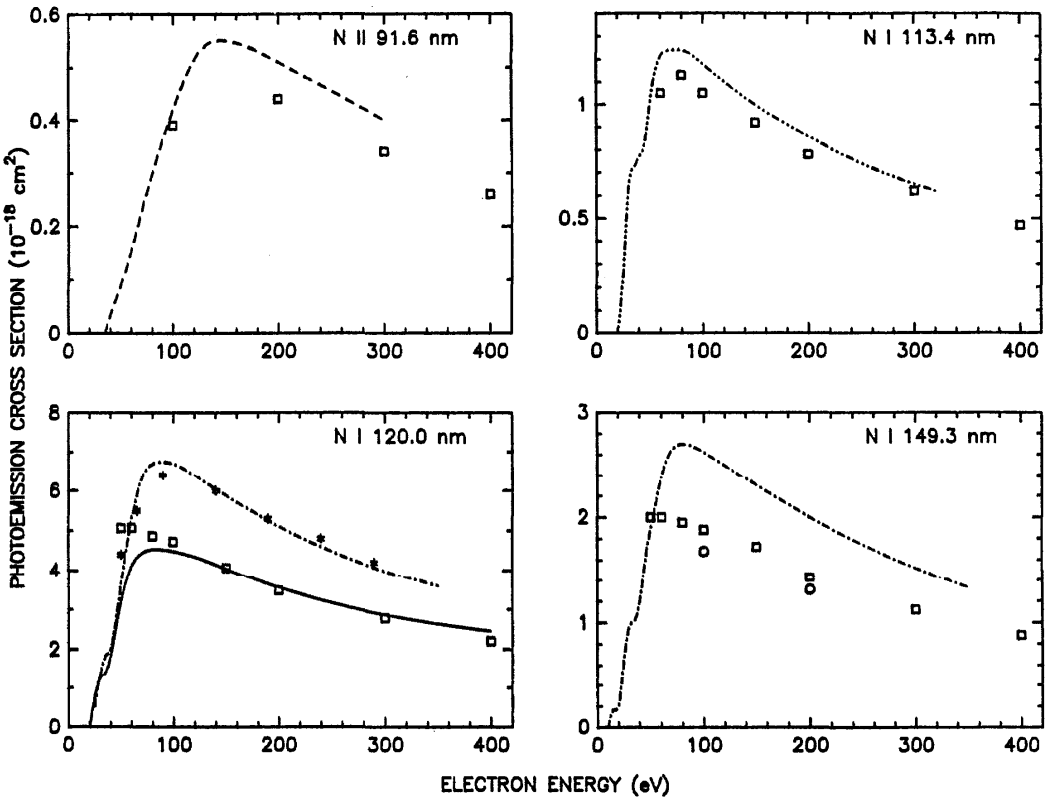

FIG. 4. Comparison of excitation functions for nitrogen transitions. All photoemission cross sections are in 10^{-18} cm^2. Measurements shown are: □ Aarts and de Heer (1971a), - · Mumma and Zipf (1971b), - · · · Stone and Zipf (1973), *Huschilt *et al.* (1981), --- Morgan and Mental (1983), and — and ○ Ajello and Shemansky (1985).

4.8. Nitric Oxide

Nitric oxide was the focus of some activity during the early seventies. Lawrence (1970) measures the NO(O I 130.4 nm) photoemission cross section, Mentall and Morgan (1972) measure eight O I and N I cross sections between 113.3 and 174.3 nm, and Stone and Zipf (1972a) measure three N I cross sections between 120.0 and 149.3 nm. An extensive study of the NO emissions between 40 and 270 nm has been made by Ajello and co-workers and will be published in a forthcoming paper (Ajello *et al.* 1989).

Lawrence (1970) bases his measurement on a cascade analysis (see Sec. 3.5). Stone and Zipf (1972a) use the N_2 LBH bands for the relative calibration of their monochromator, extended downward to 110 nm by using HD Lyman bands excited with Ar resonance radiation. Their relative calibration is normalized on the NO(O I 130.4 nm) cross section from Lawrence (1970). Mentall and Morgan (1972) use the N_2 LBH bands for relative calibration in combination with some N I transitions, and normalize their measurements on an average 3.3×10^{-18} cm^2 of three determinations of the O_2(O I 130.4 nm) cross section at 100 eV. Contrary to the measurements of Mumma and Zipf (1971a) and Ajello (1971a), Lawrence's (1970) measurement of the O_2(O I 130.4 nm) cross section, 3.05×10^{-18} cm^2, is the only one in agreement with more recent measurements (see Sec. 4.4). This suggests a small renormalization of the NO cross sections of Morgan and Mentall (1972) with a factor 3.05/3.3.

Lawrence's (1970) value 1.14×10^{-18} cm^2 for the NO(O I 130.4 nm) cross section at 100 eV is in good agreement with the value of 1.1×10^{-18} cm^2 measured by Mentall and Morgan (1972). The shapes of the optical excitation functions presented by these authors are also in agreement (see Fig. 7 of Mentall and Morgan 1972). The cross sections measured by Stone and Zipf (1972a) are slightly lower than the cross sections of Mentall and Morgan (1972), except the NO(O I 120.0 nm) cross section. There is good agreement between the shapes of the optical excitation functions but the reported cross sections at 100 eV are 4.8×10^{-18} cm^2 and 3.04×10^{-18} cm^2, respectively.

4.9. Water

Cross sections for many transitions have been measured by Böse and Sroka (1973) (fourteen transitions between

Table 6. Comparison of photoemission cross sections for dissociative excitation of water molecules in 10^{-18} cm^2 at 200 eV

Authors	H I, O I 121.7	O I 130.4	Reported uncertainty	Renormalization
Vroom and de Heer (1969c)	12.2		32%	7.3/14
McGowan et al. (1969)	3.7		factor 2	7.3/14
Lawrence (1970)		0.28	14%	–
Morgan and Mentall (1974)	7.3	0.22	13%	3.05/3.3
Möhlmann et al. (1978)	9.5		–	7.3/12
Ajello (1984)	5.6	0.19	16, 22%	7.3/8.18

53.9 and 121.7 nm) and Ajello (1984) (23 transitions between 48.4 and 130.4 nm). These measurements are difficult to compare as the cross sections are given only for 100 and 200 eV, respectively. Böse and Sroka (1973) do not measure the relative spectral response of their monochromator but determine the relative spectral response by using literature data for the grating reflection and the quantum efficiency of the multiplier cathode; therefore their results may be inaccurate. Ajello (1984) determines the relative spectral response by using a combination of the double-monochromator technique and the molecular branching-ratio technique for H_2 Rydberg band systems, and normalizes on the H_2(H I Ly-α) cross section from Shemansky *et al.* (1985a).

In addition Vroom and de Heer (1969c) McGowan *et al.* (1969), Morgan and Mentall (1974), and Möhlmann *et al.* (1978) measure the H_2O(H I, O I 121.7 nm) photoemission cross section, and Lawrence (1970) and Morgan and Mentall (1974) measure the H_2O(O I 130.4 nm) photoemission cross section. Lawrence (1970) bases his measurement on a cascade analysis of the 130.4 nm time decay curve (see Sec. 3.5). Morgan and Mentall (1974) determine the relative spectral response by using the atomic and molecular branching-ratio technique with H_2 Werner bands and N I multiplets, and normalize on an average of three determinations of the O_2(O I 130.4 nm) cross section at 100 eV. Contrary to the measurements of Mumma and Zipf (1971a) and Ajello (1971a) the measurement of Lawrence (1970), 3.05×10^{-18} cm^2, is in agreement with more recent measurements (see Sec. 4.4). This suggests a small renormalization of the H_2O cross sections of Morgan and Mentall (1974) by 3.05/3.3. The other measurements are all normalized to different values of the H_2(H I Ly-α) cross section; appropriate renormalizations are given in Table 6.

Although the shapes of the H_2O(H I, O I, 121.7 nm) optical excitation functions are in reasonable agreement (see Fig. 5), Table 6 shows a wide spread among different renormalized measurements of the H_2O(H I, O I 121.7 nm) cross section. The shapes of the H_2O(O I 130.4 nm) optical excitation functions as measured by Lawrence (1970) and Morgan and Mentall (1974) are in agreement, but it is remarkable that the carefully measured H_2O(O I 130.4 nm) cross section of Lawrence (1970) is significantly higher than the

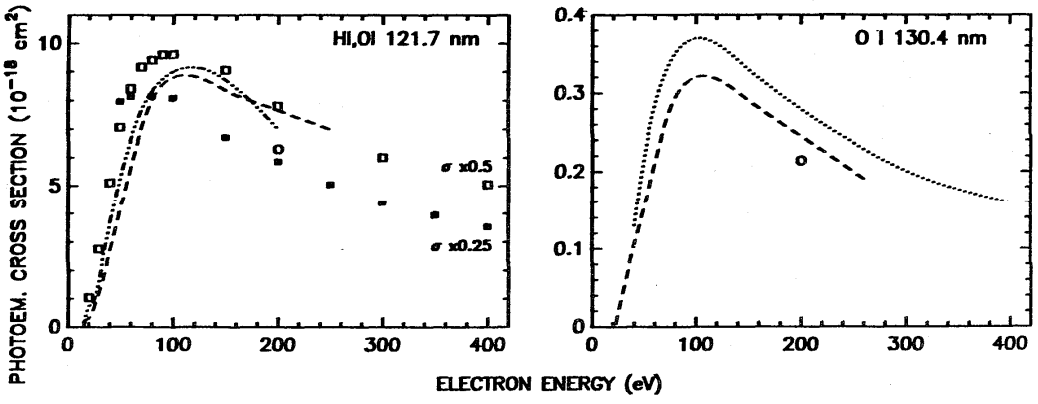

FIG. 5. Comparison of excitation functions for H I and O I transitions in dissociative excitation of water molecules. All photoemission cross sections are in 10^{-18} cm^2. Measurements shown are: ■ Vroom and de Heer (1969c), -··· McGowan *et al.* (1969), ····Lawrence (1970), ---Morgan and Mentall (1974), □ Möhlmann *et al.* (1978), and O Ajello (1984).

Table 7. Comparison of photoemission cross sections for dissociative excitation of methane molecules in 10^{-18} cm^2 at 100 eV

Authors	H I 102.6	H I 121.6	C I 165.7	C I, II 193.1	Reported uncertainty	Renormalization
Vroom and de Heer (1969a)		6.5			32%	7.3/14
Sroka (1969b)	0.29	2.5	0.22	0.18	–	–
McGowan et al. (1969)		7.3			factor 2	7.3/14
Morgan and Mentall (1974)		1.1	0.031	0.058	13%	3.05/3.3
Möhlmann et al. (1978)		7.4			–	7.3/12
McLaughlin and Zipf (1978)	1.04				–	7.3/12
Orient and Srivastava (1981)		5.5			17%	7.3/12
Pang et al. (1987)	0.86	6.3	0.49	0.23	22%	–

(renormalized) cross sections of Morgan and Mentall (1974) and Ajello (1984). Möhlmann *et al.* (1978) explain the difference between their data and the data measured earlier in the same laboratory by Vroom and de Heer (1969c) as being due to problems with determining the target gas density in the earlier experiment.

4.10. Methane and Other Hydrocarbons

Several groups have measured photoemission cross sections for a variety of hydrocarbons, but methane is the most frequently studied target gas and therefore the most interesting for a comparing photoemission cross sections.

Vroom and de Heer, (1969a), McGowan *et al.* (1969) Möhlmann *et al.* (1978) and Orient and Srivastava (1981) measure only the CH_4(H I Ly-α) cross section and normalize on the H_2(H I Ly-α) cross section either from Fite and Brackmann (1958) or from Mumma and Zipf (1971a). All authors except Vroom and de Heer (1969a) use an oxygen optical filter to detect Ly-α radiation. Based on emission spectra of Morgan and Mentall (1974), Möhlmann *et al.* (1978) argue that for an oxygen pressure of 500 Torr in the filter more than 99% of the transmitted radiation from dissociative excitation of CH_4 is Ly-α radiation. A factor to be taken into account in the normalization to the H_2(H I Lyα) cross section is the amount of Ly-α radiation in proportion to all radiation from dissociative excitation of H_2 transmitted by the filter. This factor is about 0.75 or 0.80 according to measurements by Carrière and de Heer (1972) and McGowan *et al.* (1969), but recent measurements of the H_2(H I Ly-α) cross section suggests that the factor might be close to 0.50 (see discussion in Sec. 4.3). When MgF_2 is present in the optical system we would expect this factor to be closer to 1 due to the higher cutoff at 114 nm of MgF_2. Since Möhlmann *et al.* (1978) use a photomultiplier with a MgF_2 window, and Orient and Srivastava (1981) use MgF_2 windows in the oxygen filter, the cross sections of both these groups might be somewhat on the low side.

McLaughlin and Zipf (1978) measure the CH_4(H I-Ly-β) cross section based on a relative calibration with H_2 Werner bands and a normalization on the N_2(N I 120.0 nm) cross section from Mumma and Zipf (1971b).

Three groups report cross sections for several transitions. Sroka (1969b) measures cross sections for six transitions between 95.0 and 165.7 nm. He determines the relative spectral response of his spectrometer by using literature data for the grating reflection and the quantum efficiency of the multiplier cathode, and normalizes on the He I(58.4 nm) cross section from Jobe and St. John (1967) and Gabriel and Heddle (1960). Morgan and Mentall (1974) measure cross sections for five transitions between 121.6 and 193.1 nm, based on a relative calibration using H_2 Werner bands, N_2 LBH bands and N I multiplets, and a normalization on an average of the O_2(O I 130.4 nm) cross section from three different groups. Pang *et al.* (1987) measure cross sections for thirteen transitions between 93.1 and 193.1 nm, based on a relative calibration using the molecular branching-ratio technique for N_2 LBH bands (127–260 nm) and H_2 Rydberg band systems (80–170 nm) and a normalization on an average of the H_2(H I Ly-α) cross section of 7.3×10^{-18} cm^2 of four measurements at 100 eV by Shemansky *et al.* (1985a), Woolsey *et al.* (1986), Ligtenberg *et al.* (1985), and Van Zyl *et al.* (1985).

To make a meaningful comparison of cross sections we renormalize to the above mentioned average of the H_2 (H I Ly-α) cross section. Table 7 shows the results for some of the most important transitions. The cross sections of Morgan and Mentall (1974) are normalized to an average 3.3×10^{-18} cm^2 of the O_2(O I 130.4 nm) cross section from Mumma and Zipf (1971a), Ajello (1971a), and Lawrence (1970). Contrary to the other two measurements, the measurement of Lawrence (1970), 3.05×10^{-18} cm^2, is in agreement with more recent measurements (see Sec. 4.4), leading to a renormalization by 3.05/3.3. McLaughlin and Zipf (1978) normalize on the N_2(N I 120.0 nm) of Mumma and Zipf (1971b), which was normalized on the H_2(H I Ly-α) cross section of Mumma and Zipf (1971a), leading to a renormalization by 7.3/12.

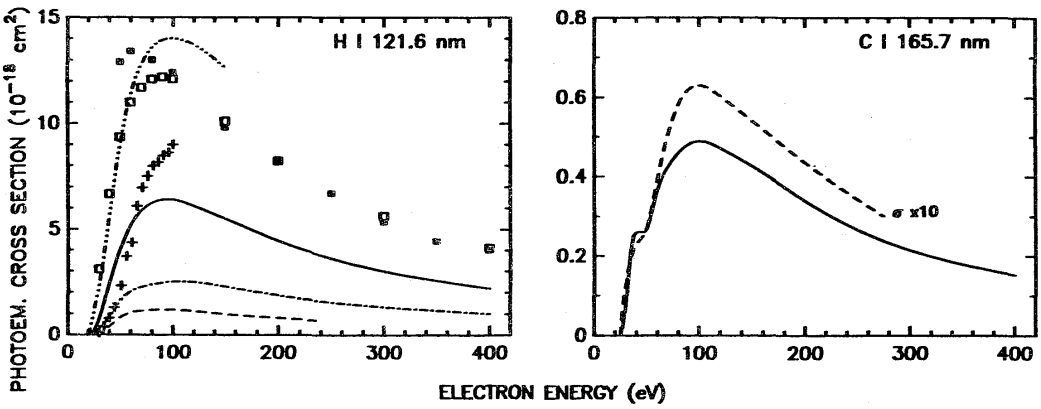

FIG. 6. Comparison of excitation functions for H I and C I transitions in dissociative excitation of methane molecules. All photoemission cross sections are in 10^{-18} cm^2. Measurements shown are: ■ Vroom and de Heer (1969a), -· Sroka (1969b), -··· McGown *et al.* (1969), --- Morgan and Mentall (1974), □ Möhlmann *et al.* (1978), + Orient and Srivastava (1981), and — Pang *et al.* (1987).

Most measurements of the CH_4(H I Ly-α) cross section are in agreement with the most recently measured value of Pang *et al.* (1987). Serious discrepancy exists among the measurements of Sroka (1969b), Morgan and Mentall (1974), and Pang *et al.* (1987). As Sroka (1969b) did not measure the relative spectral response but used literature data, his cross sections are only reliable to an order of magnitude. The reason for the discrepancy between Morgan and Mentall (1974) and Pang *et al.* (1987) is not clear. We note good agreement between the CH_4(H I Ly-β) cross section of McLaughlin and Zipf (1978) and Pang *et al.* (1987).

Figure 6 shows a comparison of optical excitation functions for the Ly-α transition. The shapes are in good agreement. Discrepancies are that the data from Vroom and de Heer (1969a) are too high below 70 eV, and the data from Orient and Srivastava (1981) are too low below 70 eV. Other optical excitation functions are measured by Sroka (1969b), McLaughlin and Zipf (1978), and Pang *et al.* (1987) for CH_4(H I Ly-β), and by Morgan and Mentall (1974) and Pang *et al.* (1987), for CH_4(C I 165.7 nm) and CH_4(C I, II 193.1 nm) The shapes of these curves are in good agreement on a relative scale.

There are also a number of measurements for other hydrocarbons. Vroom and de Heer (1969a) also measure (H I Ly-α) cross sections for dissociative excitation of C_2H_6, C_2H_4, and C_6H_6. Beenakker and de Heer (1974) measure the C_2H_2(C I,II 193.1 nm) cross section based on a relative calibration with a deuterium lamp and a quartz-iodine lamp with a coiled-coil tungsten filament, and a normalization above 300 nm to a tungsten ribbon lamp. Pang *et al* (1987) also measure cross sections for dissociative excitation of C_2H_2 for twenty-four transitions between 68.7 and 193.1 nm.

4.11. Ammonia

Cross sections for a number of transitions in dissociative excitation of ammonia are reported by Böse and Sroka (1971) (nine transitions between 93.1 and 121.6 nm) and Morgan and Mentall (1974) (six transitions between 113.4 and 174.3 nm). Böse and Sroka (1971) normalize their measurement on a value of 7.4×10^{-18} cm^2 for the H_2(H I Ly-α) cross section (a correction, of unclear origin, of the cross section from Vroom and de Heer (1969b), so their cross sections do not need renormalization). Morgan and Mentall (1974) normalize their measurements on an average 3.3×10^{-18} cm^2 of three determinations of the O_2(O I 130.4 nm(cross section at 100 eV. The measurement of Lawrence (1970), 3.05×10^{-18} cm^2, seems the most reliable (see Sec. 4.4), suggesting a small renormalization of Morgan and Mentall's cross sections by a factor of 3.05/3.3. After renormalization a comparison of cross sections for the three transitions measured by these authors shows a very serious but not surprising discrepancy, since Böse and Sroka (1971) do not measure the relative spectral response of their monochromator, but use literature data for the grating reflection and the quantum efficiency of the multiplier cathode. Morgan and Mentall (1974) measure the relative spectral response by using the atomic and molecular branching-ratio technique for H_2 Werner bands, N_2 LBH bands and N I multiplets.

McGowan *et al.* (1969) and Möhlmann *et al.* (1978) measure the NH_3(H I Ly-α) cross section. These measurements are normalized on the H_2(H I Ly-α) cross section of Fite and Brackmann (1958) and Mumma and Zipf (1971a), respectively, suggesting a renormalization by 7.3/14 and 7.3/12, respectively. McGowan *et al.* (1969) remark that their cross section is inaccurate to within a factor of 2 due to

the determination of the target gas density in their experiment. The renormalized NH_3(H I Ly-α) cross section 11.7×10^{-18} cm^2 of Möhlmann *et al.* (1978) is in good agreement with 10.0×10^{-18} cm^2 of Morgan and Mentall (1974).

Optical excitation functions for the NH_3(H I Ly-α) transition are measured by all four authors mentioned above. The shapes are in good agreement on a relative scale. Morgan and Mentall (1974) and Böse and Sroka (1971) both measure optical excitation functions for the NH_3(N I 120.0 nm) transition, but the results are in serious disagreement between threshold and 180 eV.

4.12. Other Target Gases

4.12.a. Carbon Disulphide

Ajello and Srivastava (1981) measure photoemission cross sections for thirty transitions between 114.0 and 191.5 nm. Optical excitation functions are measured in a crossed beams experiment using a spectrometer-detector system at 90° with respect to both beams. The relative spectral response is determined by using the molecular branching-ratio technique for N_2 LBH bands. Normalization is performed by measuring the intensities of the CS_2 transitions relative to the intensity of the H_2(H I Ly-α) transition, by operating in a static-gas arrangement and using the H_2(H I Ly-α) dissociative cross section from Mumma and Zipf (1971a). Recent measurements of this cross section suggest a renormalization of the CS_2 cross sections by a factor of 7.3/12.

4.12.b. Sulphur Dioxide

Becker *et al.* (1983) measure photoemission cross sections for twenty-two transitions between 44.6 and 104.0 nm. They use a crossed beams configuration with the spectrometer-detector system at 90° with respect to both beams. The spectral response of the spectrometer is determined for a number of discrete wavelengths by using the He II(30.4 nm) cross section from Bloemen *et al.* (1981), the He I(52.2, 53.7, and 58.4 nm) cross sections from van Eck and de Jongh (1970), Donaldson *et al.* (1972) and Westerveld *et al.* (1979), the Ne I(73.6 nm) cross section from Tan *et al.* (1974), the Ar II(92.0, 93.2 nm) cross sections from van Raan (1973) and Tan *et al.* (1974), and the Ar I(104.8, 106.7 nm) cross sections from McConkey and Donaldson (1973). The spectral response at other wavelengths is determined by interpolation. The optical excitation functions for the SO_2 transitions are brought on an absolute scale by interpolation on nearby noble gas transitions through comparison of slopes of intensity versus pressure.

4.12.c. Sulphur Hexafluoride

Forand *et al.* (1986) measure photoemission cross sections for forty-four transitions between 47.3 and 182.3 nm, using the same apparatus that Becker *et al.* (1983) use for measuring SO_2 cross sections. The spectral response below 117 nm is determined in the same way as by Becker *et al.* (1983) (see above), except an average of the Ar I(92.0, 93.2 nm) cross sections from Tan *et al.* (1974) and McPherson (1984) is used. Above 117 nm the relative spectral response is determined using the molecular branching-ratio technique for the CO fourth positive band system and the H_2 Werner band system, and is normalized to the H_2(H I Ly-α) cross section from Ligtenberg *et al.* (1985), Shemansky *et al.* (1985a) and Van Zyl *et al.* (1985) Different gratings are used in the spectrometer for the two wavelength regions. Intensities for transitions in different gases are compared through the relative gas-flow technique.

4.12.d. Atomic Oxygen and Nitrogen

Measurements of photoemission cross sections for electron scattering by atomic oxygen and atomic nitrogen have been performed by Zipf and co-workers. In their experiments atomic oxygen or nitrogen, produced by dissociation in a microwave discharge, flows into the collision chamber. The metastable atoms formed in the discharge rapidly decay through numerous collisions with the wall of the flow tube. The gas density is determined either by observation of absorption of O I and N I resonance radiation from an external helium discharge (1971–1974), or by a quadrupole mass spectrometer attached to the collision chamber (since 1985). Photons are detected at 90° with respect to the electron beam by a spectrometer and a photomultiplier.

Stone and Zipf (1973) measure cross sections for six N I transitions between 113.4 and 174.4 nm. These cross sections are normalized on the H_2(H I Ly-α) cross section of Mumma and Zipf (1971a), suggesting a renormalization by 7.3/12. (Preliminary results for the 120.0 nm transition are reported by Stone and Zipf 1971).

Stone and Zipf (1974) measure the O I(130.4 nm) and O I(135.6 nm) cross sections normalized on a value of 3.5×10^{-18} cm^2 for the O_2(O I 130.4 nm) cross section, which is an average of four different measurements. Based on recent measurements of the O_2(O I 130.4 nm) cross section (see Sec. 4.4), we suggest a renormalization by 3.05/3.5. Stone and Zipf (1973, 1974) determine the relative spectral response of their optical system by using the molecular branching-ratio technique for the N_2 LBH bands and the HD Lyman bands excited with resonance radiation.

Zipf and Erdman (1985), Zipf *et al.* (1985), Zipf (1986), and Zipf and Kao (1986) measure cross sections for six O I transitions between 79.2 and 130.4 nm. The relative spectral response is determined using the molecular and atomic branching-ratio technique for the H_2 Werner bands and the H I Lyman series. The cross sections are normalized on the H_2(H I Ly-α) cross section (7.5×10^{-18} cm^2, Risley, private communication to Zipf 1986; this suggests a small renormalization by 7.3/7.5). The O I(130.4 nm) cross sections reported by Zipf and Erdman (1985) and Zipf (1986) are a factor of 2.8 smaller than the renormalized cross sections of Stone and Zipf (1974), due to a more accurate determination of the atomic oxygen density in the recent experiments.

4.12.e. Hydrogen Chloride

Möhlmann *et al* (1978) measure the HCl(H I Ly-α) photoemission cross section by using a LiF-O_2 filter and a

Table 8. List of selected photoemission cross sections in 10^{-18} cm^2 at 200 eV. All photoemission cross sections normalized to H_2(H I Ly-α) or N_2(N I 120.0 nm) have been renormalized as described in the text

Transition		Cross section	Reported uncertainty	Normalization	Authors
30.4	He II	0.56	25%	photoionization chamber	Bloemen et al. (1981)
		0.62	28%	He I(58.4-50.5 nm)	Forand et al. (1985)
46.1 + 46.2	Ne II	2.26	26%	Bethe approximation	Dijkkamp and de Heer (1981)
		3.05	35%	He I(58.4, 53.7, 52.2 nm)	Eckhardt and Schartner(1983)
52.2	He I	0.88	–	oscillator strength	de Jongh and van Eck (1971b)
		0.87	38%	oscillator strength	Donaldson et al. (1972)
		0.79	22%	H_2(H I Ly-α)	Shemansky et al. (1985b)
53.7	He I	2.39	10%	oscillator strength	Donaldson et al. (1972)
		2.11	5%	oscillator strength	Westerveld et al. (1979)
		1.89	22%	H_2(H I Ly-α)	Shemansky et al. (1985b)
58.4	He I	8.66	8%	oscillator strength	Donaldson et al. (1972)
		8.78	5%	oscillator strength	Westerveld et al. (1979)
		7.44	22%	H_2(H I Ly-α)	Shemansky et al. (1985b)
83.4	O_2(O II)	1.92	22%	H_2(H I Ly-α)	Ajello and Franklin (1985)
		2.09	–	O_2(O I 130.4 nm)	Zipf et al. (1985)
92.0	Ar II	5.50	8%	synchrotron radiation	McPherson (1984)
		3.89	15%	H_2(H I Ly-α)	Forand et al. (1988)
93.2	Ar II	2.75	8%	synchrotron radiation	McPherson (1984)
		2.01	15%	H_2(H I Ly-α)	Forand et al. (1988)
98.9	O_2(O I)	0.91	–	N_2(N I 120.0 nm)	Zipf et al. (1979)
		0.86	13%	N_2(N I 120.0 nm)	Morgan and Mentall (1983)
		0.89	22%	H_2(H I Ly-α)	Ajello and Franklin (1985)
102.7	O_2(O I)	0.73	–	N_2(N I 120.0 nm)	Zipf et al. (1979)
		0.64	13%	N_2(N I 120.0 nm)	Morgan and Mentall (1983)
		0.63	22%	H_2(H I Ly-α)	Ajello and Franklin (1985)
113.4	N_2(N I)	0.52	25%	H_2(H I Ly-α)	Stone and Zipf (1973)
		0.59	13%	N_2(N I 120.0 nm)	Morgan and Mentall (1983)
120.0	N_2(N I)	3.11	18%	H_2(H I Ly-α)	Mumma and Zipf (1971b)
		3.11	16%	H_2(H I Ly-α)	Ajello and Franklin (1985)
		3.05	12%	H_2(H I Ly-α)	Forand et al. (1988)
121.6	H_2(H I)	5.10[a]	19%	Ly-α rad. from H+Ne	Van Zyl et al. (1985)
		4.64[a]	8%	synchrotron radiation	Ligtenberg et al. (1985)
		5.78	15%	Bethe approximation	Shemansky et al. (1985a)
		5.04[a]	8%	H I(Ly-α)	Woolsey et al. (1986)
124.3	N_2(N I)	0.60	22%	H_2(H I Ly-α)	Mumma and Zipf (1971b)
		0.79	20%	H_2(H I Ly-α)	Ajello and Shemansky (1985)
130.4	O_2(O I)	2.20	14%	cascade analysis	Lawrence (1970)
		2.76	30%	CO(159.7 nm band)	Aarts and de Heer (1971b)

Table 8. List of selected photoemission cross sections in 10^{-18} cm^2 at 200 eV. All photoemission cross sections normalized to H_2(H I Ly-α) or N_2(N I 120.0 nm) have been renormalized as described in the text -- Continued

Transition		Cross section	Reported uncertainty	Normalization	Authors
		2.11	22%	H_2(H I Ly-α)	Ajello and Franklin (1985)
		2.10	15%	H_2(H I Ly-α)	Zipf (1986)
131.1	N_2(N I)	0.23	30%	CO(159.7 nm band)	Aarts and de Heer (1971b)
		0.17[b]	30%	H_2(H I Ly-α)	Stone and Zipf (1973)
		0.16	20%	H_2(H I Ly-α)	Ajello and Shemansky (1985)
149.3	N_2(N I)	1.43	30%	CO(159.7 nm band)	Aarts and de Heer (1971b)
		1.20	21%	H_2(H I Ly-α)	Mumma and Zipf (1971b)
		1.17	20%	H_2(H I Ly-α)	Ajello and Shemansky (1985)
174.3	N_2(N I)	0.59	30%	CO(159.7 nm band)	Aarts and de Heer (1971b)
		0.43	–	H_2(H I Ly-α)	Mumma and Zipf (1971b)
		0.45	20%	H_2(H I Ly-α)	Ajello and Shemansky (1985)

[a] Scaled to 200 eV using σ(200 eV) / σ(100 eV) from Shemansky et al. (1985a).
[b] Scaled to 200 eV using σ(200 eV) / σ(100 eV) from Ajello and Shemansky (1985).

channel electron multiplier at 90° to the electron beam in a static gas experiment. They normalize on the H_2(H I Ly-α) cross section of Mumma and Zipf (1971a) (suggested renormalization 7.3/12). Some (Cl I 118.9 nm) radiation might have contributed to the radiation transmitted by the filter.

4.12.f. Deuterium Oxide

McGowan *et al.* (1969) measure the D_2O(D I Ly-α) photoemission cross section, normalized on the H_2(H I Ly-α) (CUV) cross section of Fite and Brackman (1958) by using a LiF-O_2 filter and a photomultiplier at 54.7° with respect to the electron beam. Their cross sections are approximate within a factor of 2 due to questionable operation of the ionization gauge used.

5. List of Selected Photoemission Cross Sections

Based on the reviews of cross sections in Sec. 4, we present a list of selected photoemission cross sections in the EUV (see Table 8). Most of the experimental reports on photoemission cross sections in the EUV do not give sufficient information on the techniques used to warrant judgment on their uncertainties. In this respect reports on EUV measurements differ from, for instance, the very careful and accurate measurement of the He $1^1S \rightarrow n^1S$ excitation cross sections in the visible reported by Van Zyl *et al.* (1980). Because of the wide range of results, we apply the following criterion to the assembly of our list: we consider only those cross sections for which recent measurements by different researchers using different techniques are in agreement.

Based on this criterion, we exclude cross sections for a number of target gases from the list. Many cross sections have been reported for CS_2, SO_2, and SF_6, but each by only one group. At this moment no independent check exists to compare the uncertainty of the reported cross sections. A number of other target gases are also excluded, because no recent measurements exist or because there are discrepancies between measurements reported by different groups. CO, NO, CO_2, and NH_3 are excluded because the relevant measurements have been performed almost exclusively around 1970 and only a few cross sections can be compared. H_2O and CH_4 are excluded because of serious discrepancies among the available measurements. As a result, only photoemission cross sections for some noble gas transitions, for the Lyman-alpha emission in dissociative excitation of hydrogen, and for dissociative excitation of oxygen and nitrogen molecules are included in our list. All photoemission cross sections normalized to the H_2(H I Ly-α) dissociative cross section have been renormalized to the same value of 7.3×10^{-18} cm^2 for this cross section (see Sec. 4). The cross sections normalized to N_2(N I 120.0 nm) have been renormalized as described in Sec. 4.4.

By far the most reliable EUV photoemission cross sections are the He I(58.4 nm) and He I(53.7 nm) cross sections and the H_2(H I Ly-α) cross section. As discussed in Sec. 4.1, the He I(58.4 nm) and He(53.7 nm) cross sections are the most accurately known photoemission cross sections in the EUV. The H_2(H I Ly-α) cross section has recently been measured by four different groups using widely different experimental methods and normalizations, and good agreement has been obtained.

Also very important are the N_2(N I 120.0 nm) and the O_2(O I 130.4 nm) cross sections. The N_2(N I 120.0 nm) cross section is considered reliable because it is directly linked to the H_2(H I Ly-α) cross section. For the O_2(O I 130.4 nm) cross section two measurements normalized on the H_2(H I Ly-α) cross section exist, and these are in agreement with a third, independent, measurement of Lawrence (1970).

Next in order of importance are the O_2(O I 98.9, 102.7 nm) transitions, the N_2(N I 113.4–174.3 nm) transitions, and the He II(30.4 nm), He I(52.2 nm), Ne II(46.1, 46.2 nm), Ar II(92.0, 93.2 nm) noble gas transitions. Some of the O I and N I cross sections show agreement among three different groups. The Ar II(92.0, 93.2 nm) cross sections listed in Table 8 are not in agreement within reported accuracies, but are included because these transitions provide important calibration lines and two of the measurements are independent of other cross sections in the EUV.

In principle the cross sections listed in Table 8 could be used for the calibration of spectrometers, but the number of calibration lines is sparse and most of the results are not of high accuracy. Uncertainties claimed by the authors are listed, and for the majority of cross sections are in the range of 15% to 25%. Substantial improvements are possible to reduce the uncertainties of these photoemission cross section measurements. Also it would be convenient to use only photoemission cross sections for transitions of one particular target gas for calibration. An interesting target gas is SF_6, because it provides discrete transitions over a wide wavelength region in the EUV. However at the present time limited information is available on the dissociative excitation of this molecule. Hopefully in the near future a more extensive table can be assembled of accurate photoemission cross sections that are suitable for calibration of spectrometers.

6. Conclusions

Many photoemission cross sections in the EUV have been measured for electron impact on a variety of atomic and molecular targets. Especially in the last few years measurements for many transitions for a few important molecular gases have become available. The available literature on the individual target gases reveals severe inconsistencies between cross sections reported by different laboratories, extending outside the reported uncertainties. Although the reported uncertainty is sometimes below 15%, we estimate that most cross sections are not known to better than 25% or even 50%, and that only very few cross sections are known to better than 10%. Most descriptions of experiments in the literature lack detail sufficient to warrant assessment of the uncertainty claimed by the researchers.

A small number of photoemission cross sections in the EUV are used for normalization and have been measured *independently* of other photoemission cross sections in the EUV. Independent measurements exist for the He II(30.4 nm), Ne II(46.1, 46.2 nm), He I(52.2, 53.7, 58.4 nm), Ne I(73.6 nm), Ar II(92.0, 93.2 nm), Ar I(104.8, 106.7 nm), H_2(H I Ly-α), and O_2(O I 130.4 nm), cross sections. The H_2(H I Ly-α) cross section is the most frequently used for normalization. These independent cross sections are very important, because their accuracy affects the accuracy of all cross sections that are normalized to them. For example, a great number of cross sections, normalized on the H_2(H I-Ly-α) cross section, have to be renormalized due to recent updated measurements of the H_2(H I Ly-α) cross section. Therefore, any measurement of cross sections, relative to the H_2(H I Ly-α) cross section or to any of the other independent cross sections, although important for applications, does not improve the accuracy in this field of research beyond the accuracy of the independent cross sections. Cross sections measured independently from any other cross sections in the EUV, e.g., by absolute calibration of the efficiency of the spectrometer-detector system by using a radiometric standard or by normalizing to a cross section in the visible wavelength region, are extremely important.

Inconsistencies in the reported EUV photoemission cross sections are likely to be the result of systematic errors in the normalization methods. Most of the photoemission cross sections for the dissociative excitation of molecules are normalized on the H_2(H I Ly-α) cross section (in some cases via the N_2(N I 120.0 nm) cross section). An important element in this normalization is the molecular branching-ratio technique used mostly for the H_2 Rydberg band systems and the N_2 LBH band system. The available literature leaves us with the impression that the molecular branching-ratio technique is less straightforward to use than some researchers want us to believe. Application of this technique requires precise modeling of molecular spectra and convolution with the spectrometer slit function (Ajello *et al.* 1988). Future research would therefore greatly benefit from independent checks of the molecular branching-ratio technique. Such checks can be made where a cross section normalized on the H_2(H I Ly-α) cross section via the molecular branching-ratio technique can be compared with an accurate measurement of the same cross section normalized in an other way. Only few of such comparisons can be made at this time. Shemansky *et al.* (1985a) measure the He I(58.4 nm) cross section relative to the H_2(H I Ly-α) cross section. Their result is in agreement within the reported uncertainties with other measurements that are normalized to the Bethe approximation (see Sec. 4.1). Ajello and Franklin (1985) measure the O_2(O I 130.4 nm) cross section relative to the H_2(H I Ly-α) cross section. Their result is in very good agreement with the measurement of Lawrence (1970). Forand *et al.* (1988) measure the Ar I(92.0 nm) cross section relative to the H_2(H I Ly-α) cross section and obtain a cross section that is smaller than the absolute measurement of McPherson (1984). In all three cases, the molecular branching-ratio technique has been applied to the H_2 Rydberg band systems.

We conclude that the majority of publications in this field pay more attention to the many transitions for which cross sections can be measured than to the many experimental details that are important for high accuracy even in a relative measurement. The field of photoemission cross sections in the EUV needs: (1) more careful attention for the difficulties associated with accurate measurement of the essential parameters, and (2) accurate measurements, inde-

pendent of the molecular (and atomic) branching-ratio technique, that are absolute by calibrating the efficiency of the spectrometer-detector system using an absolute radiometric standard.

7. Acknowledgments

We are indebted to many colleagues for valuable comments on the manuscript. Especially, thanks are due to Dr. J. M. Ajello, Dr. F. J. de Heer, Dr. G. H. Dunn, Prof. J. W. McConkey, Prof. K.- H. Schartner, Dr. S. Trajmar, Dr. J. van Eck, and Dr. B. Van Zyl.

This work was supported in part by the Aeronomy Program of NSF, Grant No. ATM85-01865, and in part by the Experimental Plasma Research of the DOE, Grant No. DE-FG05-87-ER53259.

8. References

Aarts, J. F. M., and F. J. de Heer, J. Opt. Soc. Am. **58**, 1666 (1968).
Aarts, J. F. M., and F. J. de Heer, J. Chem. Phys. **52**, 5354 (1970).
Aarts, J. F. M., and F. J. de Heer, Physica **52**, 45 (1971a).
Aarts, J. F. M., and F. J. de Heer, Physica **56**, 294 (1971b).
Ajello, J. M., J. Chem. Phys. **53**, 1156 (1970).
Ajello, J. M., J. Chem. Phys. **55**, 3156 (1971a).
Ajello, J. M., J. Chem. Phys. **55**, 3158 (1971b).
Ajello, J. M., J. Chem. Phys. **55**, 3169 (1971c).
Ajello, J. M., Geophys. Res. Lett. **11**, 1195 (1984).
Ajello, J. M., and B. Franklin, J. Chem. Phys. **82**, 2519 (1985).
Ajello, J. M., and D. E. Shemansky, J. Geophys. Res. **90**, 9845 (1985).
Ajello, J. M. and S. K. Srivastava, J. Chem. Phys. **75**, 4454 (1981).
Ajello, J. M., S. K. Srivastava, and Y. L. Yung, Phys. Rev. A **25**, 2485 (1982).
Ajello, J. M., D. E. Shemansky, T. L. Kwok, and Y. L. Yung, Phys. Rev. A **29**, 636 (1984).
Ajello, J. M., D. E. Shemansky, B. Franklin, J. Watkins, S. Srivastava, G. K. James, W. T. Simms, C. W. Hord, W. Pryor, W. McClintock, V. Argabright, and D. Hall, Appl. Opt. **27**, 890 (1988).
Ajello, J. M., K. D. Pang, B. O. Franklin, S. K. Howell, and N. J. Bowring, J. Geophys. Res. **94**, 9093 (1989).
Arai, S., M. Morita, K. Hironaka, N. Kouchi, N. Oda, and Y. Hatano, Abstracts of Contributed Papers, ICPEAC XIV, (SRI International, Menlo Park, 1985), p. 277.
Becker, K., and J. W. McConkey, Can. J. Phys. **62**, 1 (1984).
Becker, K., W. van Wijngaarden, and J. W. McConkey, Planet, Space Sci. **31**, 197 (1983).
Becker, K. H., E. H. Fink, and A. C. Allison, J. Opt. Soc. Am. **61**, 495 (1971).
Beenakker, C. I. M., and F. J. de Heer, Chem. Phys. **6**, 291 (1974).
Bell, K. L., D. J. Kennedy, and A. E. Kingston, J. Phys. B: At. Mol. Phys. **2**, 26 (1969).
Bethe, H., Ann. Physik **5**, 325 (1930).
Beyer, H. F., R. Hippler, K. -H. Schartner, and R. Albat, Z. Phys. A **289**, 239 (1979).
Bloemen, E. W. P., H. Winter, T. D. Mark, D. Dijkkamp, D. Barends, and F. J. de Heer, J. Phys. B: At. Mol. Phys. **14**, 717 (1981).
Böse, N., and W. Sroka, Z. Naturforsch, **26a**, 1491 (1971).
Böse, N., and W. Sroka, Z. Naturforsch. **28a**, 22 (1973).
Bransden, B. H. and M. R. C. McDowell, Phys. Rep. **46**, 249 (1978).
Brinkmann, R. T., and S. Trajmar, J. Phys. E: Sci. Instrum. **14**, 245 (1981).
Carrière, J. D. and F. J. de Heer, J. Chem. Phys. **56**, 2993 (1972).
Clout, P. N., and D. W. O. Heddle, J. Opt. Soc. Am. **59**, 715 (1969).
Cox, D. M. and S. J. Smith, Phys. Rev. A **5**, 2428 (1972).
Dassen, H., I. C. Malcolm, and J. W. McConkey, J. Phys. B: At. Mol. Phys. **10**, L493 (1977).
de Heer, F. J. and J. D. Carriére, J. Chem. Phys. **55**, 3829 (1971).
de Heer, F. J., H. R. Moustafa Moussa, and M. Inokuti, Chem. Phys. Lett. **1**, 484 (1967).
de Jongh, J. P., Ph.D. Thesis, University of Utrecht, Utrecht, The Netherlands, 1971 (unpublished).
de Jongh, J. P. and J. van Eck, Physica **51**, 104 (1971a).
de Jongh, J. P. and J. van Eck, Abstracts of Contributed Papers, ICPEAC VII, (North-Holland, Amsterdam, 1971b), p. 701.
Dijkkamp, D. and F. J. de Heer, J. Phys. B: At. Mol. Phys. **14**, 1327 (1981).
Dillon, M. A. and E. N. Lassettre, J. Chem. Phys. **62**, 2372 (1975).
Donaldson, F. G., M. A. Hender, and J. W. McConkey, J. Phys. B: At. Mol. Phys. **5**, 1192 (1972).
Dunn, G. H., Phys. Rev. Lett. **8**, 62 (1962).
Dunn, G. H., R. Geballe, and D. Pretzer, Phys. Rev. **128**, 2200 (1962).
Eckhardt, M. and K. -H. Schartner, Z. Phys. A **312**, 321 (1983).
Fano, U., Phys. Rev. **95**, 1198 (1954).
Filipelli, A. R., F. A. Sharpton, C. C. Lin, and R. E. Murphy, J. Chem. Phys. **76**, 3597 (1982).
Fischer, J., M. Kühne, and B. Wende, Appl. Opt. **23**, 4252 (1984).
Fite, W. L. and R. T. Brackmann, Phys. Rev. **112**, 1151 (1958).
Flaig, H. -J., K. -H. Schartner, and H. Kaase, Nucl. Instr. Meth. **208**, 405 (1983).
Forand, J. L., K. Becker, and J. W. McConkey, J. Phys. B: At. Mol. Phys. **18**, 1409 (1985).
Forand, J. L., K. Becker, and J. W. McConkey, Can. J. Phys. **64**, 269 (1986).
Forand, J. L., S. Wang, J. M. Woolsey, and J. W. McConkey, Can. J. Phys. **66**, 349 (1988).
Fremeney, J. K. J. Vac. Sci. Technol. A **3**, 1715 (1985).
Gabriel, A. H. and D. W. O. Heddle, Proc. Roy. Soc. London **258A**, 124 (1960).
Gaily, T. D. J. Opt. Soc. Am. **59**, 536 (1969).
Heddle, D. W. O., Adv. At. Mol. Phys. **15**, 381 (1979).
Heddle, D. W. O. and R. G. W. Keesing, Adv. At. Mol. Phys. **4**, 267 (1968).
Heddle, D. W. O. and J. W. Gallagher, Rev. Mod. Phys. **61**, 221 (1989).
Hertz, H. Z. Naturforsch. **24a**, 1937 (1969).
Hughey, L. R. and A. R. Schaefer, Nucl. Instr. Meth. **195**, 367 (1982).
Huschilt, J. C., H. W. Dassen, and J. W. McConkey, Can. J. Phys. **59**, 1893 (1981).
Inokuti, M., Rev. Mod. Phys. **43**, 297 (1971).
Inokuti, M., Y. Itikawa, and J. E. Turner, Rev. Mod. Phys. **50**, 23 (1978).
Itikawa, Y., M. Hayashi, A. Ichimura, K. Onda, K. Sakimoto, K. Takayanagi, M. Nakamura, N. Nishimura, and T. Takayanagi, J. Phys. Chem. Ref. Data **15**, 985 (1986).
Jobe, J. D. and R. M. St. John, Phys. Rev. **164**, 117 (1967).
Kauppila, W. E., P. J. O. Teubner, W. L. Fite, and R. J. Girnius, J. Chem. Phys. **55**, 1670 (1971).
Kendrick, R. L., A. McPherson, N. Rouze, W. B. Westerveld, and J. S. Risley, Appl. Opt. **26**, 2029 (1987).
Khakoo, M. A., and S. Trajmar, Phys. Rev. A **34**, 138 (1986).
Kim, Y. K., and M. Inokuti, Phys. Rev. **175**, 176 (1968).
Kühne, M. and B. Wende, J. Phys. E: Sci. Instrum. **18**, 637 (1985).
Lassettre, E. N. and S. M. Silverman, J. Chem. Phys. **40**, 1256 (1964).
Lassettre, E. N. and A. Skerbele, J. Chem. Phys. **54**, 1597 (1971).
Lawrence G. M., Phys. Rev. **175**, 40 (1968).
Lawrence, G. M. Phys. Rev. A **2**, 397 (1970).
Lee, P. J. Opt. Soc. Am. **45**, 703 (1955).
Li, G. P., T. Takayanagi, K. Wakiya, H. Suzuki, T. Ajiro, S. Yagi, S. S. Kano, and H. Takuma, Phys. Rev. A **38**, 1240 (1988a).
Li, G. P., T. Takayanagi, K. Wakiya, and H. Suzuki, Phys. Rev. A **38**, 1831 (1988b).
Ligtenberg, R., D. Graves, A. McPherson, N. Rouze, W. B. Westerveld, and J. S. Risley, EOS Trans. AGU **66**, 993 (1985).
Lloyd, C. R., P. J. O. Teubner, E. Weigold, and T. S. Hood, J. Phys. B: At. Mol. Phys. **5**, L44 (1972).
Long, R. L. Jr., D. M. Cox, and S. J. Smith, J. Res. NBS **72A**, 521 (1968).
Luyken, B. F. J., Physica **60**, 432 (1972).
Luyken, B. F. J., F. J. de Heer, and R. Ch. Baas, Physica **61**, 200 (1972).
Malcolm, I. C., H. W. Dassen, and J. W. McConkey, J. Phys. B: At. Mol. Phys. **12**, 1003 (1979).
Massey, H. S. W., *Encyclopedia of Physics, Volume 36* (Springer, Berlin, 1956) p. 354.
Massey, H. S. W. and D. R. Bates, *Applied Atomic Collision Physics, Volume 1, Atmospheric Physics and Chemistry* (Academic, New York, 1982).
McConkey, J. W. J. Opt. Soc. Am. **59**, 110 (1969).
McConkey, J. W., Argonne National Lab. Report, No. ANL84-28, p. 129, 1984.

McConkey, J. W. and F. G. Donaldson, Can. J. Phys. **50**, 2211 (1972).
McConkey, J. W. and F. G. Donaldson, Can. J. Phys. **51**, 914 (1973).
McConkey, J. W., H. W. Dassen, and J. C. Huschilt, J. Phys. B: At. Mol. Phys. **14**, L223 (1981).
McFarlane, S. C., J. Phys. B: At. Mol. Phys. **7**, 1756 (1974).
McGowan, J. W. and J. F. Williams, Abstracts of Contributed Papers, ICPEAC VI, (MIT, Cambridge, 1969), p. 431.
McGowan, J. W., J. F. Williams, and D. A. Vroom, Chem. Phys. Lett. **3**, 614 (1969).
McLaughlin, R. W. and E. C. Zipf, Chem. Phys. Lett. **55**, 62 (1978).
McPherson, A. Ph.D. Thesis, North Carolina State University, Raleigh, NC, 1984, unpublished.
McPherson, A., N. Rouze, W. B. Westerveld, and J. S. Risley, Appl. Opt. **25**, 298 (1986).
Mentall, J. E. and H. D. Morgan, J. Chem. Phys. **56**, 2271 (1972).
Mentall, J. E. and H. D. Morgan, Phys. Rev. A **14**, 954 (1976).
Mitchell, A. C. G. and M. W. Zemansky, *Resonance Radiation and Excited Atoms* (Cambridge University, New York, 1934).
Möhlmann, G. R., K. H. Shima, and F. J. de Heer, Chem. Phys. **28**, 331 (1978).
Moiseiwitsch, B. L. and S. J. Smith, Rev. Mod. Phys. **40**, 238 (1968).
Morgan, H. D. and J. E. Mentall, J. Chem. Phys. **60**, 4734 (1974).
Morgan, H. D. and J. E. Mentall, J. Chem. Phys. **78**, 1747 (1983).
Moustafa Moussa, H. R. and F. J. de Heer, Physica **36**, 646 (1967).
Moustafa Moussa, H. R., F. J. de Heer, and J. Schutten, Physica **40**, 517 (1969).
Mumma, M. J., J. Opt. Soc. Am. **62**, 1459 (1972).
Mumma, M. J. and E. C. Zipf, J. Chem. Phys. **55**, 1661 (1971a).
Mumma, M. J. and E. C. Zipf, J. Chem. Phys. **55**, 5582 (1971b).
Mumma, M. J. and E. C. Zipf, J. Opt. Soc. Am. **61**, 83 (1971c).
Mumma, M. J., E. J. Stone, W. L. Borst, and E. C. Zipf, J. Chem. Phys. **57**, 68 (1972).
Mumma, M. J., M. Misakian, W. M. Jackson, and J. L. Faris, Phys. Rev.A **9**, 203 (1974).
Nickel, J. C., P. W. Zetner, G. Shen, and S. Trajmar, J. Phys. E: Sci. Instrum. **22**, 730 (1989).
Nienhuis, G., in Coherence and Correlation in Atomic Collisions, edited by H. Kleinpoppen and J. F. Williams (Plenum, New York, 1980), p.121.
Ogawa, M., J. Geophys. Res. **73**, 6759 (1968).
Olander, D. R., and V. Kruger, J. Appl. Phys. **41**, 2769 (1970).
O'Neill, E. L., *Introduction to Statisical Optics* (Addison–Wesley, Reading, Mass., 1963).
Orient, O. J. and S. K. Srivastava, Chem. Phys. **54**, 183 (1981).
Ott, W. R., W. E. Kauppila, and W. L. Fite, Phys. Rev. Lett. **19**, 1361 (1967).
Ott, W. R., W. E. Kauppila, and W. L. Fite, Phys. Rev. A **1**, 1089 (1970).
Ott, W. R., L. R. Canfield, S. C. Ebner, L. R. Hughey, and R. P. Madden, SPIE **689**. 178 (1986)..
Papp, W. -F. Z., V. S. Shevera, and I. P. Zapesochnyi, JETP Lett. **25**, 29 (1977).
Pang, K. D., J. M. Ajello, B. Franklin, and D. E. Shemansky, J. Chem. Phys. **86**, 2750 (1987).
Pavlov, P. A. and V. E. Yakhontova, Opt. Spectrosc. (USSR) **39**, 130 (1975).
Percival, I. C. and M. J. Seaton, Phil. Trans. Roy. Soc. **A251**, 113 (1958).
Phillips, M. H., L. W. Anderson, and C. C. Lin, Phys. Rev. A **32**, 2117 (1985).
Plessis, P., W. Karras, M. A. Khakoo, P. Hammond, and J. W. McConkey, Bull, Am. Phys. Soc. **33**, 935 (1988).
Poulter, K. F., M. -J. Rodgers, P. J. Nash, T. J. Thompson, and M. P. Perkin, Vacuum **33**, 311 (1983).
Rall, D. L. A., A. R. Filippelli, F. A. Sharpton, S. Chung, and C. C. Lin, J. Chem. Phys. **87**, 2466 (1987).
Samson, J. A. R., J. Opt. Soc. Am. **54**, 6 (1964).
Samson, J. A. R., *Techniques of Vacuum Ultraviolet Spectroscopy* (Wiley, New York, 1967).
Schartner, K. -H., B. Kraus, W. Pöffel, and K. Reymann, Nucl. Instr. Meth. B **27**, 519 (1987).
Schiff, B. and C. L. Pekeris, Phys. Rev. **134**, A638 (1964).
Schiff, B., C. L. Pekeris, and Y. Accad., Phys. Rev. A **4**, 885 (1971).
Shemansky, D. E., J. M. Ajello, and D. T. Hall, Astrophys. J. **296**, 765 (1985a).
Shemansky, D. E., J. M. Ajello, D. T. Hall, and B. Franklin, Astrophys. J. **296**, 774 (1985b).
Srivastava, S. K., A. Chutjian, and S. Trajmar, J. Chem. Phys. **63**, 2659 (1975).
Sroka, W. Phys. Lett. **25A**, 770 (1967).
Sroka, W., Z. Naturforsch, **23a**, 2004 (1968).
Sroka, W., Z. Naturforsch. **24a**, 398 (1969a).
Sroka, W., Z. Naturforsch. **24a**, 1724 (1969b).
Sroka, W., Z. Naturforsch. **25a**, 1434 (1970).
Standage, M. C. J. Phys. B: At. Mol. Phys. **10**, 2789 (1977).
Stone, E. J. and E. C. Zipf, Phys. Rev. A **4**, 610 (1971).
Stone, E. J. and E. C. Zipf, J. Chem. Phys. **56**, 2870 (1972a).
Stone, E. J. and E. C. Zipf, J. Chem. Phys. **56**, 4646 (1972b).
Stone, E. J. and E. C. Zipf, J. Chem. Phys. **58**, 4278 (1973).
Stone, E. J. and E. C. Zipf, J. Chem. Phys. **60**, 4237 (1974).
Suzuki, H., Sing. J. Phys. **3**, 1 (1986).
Suzuki, H., T. Takayanagi, K. Morita, and Y. Iketaki in *Electron-Molecule Collisions and Photoionization Processes*, edited by V. McKoy, H. Suzuki, K. Takayanagi, and S. Trajmar (Verlag Chemie International, Florida, 1983), p. 43.
Tan, K. -H. and J. W. McConkey, Phys. Rev. A **10**, 1212 (1974).
Tan, K. -H., F. G. Donaldson, and J. W. McConkey, Can. J. Phys. **52**, 782 (1974).
Tilford, C. R., J. Vac. Sci. Technol. A **1**, 152 (1983).
Trajmar, S. and D. Register, in *Electon-Molecule Collisions*, edited by I. Shinamura and K. Takanayagi (Plenum, New York, 1984), p. 465.
Trajmar, S., D. Register, and A. Chutjian, Phys. Rep. **97**, 219 (1983).
Van Brunt, R. J. and R. N. Zare, J. Chem. Phys. **48**, 4304 (1968).
van Eck, J and J. P. de Jongh, Physica **47**, 141 (1970).
van Raan, A. F. J., Physica **65**, 566 (1973).
van Raan, A. F. J., J. P. de Jongh, and J. van Eck, Abstracts of Contributed Papers ICPEAC VII, (North-Holland, Amsterdam, 1971), p. 704.
van Sprang, H. A., H. H. Brongersma, and F. J. de Heer, Chem. Phys. Lett. **65**, 55 (1979).
Van Zyl, B., G. E. Chamberlain, G. H. Dunn, and S. Ruthberg, J. Vac. Sci. Technol. **13**, 721 (1976).
Van Zyl, F., G. H. Dunn, G. Chamberlain,a nd D. W. O. Heddle, Phys. Rev. A **22**, 1916 (1980).
Van Zyl, B., M. W. Gealy, and H. Neumann, Phys. Rev. A **31**, 2922 (1985).
Vroom, D. A. and F. J. de Heer, J. Chem. Phys. **50**, 573 (1969a).
Vroom, D. A. and F. J. de Heer, J. Chem. Phys. **50**, 580 (1969b).
Vroom, D. A. and F. J. de Heer, J. Chem. Phys. **50**, 1883 (1969c).
Watanabe, K., E. C. Y. Inn, and M. Zelikoff, J. Chem. Phys. **21**, 1026 (1953).
Weiss, A. W., J. Res. NBS **71a**, 163 (1967).
Wells, W. C., W. L. Borst, and E. C. Zipf, Chem. Phys. Lett. **12**, 288 (1971).
Westerveld, W. B., H. G. M. Heideman, and J. van Eck, J. Phys. B: At. Mol. Phys. **12**, 115 (1979).
Wiese, W. L., M. W. Smith, and B. M. Glennon, *Atomic Transition probabilities. Vol. 1. Hydrogen through Neon*, NSRDS-NBS 4 (U.S. GPO, Washington, D.C., 1966).
Williams, W., S. Trajmar, and A. Kuppermann, J. Chem. Phys. **62**, 3031 (1975).
Woolsey, J. M., J. L. Forand, and J. W. McConkey, J. Phys. B: At. Mol. Phys. **19**, L493 (1986).
Zapesochnyi,I. P., I. G. Zhukov, and P. V. Fel'tsan, Sov. Phys. JETP **38**, 675 (1974).
Zipf, E. C. in *Electron-Molecule Interactions and Their Applications, Volume I*, edited by L. G. Christophorou (Academic, Orlando, 1984), p. 335.
Zipf, E. C., J. Phys. B: At. Mol. Phys. **19**, 2199 (1986).
Zipf, E. C. and P. W. Erdman, J. Geophys. Res. **90**, 11087 (1985).
Zipf, E. C. and W. W. Kao, Chem. Phys. Lett. **125**, 394 (1986).
Zipf, E. C., R. W. McLaughlin, and M. R. Gorman, Planet. Space Sci. **27**, 719 (1979).
Zipf, E. C. W. W. Kao, and R. W. McLaughlin, Chem. Phys. Lett. **118**, 591 (1985).

Appendix A. Instrumental Polarization and the Detection of Photons

When photons are detected with a spectrometer-photomultiplier combination, two polarization effects enter the relationship between the photoemission cross section and the photon count rate. First, the photoemission by excited

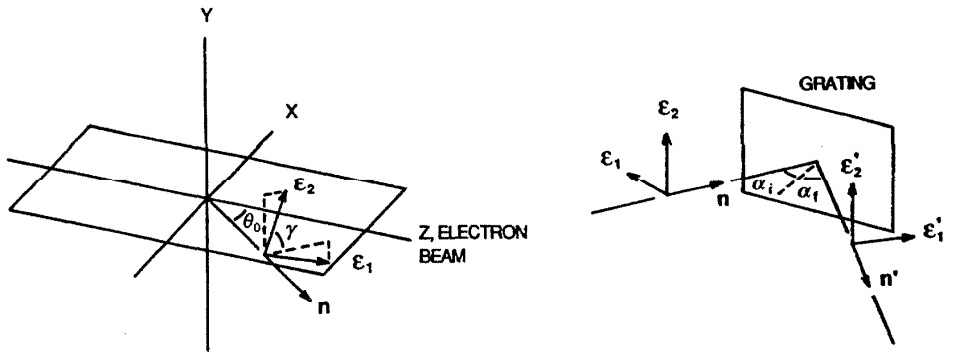

FIG. 7. (a) Coordinate system used to describe emission of light by excited atoms. The z-axis is coincident with the electron beam. Photons emitted at an angle ϑ_0 pass through the entrance slit of the spectrometer. (b) Coordinate systems used to describe reflection of light by the spectrometer grating. Photons incident in the direction **n** are reflected by the grating into the direction **n'** towards the exit slit.

atoms is in general anisotropic, so the photon count rate depends on the direction of observation of the photons. Second, the emitted photons are polarized, so any polarization sensitivity of the reflection at the grating in the spectrometer or the cathode of the photomultiplier will affect the observed photon count rate. For electric-dipole radiation the anisotropy and the polarization of the emitted radiation are correlated (Eq. 2.4). In this appendix we derive an expression for the photon count rate that contains these polarization effects and we show how polarization effects can be eliminated. We employ the coherency matrix formalism (see O'Neill 1963) in the derivation.

A.1. Emission of Light from Excited Atoms

Consider an ensemble of unpolarized atoms, subject to excitation by electron impact. The intensity and polarization of photons emitted upon decay of excited atoms can be described by a 3×3 cartesian polarization matrix **C** that determines the photon emission in every direction with any polarization (see Nienhuis 1980). The elements of the polarization matrix are proportional to the electric-dipole operator between the excited state and the final state of the atom and the density matrix elements of the excited state. Scattered electrons are not detected in measurements of photoemission cross sections. Due to azimuthal symmetry of the excited atoms around the quantization axis [z-axis, coinciding with the electron beam, see Fig. 7(a)] the off-diagaonal elements of the polarization matrix are zero. The polarization matrix can in this case be expressed in measurable quantities as

$$\mathbf{C}=\frac{1}{2}I(90°)\begin{pmatrix}1-\Pi & 0 & 0\\ 0 & 1-\Pi & 0\\ 0 & 0 & 1+\Pi\end{pmatrix}. \qquad (A.1)$$

where $I(90°)$ and Π are the intensity and linear polarization, respectively, of the photons emitted perpendicular to the electron beam. $I(90°)$ is related to the total intensity, according to Eq. (2.4):

$$I(90°)=\frac{I_{\text{tot}}}{4\pi(1-\frac{1}{3}\Pi_{ij})}.$$

We now introduce the right-handed set of unit vectors $\{\boldsymbol{\epsilon}_1,\boldsymbol{\epsilon}_2,\mathbf{n}\}$ [see Fig. 7(a)], where $\mathbf{n}=(-\sin\theta_0,0,\cos\theta_0)$ is the direction of the optic axis of the spectrometer, $\boldsymbol{\epsilon}_1=(\sin\gamma\cos\theta_0,-\cos\gamma,\sin\gamma\sin\theta_0)$ is perpendicular to the entrance slit of the spectrometer, and $\boldsymbol{\epsilon}_2=(\cos\gamma\cos\theta_0,\sin\gamma,\cos\gamma\sin\theta_0)$ is parallel to the entrance slit. The entrance slit is at an angle γ with respect to the plane containing the electron beam and the optic axis.

The 2×2 density matrix **c** (known in optics as the coherency matrix, see O'Neill 1963) for the photons emitted in the direction **n** has elements given by $c_{ij}=\boldsymbol{\epsilon}_i\cdot\mathbf{C}\cdot\boldsymbol{\epsilon}_j$, i.e.:

$$\mathbf{c}=\frac{1}{2}I(90°)\begin{pmatrix}1-\Pi\cos^2\theta_0-\Pi\sin^2\theta_0\cos2\gamma & \Pi\sin^2\theta_0\sin2\gamma\\ \Pi\sin^2\theta_0\sin2\gamma & 1-\Pi\cos^2\theta_0+\Pi\sin^2\theta_0\cos2\gamma\end{pmatrix} \qquad (A.2)$$

The density matrix **c** can be expressed in terms of the Stokes parameters of the light emitted in the direction **n**:

$$\mathbf{c}=\frac{1}{2}\begin{pmatrix}S_0+S_1 & S_2-iS_3\\ S_2+iS_3 & S_0-S_1\end{pmatrix}, \qquad (A.3)$$

from which

$$S_0=I(90°)(1-\Pi\cos^2\theta_0)$$

$$S_1=-I(90°)\Pi\sin^2\theta_0\cos2\gamma$$

$$S_2=I(90°)\Pi\sin^2\theta_0\sin2\gamma$$

$$S_3=0. \qquad (A.4)$$

A.2. Reflection of Light by the Spectrometer Grating

According to the coherency matrix formalism the transformation law for the density (coherency) matrix for

light passing through an optical instrument is

$$\mathbf{c}' = \mathbf{A}\mathbf{c}\mathbf{A}^{\dagger}, \tag{A.5}$$

where $\mathbf{A}$ is the Jones matrix representing the operation of the optical instrument. For reflection from a grating, the Jones matrix has the form

$$\mathbf{A} = \begin{pmatrix} r_{\perp}\exp(i\delta_{\perp}) & 0 \\ 0 & r_{\parallel}\exp(i\delta_{\parallel}) \end{pmatrix}. \tag{A.6}$$

Here, $r_{\perp}\exp(i\delta_{\perp})$ and $r_{\parallel}\exp(i\delta_{\parallel})$ are the complex reflection coefficients for light polarized perpendicular and parallel to the grating grooves, respectively. For reflection from a flat surface the reflection coefficients can be expressed in terms of the complex index of refraction of the medium. However, interference greatly complicates the details of the reflection from a grating, and in general the expression for reflection from a flat surface cannot be assumed valid.

The density matrix for the reflected light follows from Eq. (A.5):

$$\mathbf{c}' = \frac{1}{2}I(90°)\begin{pmatrix} r_{\perp}^2(1-\Pi\cos^2\theta_0-\Pi\sin^2\theta_0\cos 2\gamma) & r_{\perp}r_{\parallel}e^{i\delta_{\perp}-i\delta_{\parallel}}\Pi\sin^2\theta_0\sin 2\gamma \\ r_{\perp}r_{\parallel}e^{-i\delta_{\perp}+i\delta_{\parallel}}\Pi\sin^2\theta_0\sin 2\gamma & r_{\parallel}^2(1-\Pi\cos^2\theta_0+\Pi\sin^2\theta_0\cos 2\gamma) \end{pmatrix} \tag{A.7}$$

This density matrix is given with respect to $\boldsymbol{\epsilon}_1'$, $\boldsymbol{\epsilon}_2'$, and $\mathbf{n}'$ [see Fig. 7(b)], where $\mathbf{n}'$ is the direction of the reflected radiation passing through the exit slit of the spectrometer, $\boldsymbol{\epsilon}_1'$ is perpendicular to the exit slit, and $\boldsymbol{\epsilon}_2'$ is parallel to the exit slit.

A.3. Detection of Light by the Photomultiplier

Assume that the photomultiplier is insensitive to polarization and has an efficiency e_0 for the total intensity of the light incident on the cathode. In this case the photomultiplier can be characterized by the efficiency matrix $\mathbf{E}$

$$\mathbf{E} = \frac{1}{2}\begin{pmatrix} e_0 & 0 \\ 0 & e_0 \end{pmatrix}. \tag{A.8}$$

The detected sign $S(\theta_0,\gamma)$ follows from

$$\begin{aligned} S(\vartheta_0,\gamma) &= \mathrm{Tr}(\mathbf{E}\mathbf{c}') = \sum_{klij} E_{kl}A_{li}\boldsymbol{\epsilon}_i\cdot\mathbf{C}\cdot\boldsymbol{\epsilon}_j A^{*}_{kj} \\ &= \frac{1}{2}I(90°)\left\{\frac{1}{2}e_0(r_{\perp}^2+r_{\parallel}^2)(1-\Pi\cos^2\theta_0)+\frac{1}{2}e_0(r_{\perp}^2-r_{\parallel}^2)(-\Pi\sin^2\theta_0\cos 2\gamma)\right\} \end{aligned} \tag{A.9}$$

The products $\frac{1}{2}e_0r_{\perp}^2$ and $\frac{1}{2}e_0r_{\parallel}^2$ are abbreviated to $k_{\perp}$ and $k_{\parallel}$, respectively, representing the efficiencies for detection of light linearly polarized perpendicular and parallel to the grating grooves (see Sec. 2.2). Eq. (A.9) takes a simpler form

$$\begin{aligned} S(\theta_0,\gamma) = \frac{1}{2}I(90°)\{&(k_{\perp}+k_{\parallel})(1-\Pi\cos^2\theta_0) \\ &+(k_{\perp}-k_{\parallel})(-\Pi\sin^2\theta_0\cos 2\gamma)\} \end{aligned} \tag{A.10}$$

As is shown by Clout and Heddle (1969), the effects of polarization can be eliminated from the photon count rate by choosing suitable values for the angles θ_0 and γ. For $\theta_0 = 54.7°$ and $\gamma = 45°$, Eq. (A.10) in combination with Eq. (2.4) results in

$$\begin{aligned} S(54.7°,45°) &= \frac{1}{2}I(90°)(k_{\perp}+k_{\parallel})(1-\tfrac{1}{3}\Pi) \\ &= \frac{I_{\mathrm{tot}}}{4\pi}\frac{1}{2}(k_{\perp}+k_{\parallel}). \end{aligned} \tag{A.11}$$

In most experiments photons are observed perpendicular to the electron beam with the entrance slit of the spectrometer perpendicular to the electron beam. In that situation $\theta_0 = 90°$ and $\gamma = 90°$, and Eq. (A.10) results in

$$\begin{aligned} S(90°,90°) &= \frac{1}{2}I(90°)\{(k_{\perp}+k_{\parallel})+\Pi(k_{\perp}-k_{\parallel})\} \\ &= \frac{I_{\mathrm{tot}}}{4\pi(1-\frac{1}{3}\Pi)}\frac{1}{2}\{(1+\Pi)k_{\perp}+(1-\Pi)k_{\parallel}\}. \end{aligned} \tag{A.12}$$

Eqs. (A.11) and (A.12) are equivalent to Eqs. (2.9) and (2.13), respectively, and are discussed in more detail in Sec. 2.2

Finally we consider the case that the photomultiplier is sensitive to linear polarization or to circular polarization. In the most general situation the efficiency matrix is

$$\mathbf{E} = \frac{1}{2}\begin{pmatrix} e_0+e_1 & e_2-ie_3 \\ e_2+ie_3 & e_0-e_1 \end{pmatrix}. \tag{A.13}$$

By deriving the photon count rate from $S(\theta_0,\gamma) = \mathrm{Tr}(\mathbf{E}\mathbf{c}')$ it can be seen that terms with $\exp(i\delta_{\perp}-i\delta_{\parallel})$ enter the expression for the photon count rate. As a result the efficiencies $k_{\perp}$ and $k_{\parallel}$ are insufficient to characterize the spectrometer-detector system and the method of Clout and Heddle (1969) cannot be used to eliminate the effects of polarization. However, if the multiplier is sensitive only to linear polarization (i.e., $e_3 = 0$) and is properly oriented behind the exit slit (such that $e_2 = 0$), the method of Clout and Heddle (1969) can be used.

Appendix B. Summary of Experiments by Different Researchers

In this appendix we summarize the experimental equipment and procedures used by the groups that performed electron impact photoemission cross section measurements.

B. 1. Ajello and Co-workers

Photon Detection

Spectrometer: *1970s:* McPherson model 218, Czerney–Turner type, MgF_2 coated grating, 1.39 nm/mm; *1980s:* McPherson model 234, Seya Namioka type, MgF_2 coated grating for 115–550 nm and osmium coated grating for 50–550 nm, 3.4 nm/mm.

Detector: *1970s:* 541 G-08-18 EMR photomultiplier tube, MgF_2 window with CsI photocathode; *1980s:* Galileo Optics 4503 channel electron multiplier for 50–120 nm, EMI Gencom G photomultiplier with CsI photocathode and MgF_2 window for 115–220 nm, EMR photoelectric F photomultiplier with CsTe cathode and MgF_2 window for 115–300 nm.

Polarization: (He) photons detected at 54.7°, corrected for instrumental polarization; (other gases) photons detected at 90°, not corrected.

Target Gases

Gases used: *1970s:* static gas: N_2, O_2, CO, CO_2; *1980s:* crossed beams: He, H_2, N_2, O_2, H_2O, CS_2, CH_4, C_2H_2.

Gas density: *1970s:*: ionization gauge calibrated against a McLeod gauge; *1980s:* (CS_2) absolute pressure measurement with MKS Baratron capacitance manometer in static gas experiment; (other gases) relative gas-flow technique.

Normalization

Relative spectral response: *1970s:* (N_2) double-monochromator technique; (O_2, CO, CO_2) molecular branching ratio technique for N_2(LBH) bands; *1980s:* 40–130 nm: relative intensities of the H_2 Rydberg band systems (predominantly Werner and Lyman bands) and double-monochromator technique; 127–210 nm: molecular branching-ratio technique for N_2 LBH bands.

Normalization: *1970s:* (N_2) absolute calibration at Lyman-α using an NO ionization chamber; (O_2, CO, CO_2) to CO (159.7 nm band) cross section from Aarts and de Heer (1970); *1980s:* (CS_2) to H_2(H I Ly-α) cross section from Mumma and Zipf (1971a); (He, N_2, O_2, H_2O) to H_2(H I Ly-α) cross section from Shemansky *et al.* (1985a); (CH_4, C_2H_2) to an average of values of the H_2(H I Ly-α) cross section from Shemansky *et al.*, Van Zyl *et al.* (1985), Ligtenberg *et al.* (1985), and Woolsey *et al.* (1986).

References

*1970s:*Ajello (1970), Ajello (1971a, b, c); *1980s:* Ajello and Srivastava (1981), Ajello *et al.* (1982), Ajello (1984), Ajello *et al.* (1984), Ajello and Franklin (1985), Ajello and Shemansky (1985), Shemansky *et al.* (1985a, b), Pang *et al.* (1987), Ajello *et al.* (1988, 1989).

B.2. Van Eck and Co-workers

Photon Detection

Spectrometer: (1970–1973) grazing incidence, Paschen Runge type, Al grating 3.33 nm/mm; (1979) near normal incidence, Pt coated grating 0.83 nm/mm.

Detector: EMI 9642 open particle multiplier.

Polarization: (He) corrected or eliminated by experimental set up; (Ne, Ar, Kr, Xe) photons detected at 90°, unpolarized transitions.

Target Gases

Gases used: He, Ne, Ar, Kr, Xe.

Gas density: ionization gauge calibrated against a McLeod gauge or an MKS Baratron capacitance manometer.

Normalization

(He I) Bethe–Born approximation with theoretical optical oscillator strengths and experimental c_n; (Ne II, Ar II, Kr II, Xe II) used cross sections for noble gas resonance lines, normalized by using experimental optical oscillator strengths from de Jongh and van Eck (1971a).

References

Van Eck and de Jongh (1970), de Jongh (1971), de Jongh and van Eck (1971a, b) van Raan *et al.* (1971), van Raan (1973), Westerveld *et al.* (1979).

B.3. Fite and Co-workers

Photon Detection

Spectrometer: none used.

Detector: I_2 filled Geiger–Müller counter with LiF-O_2 filter.

Polarization: (1958) data taken at 90° and 54.7°, (1971) corrected, measured by Ott *et al.* (1970).

Target Gases

Gases used: crossed beams, chopped atomic beam: H, H_2.

Gas density: dissociation fraction determined by monitoring atomic and molecular ions formed with (1958) a mass spectrometer or (1971) a quadrupole mass filter.

Normalization

(1958) to first Born approximation for H $1s \rightarrow 2p$ from Massey (1956); (1971) to H I(Ly-α) cross section from Long *et al.* (1968).

References

Fite and Brackmann (1958), Ott *et al.* (1970), Kauppila *et al.* (1971).

B.4. de Heer and Co-workers

Photon Detection

Spectrometer: vacuum monochromator (both normal and grazing incidence, custom built), MgF_2 coated grating, 0.83 nm/mm.

Detector: EMI 6256 S photomultiplier, sodium salicylate coated cathode.

Polarization: not corrected.

Target Gases

Gases used: static gas: He, Ne, Ar, Kr, Xe, H_2, D_2, N_2, O_2, CO, H_2O, CH_4, CD_4, C_2H_2, C_2H_4, C_2H_6, C_6H_6.

Gas density: McLeod gauge; ionization gauge calibrated against an MKS Baratron capacitance manometer.

Normalization

(He I 58.4 nm) theoretical oscillator strength and Bethe approximation.

(He II) interpolation (and extrapolation) between H_2(H I Ly-α) from Fite and Brackmann (1958) and He I(53.7 nm) radiation from $He^+ + Ne$ collisions.

(H_2, D_2, H_2O, hydrocarbons) H_2(H I Ly-α) cross section from Fite and Brackmann (1958).

(CO) inelastic scattering data for CO(159.7 nm band) from Lassettre and Silverman (1964) and Lassettre and Skerbele (1971).

(N_2, H_2, Ne, Ar, Kr, Xe) 127–180 nm: N_2 (LBH) branching-ratio method, normalization to CO(159.7 nm band) from Aarts and de Heer (1970); 103–124 nm: oscillator strengths for H_2 Werner bands; 65–100 nm: interpolation and normalization to noble gas cross sections from de Jongh and van Eck (1971a) and van Raan (1973).

(Ne II) most recently (1981): Bethe approximation.

References

Moustafa Moussa and de Heer (1967), Moustafa Moussa *et al.* (1969), Vroom and de Heer (1969a, b, c), Aarts and de Heer (1970), Aarts and de Heer (1971a, b), de Heer and Carrière (1971), Carrière and de Heer (1972), Luyken *et al.* (1972), Beenakker and de Heer (1974), Möhlmann *et al.* (1978), van Sprang *et al.* (1979), Bloemen *et al.* (1981), Dijkkamp and de Heer (1981).

B.5. Lawrence

Photon Detection

Spectrometer: McPherson model 225 near normal incidence.

Detector: Amperex 56P17 multiplier, CsI coated cathode.

Polarization: unpolarized transitions.

Target Gases

Gases used: static gas: O_2, CO, NO, H_2O.

Gas density: MKS Baratron capacitance manometer.

Normalization

To (O I 844.7 nm) cross section by means of a cascade analysis of the 130.4 nm time decay curve. The (O I 844.7 nm) cross section was measured absolutely by using a blackbody as radiation intensity standard.

References

Lawrence (1968, 1970).

B.6. McConkey and Co-workers

Photon Detection

Spectrometer: Seya-Namioka type, below 120 nm: Au coated grating, 1.7 nm/mm, above 120 nm: Al grating overcoated with MgF_2, 34 nm/mm.

Detector: Mullard channel electron multiplier, Galileo Optics BX7600 4413 channel electron multiplier, CSI cathode and a MgF_2 window.

Polarization: (He, Ne, Ar) eliminated by experimental set up; (H_2) corrected; (N_2, SO_2, SF_6) data taken at 90° and not corrected.

Target Gases

Gases used: crossed beams: He, Ne, Ar, H_2, D_2, N_2, SO_2, SF_6.

Gas density: (Ar, SO_2) comparison of slopes of intensity versus pressure; (SF_6, Ar, N_2; since 1986) relative gasflow technique; (H_2) dissociative fraction determined by comparison of intensity of molecular bands near Lyman-α with discharge source on and off.

Normalization

(He, Ne, Ar) theoretical and experimental optical oscillator strengths from Schiff and Pekeris (1964), Weiss (1967), de Jongh and van Eck (1971a), and others.

(He II) to He I resonance transitions.

(Ar II) to Ar II cross sections from van Raan (1973).

(Ar I, II) most recently (1988): to H_2(H I Ly-α) cross section from Woolsey *et al.* (1986). Relative spectral response: relative intensities of atomic hydrogen Lyman series and H_2 Rydberg band systems.

(N_2) to N_2(N I 120.0 nm) cross section from Mumma and Zipf (1971b); most recently (1988) to H_2(H I Ly-α) cross section from Woolsey *et al.* (1986).

(H_2) to H I(Ly-α) cross section from Long *et al.* (1968).

(SO_2, D_2, SF_6) above 117 nm: molecular branching-ratio technique for CO fourth positive system bands and H_2 Werner bands, normalization to H_2(H I Ly-α) cross section from Mumma and Zipf (1971a) or average of Van Zyl *et al.* (1985), Shemansky *et al.* (1985), and Ligtenberg *et al.* (1985); below 117 nm: normalization to various noble gas cross sections (see Section 4.12).

References

McConkey and Donaldson (1972, 1973), Donaldson *et al.* (1972), Tan and McConkey (1974), Tan *et al.* (1974),

Dassen *et al.* (1977), Malcolm *et al.* (1979), Huschilt *et al.* (1981), McConkey *et al.* (1981), Becker *et al.* (1983), Becker and McConkey (1984), Forand *et al.* (1985, 1986), Woolsey *et al.* (1986), Forand *et al.* (1988), Plessis *et al.* (1988).

B.7. Mentall and Morgan

Photon Detection

Spectrometer: McPherson 220 and 225, near normal incidence.

Detector: EMR 541 F-08-18 solar blind photomultiplier and Bendix 4700 channel electron multiplier.

Polarization: photons detected at 90°, not corrected; Ar measurements taken at 54.7°.

Target Gases

Gases used: static gas: N_2, O_2, NO, H_2O, NH_3, CH_4; crossed beams: Ar.

Gas density: MKS Baratron capacitance manometer.

Normalization

(NO, H_2O, NH_3, CH_4) relative spectral response: molecular branching-ratio technique for N_2 LBH bands and H_2 Werner bands, normalization to O_2 (O I 130.4 nm) cross section from Mumma and Zipf (1971a), Lawrence (1970), and Aarts and de Heer (1971b).

(Ar, N_2, O_2) relative spectral response: double-monochromator technique, normalization to N_2(N I 120 nm) cross section from Mumma and Zipf (1971b).

References

Mentall and Morgan (1972, 1976), Morgan and Mentall (1974, 1983).

B.8. Risley and Westerveld and Co-Workers

Photon Detection

Spectrometer: Minuteman model 302 VM, Seya-Namioka type, type IV J-Y holographic grating with an Al substrate overcoated with MgF_2, 1200 lines/mm, 4.0 nm/mm.

Detector: EMI model 9642/4B venetian blind PMT with a BeCu cathode.

Polarization: corrected.

Target Gases

Gases used: static gas: Ar, H_2, He.

Gas density: ionization gauge calibrated against a MKS Baratron capacitance manometer.

Normalization

Absolute calibration of spectrometer-detector system with synchrotron radiation.

References

McPherson (1984), Ligtenberg *et al.* (1985), McPherson *et al.* (1986),Kendrick *et al.* (1987).

B.9. Schartner and Co-workers

Photon Detection

Spectrometer: McPherson model 225, near normal incidence, Pt coated grating, 0.83 nm/mm.

Detector: channel electron multiplier.

Polarization: eliminated by experimental setup.

Target Gases

Gases used: static gas: Ne, Ar.

Gas density: ionization gauge, MKS Baratron capacitance manometer.

Normalization

Relative spectral response: atomic branching-ratio technique, synchrotron radiation.

Normalization: to Bethe–Born approximation with theoretical oscillator strengths from Inokuti (1971) and de Jongh and van Eck (1971).

References

Beyer *et al.* (1979), Eckhardt and Schartner (1983), Flaig *et al.* (1983),Schartner *et al.* (1987).

B.10. Smith and Co-workers

Photon Detection

Spectrometer: none used.

Detector: NO filled ion chamber with a MgF_2 window.

Polarization: not corrected, photons detected at 90°.

Target Gases

Gases used: crossed beams: H.

Pressure: ionization gauge.

Normalization

To first Born approximation at 200 eV with cascade correction, from Moiseiwitsch and Smith (1968).

References

Long *et al.* (1968), Cox and Smith (1972).

B.11. Sroka and Co-workers

Photon Detection

Spectrometer: McPherson 235, Seya Namioka type with Pt coated grating.

Detector: Bendix M306 photomultiplier with a W cathode, EMI 9502S photomultiplier with a sodium salicylate coating.

Polarization: photons detected at 90°, not corrected.

Target Gases

Gases used: static gas: Ne, N_2, O_2, CO_2, H_2O, CH_4, NH_3.

Gas density: MKS Baratron capacitance manometer.

Normalization

Relative spectral response of grating and photomultiplier cathode determined from literature.

Normalization: (N_2, O_2, CH_4, CO_2) to He (He I 58.4 nm) cross section from Jobe and St. John (1967) and Gabriel and Heddle (1960); (CO_2) to H_2 (H I Ly-α) cross section from Carrière and de Heer (1972); (NH_3) to H_2(H I Ly-α) cross section from Vroom and de Heer (1969b).

References

Sroka (1967, 1968, 1969a, b, 1970), Hertz (1969), Böse and Sroka (1971, 1973).

B.12. Suzuki and Co-workers

Photon Detection

Spectrometer: Seya Namioka type.

Detector: channel electron multiplier, channel plate.

Polarization: (1983) photons detected at 54.7°; (1988) eliminated by experimental set up.

Target Gases

Gases used: crossed beams: Ar, Kr, Xe.

Gas density: ionization gauge.

Normalization

(Kr, Xe) to excitation cross sections for some Xe I resonance transitions from Williams *et al.* (1975). Relative spectral response: relative intensities of H Lyman series in $e + NH_3$ scattering.

(Ar) to excitation cross section for the Ar I(106.7 nm) transition from Li *et al.* (1988a). Relative spectral response: relative intensities of H_2 Werner and Lyman bands.

References

Suzuki *et al.* (1983), Suzuki (1986), Li *et al.* (1988b).

B.13. Van Zyl and Co-workers

Photon Detection

Spectrometer: none used.

Detector: solar blind photomultiplier with MgF_2 window and a LiF-O_2 filter.

Polarization: corrected using data from Ott *et al.* (1970).

Target Gases

Gases used: static gas: H_2.

Pressure: calibrated MKS Baratron capacitance manometer.

Normalization

Lyman-α radiation from H + Ne collisions is measured as a function of the detector position in the target cell and fitted to a model for the population of H($2p$) by direct excitation and cascade.

References

Van Zyl *et al.* (1985).

B.14. Zipf and Co-workers

Photon Detection

Spectrometer: McPherson 225 near normal incidence.

Detector: EMR 541 G-08-18 photomultiplier, EMR541 GX solar blind photomultiplier, and a Johnston MM-1 multiplier.

Polarization: photons detected at 90°, not corrected.

Target Gases

Gases used: static gas: N, O, N_2, H_2, O_2, CO_2, CH_4.

Gas density: absolute pressure measurement with MKS Baratron capacitance manometer, ionization gauge calibrated against a McLeon gauge; (O, N) observed atomic resonance absorption or used a quadrupole mass spectrometer.

Normalization

Relative spectral response: (H_2, N_2, O_2, CO_2) molecular branching-ratio technique for N_2 LBH bands and relative intensities for N I transitions; (NO, N, O) molecular branching-ratio technique for N_2 LBH bands and HD Lyman bands excited with Ar resonance radiation; (O_2, CH_4) molecular branching-ratio technique for H_2 Werner bands.

Normalization: (H_2) to H I(Ly-α) cross section from Long *et al.* (1968); (N_2, O_2, CO_2, N) to H_2(H I Ly-α) cross section from Mumma and Zipf (1971a); (O) to average of O_2(O I 130.4 nm) cross sections from Mumma and Zipf (1971a), Ajello (1971a),Lawrence (1970) and Stone and Zipf (1974); (O, since 1985) to H_2(H I Ly-α) cross section from Risley (private communication to Zipf, 1985); (O_2, CH_4) to N_2(N I 120.0 nm) cross section from Mumma and Zipf (1971b); (NO) to NO(O I 130.4 nm) cross section from Lawrence (1970).

References

Mumma and Zipf (1971a, b, c), Wells *et al.* (1971), Mumma (1972),Mumma *et al.* (1972, 1974), Stone and Zipf (1971, 1972a, b, 1973, 1974), McLaughlin and Zipf (1978), Zipf *et al.* (1979), Zipf (1984), Zipf and Erdman (1985), Zipf *et al.* (1985) Zipf (1986), Zipf and Kao (1986).

Appendix C. List of Reported Photoemission Cross Sections in the Extreme Ultraviolet

Table C1. List of reported photoemission cross sections in the extreme ultraviolet

Wavelength (nm)	Target gas	Species	Energy (eV)	Cross section (10^{-18} cm^2)	Authors
25.6	He	He II	300	0.0268	Moustafa Moussa and de Heer (1967)
30.4	He	He II	200	0.56	Bloemen et al. (1981)
30.4	He	He II	300	0.58	Forand et al. (1985)
30.4	He	He II	300	0.307	Moustafa Moussa and de Heer (1967)
37.9	Ne	Ne III	200	0.03	Papp et al. (1977)
42.5 – 43.0	O_2	O II	200	0.021	Ajello and Franklin (1985)
43.7 – 44.6	O_2	O II	200	0.032	Ajello and Franklin (1985)
43.7 – 44.6	SO_2	O II	150	0.15	Becker et al. (1983)
46.1	Ne	Ne II	300	5.21	van Raan (1973)
46.1 – 46.2	Ne	Ne II	1000	1.65	Beyer et al. (1979)
46.1 – 46.2	Ne	Ne II	300	2.13	Dijkkamp and de Heer (1981)
46.1 – 46.2	Ne	Ne II	300	2.9	Eckhardt and Schartner (1983)
46.1 – 46.2	Ne	Ne II	300	7.82	Luyken et al. (1972)
46.1 – 46.2	Ne	Ne II	200	19.	Zapesochnyi et al. (1974)
46.2	Ne	Ne II	300	2.61	van Raan (1973)
46.4 – 47.0	O_2	O II	200	0.023	Ajello and Franklin (1985)
47.3	SF_6	F II	200	0.016	Forand et al. (1986)
48.2 – 48.6	H_2O	O II	200	0.008	Ajello (1984)
48.2 – 48.6	O_2	O II	200	0.106	Ajello and Franklin (1985)
48.7	Ar	Ar II	100	0.42	Tan and McConkey (1974)
48.9	Ar	Ar II	100	0.56	Tan and McConkey (1974)
49.0	Ne	Ne III	200	0.21	Eckhardt and Schartner (1983)
49.0	Ne	Ne III	200	0.34	Papp et al. (1977)
49.1	Ar	Ar II	100	0.48	Tan and McConkey (1974)
49.2	Ar	Ar II	100	0.05	Tan and McConkey (1974)
50.0	O_2	O II	200	0.023	Ajello and Franklin (1985)
51.5 – 51.8	O_2	O II	200	0.072	Ajello and Franklin (1985)
51.5	SF_6	F II	400	0.0079	Forand et al. (1986)
51.6 – 51.8	H_2O	O II	200	0.004	Ajello (1984)
51.9	Ar	Ar II	100	0.91	Tan and McConkey (1974)
52.2	He	He I	300	0.72	Donaldson et al. (1972)
52.2	He	He I	300	0.69	van Eck and de Jongh (1970)
52.2	He	He I	300	0.739	de Jongh and van Eck (1971b)
52.2	He	He I	200	0.89	Shemansky et al. (1985b)
52.3	Ar	Ar II	100	0.49	Tan and McConkey (1974)
52.5	Ar	Ar II	100	0.44	Tan and McConkey (1974)
52.7	Ar	Ar II	100	0.09	Tan and McConkey (1974)
53.0	Ar	Ar II	100	0.18	Tan and McConkey (1974)
53.7	He	He I	300	1.94	Donaldson et al. (1972)
53.7	He	He I	300	1.85	van Eck and de Jongh (1970)
53.7	He	He I	300	1.82	de Jongh and van Eck (1971b)
53.7	He	He I	200	2.12	Shemansky et al. (1985b)
53.7	He	He I	300	1.83	Westerveld et al. (1979)
53.8 – 54.0	H_2O	O II	200	0.047	Ajello (1984)
53.8 – 54.0	H_2O	O II	100	0.03	Böse and Sroka (1973)
53.8 – 54.0	O_2	O II	200	0.689	Ajello and Franklin (1985)
53.8 – 54.0	O_2	O II	200	0.7	Morgan and Mentall (1983)
53.8 – 54.0	SO_2	O II	320	0.087	Becker et al. (1983)
54.29	Ar	Ar II	100	0.43	Tan and McConkey (1974)
54.3	Ar	Ar II	500	0.79	Schartner et al. (1987)
54.32	Ar	Ar II	100	0.71	Tan and McConkey (1974)
54.37	Ar	Ar II	100	0.25	Tan and McConkey (1974)
54.6	Ar	Ar II	100	0.17	Tan and McConkey (1974)
54.7	Ar	Ar II	500	0.57	Schartner et al. (1987)

Table C1. List of reported photoemission cross sections in the extreme ultraviolet -- Continued

Wavelength (nm)	Target gas	Species	Energy (eV)	Cross section (10^{-18} cm^2)	Authors
54.72	Ar	Ar II	100	0.23	Tan and McConkey (1974)
54.75	Ar	Ar II	100	0.49	Tan and McConkey (1974)
54.8	Ar	Ar II	100	0.16	Tan and McConkey (1974)
54.8	SF_6	F II	400	0.012	Forand et al. (1986)
54.9	Ar	Ar II	100	0.06	Tan and McConkey (1974)
55.0	Ar	Ar II	100	0.03	Tan and McConkey (1974)
55.1	Ar	Ar II	100	0.02	Tan and McConkey (1974)
55.5	H_2O	O II	200	0.029	Ajello (1984)
55.5	H_2O	O II	100	0.02	Böse and Sroka (1973)
55.5	O_2	O II	200	0.219	Ajello and Franklin (1985)
55.5	O_2	O II	200	0.156	Morgan and Mentall (1983)
57.2	Ar	Ar II	100	0.27	Tan and McConkey (1974)
57.3	Ar	Ar II	100	1.24	Tan and McConkey (1974)
57.7	Ar	Ar II	100	0.52	Tan and McConkey (1974)
57.8	Ar	Ar II	100	0.69	Tan and McConkey (1974)
58.0	Ar	Ar II	100	1.33	Tan and McConkey (1974)
58.0 – 58.1	O_2	O II	200	0.029	Ajello and Franklin (1985)
58.3	Ar	Ar II	100	0.61	Tan and McConkey (1974)
58.4	He	He I	300	6.85	Donaldson et al. (1972)
58.4	He	He I	300	7.51	van Eck and de Jongh (1970)
58.4	He	He I	300	7.71	de Jongh and van Eck (1971b)
58.4	He	He I	300	5.79	Moustafa Moussa et al. (1969)
58.4	He	He I	200	8.34	Shemansky et al. (1985b)
58.4	He	He I	300	7.3	Westerveld et al. (1979)
60.1	H_2O	O II	200	0.013	Ajello (1984)
60.1	O_2	O II	200	0.109	Ajello and Franklin (1985)
60.7	SF_6	F II	400	0.016	Forand et al. (1986)
61.6 – 61.7	H_2O	O II	200	0.044	Ajello (1984)
61.6 – 61.7	H_2O	O II	100	0.03	Böse and Sroka (1973)
61.6 – 61.7	O_2	O II	200	0.399	Ajello and Franklin (1985)
61.6 – 61.7	O_2	O II	200	0.22	Morgan and Mentall (1983)
62.9	N_2	N II	100	0.23	Sroka (1969a)
64.4	H_2O	O II	200	0.001	Ajello (1984)
64.4	O_2	O II	200	0.061	Ajello and Franklin (1985)
64.5	N_2	N II	100	0.25	Sroka (1969a)
66.2	Ar	Ar II	100	0.85	Tan and McConkey (1974)
66.5	Ar	Ar II	100	0.12	Tan and McConkey (1974)
66.6	Ar	Ar II	100	0.31	Tan and McConkey (1974)
67.1	Ar	Ar II	100	0.59	Tan and McConkey (1974)
67.1	N_2	N II	200	0.28	Morgan and Mentall (1983)
67.1	N_2	N II	100	4.5	Sroka (1969a)
67.2	Ar	Ar II	100	1.44	Tan and McConkey (1974)
67.3 – 67.4	H_2O	O II	200	0.007	Ajello (1984)
67.3	Ar	Ar II	100	0.06	Tan and McConkey (1974)
67.3 – 67.4	O_2	O II	200	0.073	Ajello and Franklin (1985)
67.3 – 67.4	SO_2	O II	240	0.16	Becker et al. (1983)
67.6	Ar	Ar II	100	0.13	Tan and McConkey (1974)
67.8	Ar	Ar II	100	0.11	Tan and McConkey (1974)
67.9	Ar	Ar II	100	0.9	Tan and McConkey (1974)
68.2	SO_2	S III	320	0.18	Becker et al. (1983)
68.6	Ar	Ar II	100	0.11	Tan and McConkey (1974)
68.7	C_2H_2	C II	200	0.016	Pang et al. (1987)
68.7	CO_2	C II	200	0.05	Sroka (1970)
69.0	Ar	Ar III	100	0.09	Tan and McConkey (1974)

Table C1. List of reported photoemission cross sections in the extreme ultraviolet -- Continued

Wavelength (nm)	Target gas	Species	Energy (eV)	Cross section (10^{-18} cm^2)	Authors
69.1	Ar	Ar II	100	0.08	Tan and McConkey (1974)
69.3	Ar	Ar II	100	0.15	Tan and McConkey (1974)
69.7	Ar	Ar II	100	0.05	Tan and McConkey (1974)
69.8	Ar	Ar II	100	0.08	Tan and McConkey (1974)
69.9	Ar	Ar II	100	0.16	Tan and McConkey (1974)
70.2 – 70.7	O_2	O III	200	0.034	Ajello and Franklin (1985)
70.5	Ar	Ar II	100	0.11	Tan and McConkey (1974)
71.1 – 73.6	SF_6	F I	200	0.15	Forand et al. (1986)
71.7	CO_2	O II	200	0.07	Sroka (1970)
71.8	Ar	Ar II	200	0.23	Mentall and Morgan (1976)
71.8	Ar	Ar II	100	0.38	Tan and McConkey (1974)
71.8 – 71.9	O_2	O II	200	0.388	Ajello and Franklin (1985)
71.8 – 71.9	O_2	O II	200	0.14	Morgan and Mentall (1983)
71.8 – 71.9	O_2	O II	100	2.	Sroka (1968)
71.9	H_2O	O II	200	0.046	Ajello (1984)
71.9	H_2O	O I	100	0.06	Böse and Sroka (1973)
71.9	SO_2	O II	220	0.12	Becker et al. (1983)
72.3	Ar	Ar II	200	0.92	Mentall and Morgan (1976)
72.3	Ar	Ar II	100	1.8	Tan and McConkey (1974)
72.6	Ar	Ar II	200	0.4	Mentall and Morgan (1976)
72.6	Ar	Ar II	100	0.75	Tan and McConkey (1974)
73.1	Ar	Ar II	200	0.16	Mentall and Morgan (1976)
73.1	Ar	Ar II	100	0.27	Tan and McConkey (1974)
73.6	Ne	Ne I	200	6.0	de Jongh (1971)
73.6	Ne	Ne I	60	20.	Hertz (1969)
73.6	Ne	Ne I	300	4.34	Tan et al. (1974)
74.4	Ne	Ne I	40	3.	Hertz (1969)
74.7	N_2	N II	300	1.23	Aarts and de Heer (1971a)
74.7	N_2	N II	200	0.17	Morgan and Mentall (1983)
74.7	N_2	N II	100	3.2	Sroka (1969a)
75.1	SF_6	F I	200	0.17	Forand et al. (1986)
75.5	Ar	Ar II	100	0.1	Tan and McConkey (1974)
76.2	Ar	Ar II	100	0.05	Tan and McConkey (1974)
76.8	SO_2	O I	180	0.22	Becker et al. (1983)
76.9	Ar	Ar III	500	0.14	Schartner et al. (1987)
76.9	Ar	Ar III	200	0.14	Papp et al. (1977)
77.6	N_2	N II	300	0.1	Aarts and de Heer (1971a)
77.6	N_2	N II	200	0.11	Morgan and Mentall (1983)
77.6	N_2	N II	100	2.3	Sroka (1969a)
78.0	SF_6	F I	200	0.39	Forand et al. (1986)
78.6	Kr	Kr III	200	0.31	Papp et al. (1977)
79.2	O	O I	100	4.	Zipf and Kao (1986)
79.2	SF_6	F I	200	0.13	Forand et al. (1986)
79.5	SF_6	F I	200	0.07	Forand et al. (1986)
79.7	H_2O	O II	200	0.001	Ajello (1984)
79.7	O_2	O II	200	0.061	Ajello and Franklin (1985)
80.7	SF_6	F I	200	0.19	Forand et al. (1986)
80.6 – 81.0	C_2H_2	C II	200	0.0098	Pang et al. (1987)
80.9	CO_2	C II	200	0.05	Sroka (1970)
81.0	SF_6	F I	200	0.36	Forand et al. (1986)
81.1	SO_2	O I	150	0.23	Becker et al. (1983)
83.3	CO_2	O II	200	0.24	Sroka (1970)
83.3 – 83.5	H_2O	O II & III	200	0.07	Ajello (1984)
83.3 – 83.5	O	O II & O III	300	17.	Zipf et al. (1985)

Table C1. List of reported photoemission cross sections in the extreme ultraviolet -- Continued

Wavelength (nm)	Target gas	Species	Energy (eV)	Cross section (10^{-18} cm^2)	Authors
83.3 – 83.5	O_2	O II & III	200	2.15	Ajello and Franklin (1985)
83.3 – 83.5	O_2	O II & III	300	1.06	Aarts and de Heer (1971b)
83.3 – 83.5	O_2	O II & III	200	1.29	Morgan and Mentall (1983)
83.3 – 83.5	O_2	O II & III	100	7.6	Sroka (1968)
83.3 – 83.5	O_2	O II & O III	300	1.77	Zipf et al. (1985)
83.4	H_2O	O II	100	0.1	Böse and Sroka (1973)
83.4	SO_2	O II & III	225	0.37	Becker et al. (1983)
83.8	Kr	Kr III	200	0.28	Papp et al. (1977)
85.8	C_2H_2	C II	200	0.0098	Pang et al. (1987)
85.8	CO_2	C II	200	0.07	Sroka (1970)
86.0	H_2O	O I	200	0.002	Ajello (1984)
86.2	O_2	O I	200	0.048	Ajello and Franklin (1985)
86.7	Ar	Ar I	200	1.3	Mentall and Morgan (1976)
86.7	SO_2	S II	160	0.18	Becker et al. (1983)
87.0	Ar	Ar I	200	0.73	Mentall and Morgan (1976)
87.6	Ar	Ar I	200	1.19	Mentall and Morgan (1976)
87.8 – 88.3	CO_2	O I	200	0.08	Sroka (1970)
87.8 – 88.3	H_2O	O I	200	0.047	Ajello (1984)
87.8 – 88.3	H_2O	O I	100	0.1	Böse and Sroka (1973)
87.8	O	O I	300	5.9	Zipf and Kao (1986)
87.8 – 88.3	O_2	O I	200	0.46	Ajello and Franklin (1985)
87.8 – 88.3	O_2	O I	200	0.37	Morgan and Mentall (1983)
87.8 – 88.3	O_2	O I	100	2.4	Sroka (1968)
87.8 – 88.3	SO_2	O I	90	0.21	Becker et al. (1983)
88.0	Ar	Ar I	200	0.54	Mentall and Morgan (1976)
88.7	Ar	Ar III	200	0.12	Papp et al. (1977)
89.4	Ar	Ar I	200	0.4	Mentall and Morgan (1976)
90.2	Xe	Xe III	108	0.27	Papp et al. (1977)
90.2	Xe	Xe III	300	0.80	Suzuki et al. (1983)
90.4	C_2H_2	C II	200	0.026	Pang et al. (1987)
90.4	CO_2	C II	200	0.15	Sroka (1970)
90.6	Kr	Kr III	300	2.1	Suzuki et al. (1983)
90.7	SF_6	S II	200	0.1	Forand et al. (1986)
91.0	SO_2	S II	130	1.04	Becker et al. (1983)
91.1	SF_6	S II	200	0.06	Forand et al. (1986)
91.3	SF_6	S II	200	0.033	Forand et al. (1986)
91.5 – 93.1	CH_4	H I	200	0.179	Pang et al. (1987)
91.5 – 93.1	C_2H_2	H I	200	0.165	Pang et al. (1987)
91.5 – 94.0	H_2O	H I & O I	200	0.211	Ajello (1984)
91.5	SF_6	S II	200	0.006	Forand et al. (1986)
91.6	N_2	N II	300	0.34	Aarts and de Heer (1971a)
91.6	N_2	N II	200	0.47	Morgan and Mentall (1983)
91.7 – 96.5	Kr	Kr II	300	4.65	Luyken et al. (1972)
91.7	Kr	Kr II	300	1.33	van Raan (1973)
91.7 – 96.5	Kr	Kr II	200	69.	Zapesochnyi et al. (1974)
91.7	N_2	N II	100	11.9	Sroka (1969a)
91.9	SF_6	S II	200	0.004	Forand et al. (1986)
92.0	Ar	Ar II	200	3.80	Forand et al. (1988)
92.0	Ar	Ar II	200	2.89	Li et al. (1988b)
92.0 – 93.2	Ar	Ar II	300	4.99	Luyken et al. (1972)
92.0	Ar	Ar II	100	5.81	McPherson (1984)
92.0	Ar	Ar II	200	3.53	Mentall and Morgan (1976)
92.0	Ar	Ar II	300	3.19	van Raan (1973)
92.0	Ar	Ar II	300	1.64	Tan et al. (1974)

Table C1. List of reported photoemission cross sections in the extreme ultraviolet -- Continued

Wavelength (nm)	Target gas	Species	Energy (eV)	Cross section (10^{-18} cm^2)	Authors
92.0 – 93.2	Ar	Ar II	200	61.	Zapesochnyi et al. (1974)
92.2 – 93.2	O_2	O I	200	0.144	Ajello and Franklin (1985)
92.9	O_2	O I	100	0.016	Zipf (1984)
93.1	H_2O	H I	100	0.05	Böse and Sroka (1973)
93.1	NH_3	H I	140	0.073	Böse and Sroka (1971)
93.2	Ar	Ar II	200	1.96	Forand et al. (1988)
93.2	Ar	Ar II	200	1.50	Li et al. (1988b)
93.2	Ar	Ar II	100	3.00	McPherson (1984)
93.2	Ar	Ar II	200	2.	Mentall and Morgan (1976)
93.2	Ar	Ar II	300	1.8	van Raan (1973)
93.2	Ar	Ar II	300	1.64	Tan et al. (1974)
93.5 – 94.0	CO_2	O I	200	0.07	Sroka (1970)
93.5 – 94.0	O_2	O I	200	0.122	Ajello and Franklin (1985)
93.6	O_2	O I	100	0.04	Zipf (1984)
93.7	SF_6	S II	200	0.07	Forand et al. (1986)
93.8	CH_4	H I	200	0.131	Pang et al. (1987)
93.8	C_2H_2	H I	200	0.113	Pang et al. (1987)
93.8	H_2O	H I	100	0.1	Böse and Sroka (1973)
93.8	NH_3	H I	140	0.15	Böse and Sroka (1971)
93.8	SO_2	O I	150	0.22	Becker et al. (1983)
93.8	SO_2	S II	140	0.66	Becker et al. (1983)
94.0	O_2	O I	100	0.016	Zipf (1984)
94.5 – 95.0	CH_4	H I, C I, C II	200	0.158	Pang et al. (1987)
94.9 – 95.3	CO_2	O I	200	0.07	Sroka (1970)
94.9 – 95.3	H_2O	H I & O I	200	0.154	Ajello (1984)
94.9 – 95.3	O_2	O I	200	0.12	Ajello and Franklin (1985)
95.0	CH_4	H I	156	0.07	Sroka (1969b)
95.0	CO	O I	100	0.033	Zipf (1984)
95.0	H_2O	H I	100	0.3	Böse and Sroka (1973)
95.0	NH_3	H I	140	0.31	Böse and Sroka (1971)
95.0	O_2	O I	100	0.011	Zipf (1984)
95.1	SO_2	O I	150	0.35	Becker et al. (1983)
95.2	CO	O I	100	0.034	Zipf (1984)
95.2	CO_2	O I	100	0.0712	Zipf (1984)
95.2	O_2	O I	100	0.039	Zipf (1984)
95.2	SF_6	F I	200	0.25	Forand et al. (1986)
95.5	SF_6	F I	200	1.78	Forand et al. (1986)
95.9	SF_6	F I	200	0.26	Forand et al. (1986)
96.5	Kr	Kr II	300	3.32	van Raan (1973)
97.2 – 97.9	H_2O	H I & O I	200	0.255	Ajello (1984)
97.2 – 97.9	O_2	O I	200	0.344	Ajello and Franklin (1985)
97.2	SF_6	F I	200	0.06	Forand et al. (1986)
97.3	CH_4	H I	200	0.258	Pang et al. (1987)
97.3	CH_4	H I	156	0.13	Sroka (1969b)
97.3	CO	O I	100	0.158	Zipf (1984)
97.3	CO_2	O I	100	0.173	Zipf (1984)
97.3	H_2O	H I	100	0.6	Böse and Sroka (1973)
97.3	NH_3	H I	140	0.58	Böse and Sroka (1971)
97.3	O_2	O I	100	0.37	Zipf (1984)
97.3	SO_2	O I	90	0.4	Becker et al. (1983)
97.4	CO_2	O I	200	0.13	Sroka (1970)
97.4	SF_6	F I	200	1.09	Forand et al. (1986)
97.6	SF_6	F I	200	0.33	Forand et al. (1986)
97.8	CO	O I	100	0.156	Zipf (1984)

Table C1. List of reported photoemission cross sections in the extreme ultraviolet -- Continued

Wavelength (nm)	Target gas	Species	Energy (eV)	Cross section (10^{-18} cm^2)	Authors
97.8	CO_2	O I	100	0.54	Zipf (1984)
97.8	O_2	O I	100	0.1	Zipf (1984)
97.8	SF_6	F I	200	0.17	Forand et al. (1986)
97.8	SO_2	O I	180	0.32	Becker et al. (1983)
98.9	CO	O I	100	0.842	Zipf (1984)
98.9 – 99.1	CO_2	O I	200	0.43	Sroka (1970)
98.9	CO_2	O I	100	0.56	Zipf (1984)
98.9 – 99.1	H_2O	O I	200	0.215	Ajello (1984)
98.9 – 99.1	H_2O	O I	100	0.3	Böse and Sroka (1973)
98.9	O	O I	300	8.39	Zipf and Erdman (1985)
98.9 – 99.1	O_2	O I	200	1.	Ajello and Franklin (1985)
98.9 – 99.1	O_2	O I	200	1.41	Morgan and Mentall (1983)
98.9 – 99.1	O_2	O I	100	3.7	Sroka (1968)
98.9	O_2	O I	100	1.96	Zipf (1984)
98.9 – 99.1	O_2	O I	100	1.9	Zipf et al. (1979)
98.9 – 99.1	SO_2	O I	110	0.95	Becker et al. (1983)
99.6	SF_6	S II	200	0.13	Forand et al. (1986)
99.8	SO_2	S II	160	0.31	Becker et al. (1983)
99.9	O_2	O I	200	0.318	Ajello and Franklin (1985)
99.9	O_2	O I	200	0.31	Morgan and Mentall (1983)
100.0	H_2O	O I	200	0.039	Ajello (1984)
100.1	SF_6	S II	200	0.1	Forand et al. (1986)
100.6	SF_6	S II	200	0.12	Forand et al. (1986)
101.4	SF_6	S II	200	0.07	Forand et al. (1986)
101.7	Xe	Xe III	134	0.76	Papp et al. (1977)
102.0	SF_6	S II	200	0.04	Forand et al. (1986)
102.6	CH_4	H I	300	0.79	McLaughlin and Zipf (1978)
102.6	CH_4	H I	200	0.567	Pang et al. (1987)
102.6	CH_4	H I	156	0.26	Sroka (1969b)
102.6	C_2H_2	H I	200	0.503	Pang et al. (1987)
102.6 – 102.8	CO_2	O I	200	0.29	Sroka (1970)
102.6	H_2	H I	100	0.89	Ajello et al. (1984)
102.6 – 102.8	H_2O	H I & O I	200	0.677	Ajello (1984)
102.6	H_2O	H I	100	1.4	Böse and Sroka (1973)
102.6	NH_3	H I	140	1.1	Böse and Sroka (1971)
102.6 – 102.8	O_2	O I	200	0.708	Ajello and Franklin (1985)
102.6 – 102.8	O_2	O I	200	1.05	Morgan and Mentall (1983)
102.6 – 102.8	O_2	O I	100	1.46	Zipf et al. (1979)
102.6 – 102.8	SO_2	O I	90	0.99	Becker et al. (1983)
102.7	CO	O I	100	0.164	Zipf (1984)
102.7	CO_2	O I	100	0.554	Zipf (1984)
102.7	O	O I	300	1.86	Zipf and Erdman (1985)
102.7	O_2	O I	100	1.46	Zipf (1984)
103.0	SF_6	S II	200	0.015	Forand et al. (1986)
103.7	C_2H_2	C II	200	0.020	Pang et al. (1987)
103.9 – 104.2	CO_2	O I & C II	200	0.16	Sroka (1970)
103.9 – 104.2	H_2O	O I	200	0.028	Ajello (1984)
103.9 – 104.2	O_2	O I	200	0.254	Ajello and Franklin (1985)
103.9 – 104.2	O_2	O I	200	0.48	Morgan and Mentall (1983)
103.9 – 104.2	O_2	O I	100	0.49	Zipf et al. (1979)
103.9 – 104.2	SO_2	O I	175	0.45	Becker et al. (1983)
104.0	O_2	O I	100	0.34	Zipf (1984)
104.5 – 105.3	SF_6	S II	200	0.12	Forand et al. (1986)
104.8	Ar	Ar I	200	14.	de Jongh (1971)

Table C1. List of reported photoemission cross sections in the extreme ultraviolet -- Continued

Wavelength (nm)	Target gas	Species	Energy (eV)	Cross section (10^{-18} cm^2)	Authors
104.8	Ar	Ar I	200	12.81	Forand et al. (1988)
104.8 – 106.7	Ar	Ar I	150	24.	Lloyd et al. (1972)
104.8	Ar	Ar I	300	12.6	McConkey and Donaldson (1973)
104.8	Ar	Ar I	200	24.	Mentall and Morgan (1976)
106.7	Ar	Ar I	200	5.32	Forand et al. (1988)
106.7	Ar	Ar I	300	5.02	McConkey and Donaldson (1973)
106.7	Ar	Ar I	200	9.85	Mentall and Morgan (1976)
108.4	N_2	N II	300	1.92	Aarts and de Heer (1971a)
108.4	N_2	N II	200	2.26	Morgan and Mentall (1983)
108.4	N_2	N II	100	20.4	Sroka (1969a)
108.6	NH_3	N II	140	0.12	Böse and Sroka (1971)
108.9	Xe	Xe III	300	2.3	Suzuki et al. (1983)
110.0	SF_6	S II	200	0.19	Forand et al. (1986)
110.0 – 124.5	Xe	Xe II	300	6.61	Luyken et al. (1972)
110.0	Xe	Xe II	300	5.9	van Raan (1973)
110.0 – 124.5	Xe	Xe II	200	82.	Zapesochnyi et al. (1974)
112.4 – 113.2	SF_6	S II	200	0.05	Forand et al. (1986)
113.4	N	N I	100	68	Stone and Zipf (1973)
113.4	N_2	N I	300	0.62	Aarts and de Heer (1971a)
113.4	N_2	N I	200	0.97	Morgan and Mentall (1983)
113.4	N_2	N I	100	18.9	Sroka (1969a)
113.4	N_2	N I	100	1.24	Stone and Zipf (1973)
113.4	NH_3	N I	140	0.12	Böse and Sroka (1971)
113.4	NH_3	N I	100	0.26	Morgan and Mentall (1974)
113.4	NO	N I	100	1.6	Mentall and Morgan (1972)
114.0	CS_2	?	100	0.16	Ajello and Shemansky (1981)
115.2	CO_2	O I	100	0.347	Zipf (1984)
115.2	H_2O	O I	200	0.174	Ajello (1984)
115.2	H_2O	O I	100	0.2	Böse and Sroka (1973)
115.2	NO	O I	100	0.85	Mentall and Morgan (1972)
115.2	O_2	O I	200	0.3	Ajello and Franklin (1985)
115.2	O_2	O I	200	0.69	Morgan and Mentall (1983)
115.3	CO_2	O I & CO	200	0.27	Sroka (1970)
115.6 – 115.9	C_2H_2	C I	200	0.052	Pang et al. (1987)
115.7	CS_2	?	100	0.28	Ajello and Shemansky (1981)
116.4	N	N I	18	3.4	Stone and Zipf (1973)
116.4	N_2	N I	300	0.32	Aarts and de Heer (1971a)
116.4	N_2	N I	100	0.08	Ajello and Shemansky (1985)
116.4	N_2	N I	200	0.121	Morgan and Mentall (1983)
116.4	N_2	N I	100	0.163	Mumma and Zipf (1971b)
116.4	N_2	N I	100	0.124	Stone and Zipf (1973)
116.5	Kr	Kr I	200	10.	de Jongh (1971)
116.5	Kr	Kr I	150	13.	Pavlov and Yakhontova (1975)
116.8	N	N I	18	13.	Stone and Zipf (1973)
116.8	N_2	N I	100	5.5	Sroka (1969a)
117.7	N_2	N I	100	0.33	Ajello and Shemansky (1985)
117.7	N_2	N I	100	0.516	Mumma and Zipf (1971b)
117.8	N_2	N I	300	0.23	Aarts and de Heer (1971a)
117.8	N_2	N I	200	0.39	Morgan and Mentall (1983)
118.9 – 119.5	CH_4	C I	200	0.083	Pang et al. (1987)
119.0 – 119.5	C_2H_2	C I	200	0.113	Pang et al. (1987)
119.4	CS_2	S III	100	0.56	Ajello and Shemansky (1981)
120.0	N	N I	100	160.	Stone and Zipf (1973)
120.0	N_2	N I	100	7.4	Ajello (1970)

Table C1. List of reported photoemission cross sections in the extreme ultraviolet -- Continued

Wavelength (nm)	Target gas	Species	Energy (eV)	Cross section (10^{-18} cm^2)	Authors
120.0	N_2	N I	300	2.78	Aarts and de Heer (1971a)
120.0	N_2	N I	200	3.48	Ajello and Shemansky (1985)
120.0	N_2	N I	200	2.98	Forand et al. (1988)
120.0	N_2	N I	290	4.2	Huschilt et al. (1981)
120.0	N_2	N I	300	3.98	Mumma and Zipf (1971b)
120.0	N_2	N I	100	38.5	Sroka (1969a)
120.0	NH_3	N I	140	0.51	Böse and Sroka (1971)
120.0	NH_3	N I	100	0.7	Morgan and Mentall (1974)
120.0	NO	N I	100	4.8	Mentall and Morgan (1972)
120.0	NO	N I	100	3.04	Stone and Zipf (1972a)
120.1	CS_2	S III	100	1.95	Ajello and Shemansky (1981)
120.4	SF_6	S II	200	0.34	Forand et al. (1986)
121.5	D_2	D I	100	10.	Becker and McConkey (1984)
121.5	He	He II	300	0.0218	Moustafa Moussa and de Heer (1967)
121.5	He	He II	200	0.0226	Shemansky et al. (1985b)
121.6	C_2H_4	H I	300	4.73	Vroom and de Heer (1969a)
121.6	C_2H_6	H I	300	4.45	Vroom and de Heer (1969a)
121.6	C_6H_6	H I	300	7.85	Vroom and de Heer (1969a)
121.6	CD_4	D I	300	4.5	Vroom and de Heer (1969a)
121.6	CH_4	H I	100	14.	McGowan et al. (1969)
121.6	CH_4	H I	100	1.2	Morgan and Mentall (1974)
121.6	CH_4	H I	300	5.62	Möhlmann et al. (1978)
121.6	CH_4	H I	100	8.99	Orient and Srivastava (1981)
121.6	CH_4	H I	200	4.37	Pang et al. (1987)
121.6	CH_4	H I	156	2.2	Sroka (1969b)
121.6	CH_4	H I	300	5.35	Vroom and de Heer (1969a)
121.6	C_2H_2	H I	200	0.322	Pang et al. (1987)
121.6	D_2	H I	300	4.53	Möhlmann et al. (1978)
121.6	D_2	D I	300	5.68	Vroom and de Heer (1969b)
121.6	D_2O	D I	100	8.	McGowan et al. (1969)
121.6	H	H I	200	39.	Fite and Brackmann (1958)
121.6	H	H I	199	42.8	Long et al. (1968)
121.6	H_2	H I	300	5.41	Carrière and de Heer (1972)
121.6	H_2	H I	300	7.4	Dunn et al. (1962)
121.6	H_2	H I	300	7.5	Fite and Brackmann (1958)
121.6	H_2	H I	300	5.27	de Heer and Carrière (1971)
121.6	H_2	H I	100	14.8	Kauppila et al. (1971)
121.6	H_2	H I	100	7.3	Ligtenberg et al. (1985)
121.6	H_2	H I	300	6.5	McConkey and Donaldson (1972)
121.6	H_2	H I	100	11.	McGowan et al. (1969)
121.6	H_2	H I	300	6.51	Möhlmann et al. (1978)
121.6	H_2	H I	300	6.	Mumma and Zipf (1971a)
121.6	H_2	H I	200	5.78	Shemansky et al. (1985a)
121.6	H_2	H I	300	6.94	Vroom and de Heer (1969b)
121.6	H_2	H I	100	7.22	Van Zyl et al. (1985)
121.6	H_2	H I	100	7.13	Woolsey et al. (1986)
121.6 – 121.8	H_2O	H I & O I	200	6.3	Ajello (1984)
121.6 – 121.8	H_2O	H I & O I	100	7.5	Böse and Sroka (1973)
121.6 – 121.8	H_2O	H I & O I	100	9.	McGowan et al. (1969)
121.6	H_2O	H I	100	8.8	Morgan and Mentall (1974)
121.6	H_2O	H I	300	12.	Möhlmann et al. (1978)
121.6 – 121.8	H_2O	H I & O I	300	17.5	Vroom and de Heer (1969c)
121.6	HCl	H I	300	18.3	Möhlmann et al. (1978)
121.6	HD	H I	300	6.05	Möhlmann et al. (1978)

Table C1. List of reported photoemission cross sections in the extreme ultraviolet -- Continued

Wavelength (nm)	Target gas	Species	Energy (eV)	Cross section (10^{-18} cm^2)	Authors
121.6	NH_3	H I	140	7.3	Böse and Sroka (1971)
121.6	NH_3	H I	100	7.	McGowan et al. (1969)
121.6	NH_3	H I	100	10.9	Morgan and Mentall (1974)
121.6	NH_3	H I	300	10.2	Möhlmann et al. (1978)
121.8	NO	O I	100	0.39	Mentall and Morgan (1972)
121.8	O_2	O I	200	0.143	Ajello and Franklin (1985)
121.8	O_2	O I	100	0.15	Mumma and Zipf (1971a)
123.4	CS_2	S II	100	0.14	Ajello and Shemansky (1981)
123.6	Kr	Kr I	150	40.	Pavlov and Yakhontova (1975)
124.3	N	N I	17	5.5	Stone and Zipf (1973)
124.3	N_2	N I	300	0.73	Aarts and de Heer (1971a)
124.3	N_2	N I	200	0.88	Ajello and Shemansky (1985)
124.3	N_2	N I	300	0.72	Mumma and Zipf (1971b)
124.3	N_2	N I	100	10.9	Sroka (1969a)
124.3	NH_3	N I	100	0.19	Morgan and Mentall (1974)
124.3	NO	N I	100	0.89	Mentall and Morgan (1972)
124.3	NO	N I	100	0.74	Stone and Zipf (1972a)
125.0 – 126.0	SF_6	S II	200	0.35	Forand et al. (1986)
125.3 – 126.8	C_2H_2	C I	200	0.132	Pang et al. (1987)
125.6 – 126.1	CS_2	SII & C I	100	3.56	Ajello and Shemansky (1981)
126.1	CO_2	C I	100	0.132	Ajello (1971c)
127.4 – 128.1	CH_4	C I	200	0.163	Pang et al. (1987)
127.4 – 128.1	C_2H_2	C I	200	0.329	Pang et al. (1987)
127.8 – 128.0	CO	C I	110	0.715	Ajello (1971b)
127.8 – 128.0	CO	C I	300	0.47	Aarts and de Heer (1970)
127.8 – 128.0	CO_2	C I	100	0.518	Ajello (1971c)
128.0	CS_2	C I	100	1.69	Ajello and Shemansky (1981)
129.6	CS_2	S I	100	0.32	Ajello and Shemansky (1981)
129.6	Xe	Xe I	150	5.6	Pavlov and Yakhontova (1975)
130.2 – 130.6	H_2O	O I	200	0.214	Ajello (1984)
130.2 – 130.6	O_2	O I	200	2.36	Ajello and Franklin (1985)
130.3	CS_2	S I	100	0.39	Ajello and Shemansky (1981)
130.4	CO	O I	110	0.803	Ajello (1971b)
130.4	CO	O I	100	0.84	Lawrence (1970)
130.4	CO	O I	100	1.56	Zipf (1984)
130.4	CO_2	O I	100	0.756	Ajello (1971c)
130.4	CO_2	O I	100	1.04	Mumma et al. (1972)
130.4	H_2O	O I	100	0.37	Lawrence (1970)
130.4	H_2O	O I	100	0.32	Morgan and Mentall (1974)
130.4	NO	O I	100	1.14	Lawrence (1970)
130.4	NO	O I	100	1.1	Mentall and Morgan (1972)
130.4	O	O I	300	4.63	Zipf (1986)
130.4	O	O I	300	4.2	Stone and Zipf (1974)
130.4	O_2	O I	100	3.	Ajello (1971a)
130.4	O_2	O I	300	2.08	Aarts and de Heer (1971b)
130.4	O_2	O I	100	3.05	Lawrence (1970)
130.4	O_2	O I	300	2.05	Mumma and Zipf (1971a)
130.4	O_2	O I	100	3.19	Stone and Zipf (1974)
130.4	O_2	O I	100	3.8	Zipf (1984)
130.4	O_2	O I	300	1.71	Zipf (1986)
130.4	O_2	O I	100	3.8	Zipf et al. (1979)
130.5	CO	O I	300	0.469	Aarts and de Heer (1970)
130.6	CO_2	O I	200	0.64	Sroka (1970)
131.0	N_2	N I	100	0.45	Mumma and Zipf (1971b)

Table C1. List of reported photoemission cross sections in the extreme ultraviolet -- Continued

Wavelength (nm)	Target gas	Species	Energy (eV)	Cross section (10^{-18} cm^2)	Authors
131.1	N_2	N I	300	0.16	Aarts and de Heer (1971a)
131.1	N_2	N I	200	0.183	Ajello and Shemansky (1985)
131.1	N_2	N I	100	0.35	Stone and Zipf (1973)
131.1 – 131.6	C_2H_2	C I	200	0.024	Pang et al. (1987)
132.0	CS_2	S I	100	1.47	Ajello and Shemansky (1981)
132.0	N_2	N I	200	0.16	Ajello and Shemansky (1985)
132.4	CO_2	C II	100	0.0133	Mumma et al. (1972)
132.4 – 133.6	CH_4	C I & C II	200	0.145	Pang et al. (1987)
132.4 – 133.6	C_2H_2	C I & C II	200	0.430	Pang et al. (1987)
132.7	N_2	N I	200	0.047	Ajello and Shemansky (1985)
132.7	N_2	N I	100	0.09	Mumma and Zipf (1971b)
132.9	CO_2	C I	100	0.25	Ajello (1971c)
132.9	CO_2	C I	100	0.267	Mumma et al. (1972)
133.5	CH_4	C II	100	0.023	Morgan and Mentall (1974)
133.5	CO	C II	125	5.2	Ajello (1971b)
133.5	CO	C II	300	2.85	Aarts and de Heer (1970)
133.5	CO_2	C II	150	0.83	Ajello (1971c)
133.5	CO_2	C II	100	0.76	Mumma et al. (1972)
133.5	CS_2	C II	100	1.36	Ajello and Shemansky (1981)
133.6	CO_2	C II	200	1.33	Sroka (1970)
135.4 – 135.9	C_2H_2	C I	200	0.058	Pang et al. (1987)
135.6	CO	O I	110	0.68	Ajello (1971b)
135.6	CO_2	O I	100	0.8	Ajello (1971c)
135.6	CS_2	?	100	0.15	Ajello and Shemansky (1981)
135.6	O	O I	15	25.	Stone and Zipf (1974)
135.6	O_2	O I	100	1.65	Ajello (1971a)
135.6	O_2	O I	100	7.	Wells et al. (1971)
136.4	CO_2	C I	100	0.054	Ajello (1971c)
136.4	CS_2	C I	100	0.14	Ajello and Shemansky (1981)
138.9	CS_2	S I	100	1.15	Ajello and Shemansky (1981)
140.5	CS_2	S I	100	0.16	Ajello and Shemansky (1981)
141.2	N_2	N I	100	0.124	Ajello and Shemansky (1985)
141.2	N_2	N I	100	0.16	Mumma and Zipf (1971b)
142.5	CS_2	S I	100	1.62	Ajello and Shemansky (1981)
142.5	SF_6	S I	200	0.15	Forand et al. (1986)
143.3	CS_2	S I	100	1.26	Ajello and Shemansky (1981)
143.3	SF_6	S I	200	0.09	Forand et al. (1986)
143.7	SF_6	S I	200	0.036	Forand et al. (1986)
144.8	CS_2	S I	100	0.19	Ajello and Shemansky (1981)
146.3 – 146.7	CO_2	C I	100	0.193	Ajello (1971c)
146.3	CH_4	C I	200	0.069	Pang et al. (1987)
146.3 – 147.0	C_2H_2	C I	200	0.104	Pang et al. (1987)
146.3	CS_2	C I	100	0.44	Ajello and Shemansky (1981)
147.0	Xe	Xe I	150	32.	Pavlov and Yakhontova (1975)
147.4	CS_2	S I	100	3.72	Ajello and Shemansky (1981)
147.4	SF_6	S I	200	0.32	Forand et al. (1986)
148.2	C_2H_2	C I	200	0.048	Pang et al. (1987)
148.2	CO_2	C I	100	0.024	Ajello (1971c)
148.3	CS_2	S I	100	2.64	Ajello and Shemansky (1981)
148.3	SF_6	S I	200	0.16	Forand et al. (1986)
148.7	SF_6	S I	200	0.05	Forand et al. (1986)
149.3	N_2	N I	100	5.7	Ajello (1970)
149.3	N_2	N I	200	1.31	Ajello and Shemansky (1985)
149.3	N_2	N I	300	1.52	Mumma and Zipf (1971b)

Table C1. List of reported photoemission cross sections in the extreme ultraviolet -- Continued

Wavelength (nm)	Target gas	Species	Energy (eV)	Cross section (10^{-18} cm^2)	Authors
149.3	NH_3	N I	100	0.43	Morgan and Mentall (1974)
149.3	NO	N I	100	1.5	Mentall and Morgan (1972)
149.3	NO	N I	100	1.26	Stone and Zipf (1972a)
149.4	N_2	N I	300	1.12	Aarts and de Heer (1971a)
156.1	CH_4	C I	100	0.034	Morgan and Mentall (1974)
156.1	CH_4	C I	200	0.211	Pang et al. (1987)
156.1	CH_4	C I	156	0.22	Sroka (1969b)
156.1	C_2H_2	C I	200	0.437	Pang et al. (1987)
156.1	CO_2	C I	100	0.679	Ajello (1971c)
156.1	CO_2	C I	100	0.75	Mumma et al. (1972)
156.1	CS_2	C I	100	2.74	Ajello and Shemansky (1981)
164.0	He	He II	300	0.0685	Moustafa Moussa and de Heer (1967)
164.0	He	He II	200	0.0451	Shemansky et al. (1985b)
164.1	O_2	O I	100	0.0000122	Erdman and Zipf (1986)
165.6	CS_2	C I	100	5.09	Ajello and Shemansky (1981)
165.7	C_2H_2	C I	300	0.498	Pang et al. (1987)
165.7	CH_4	C I	100	0.063	Morgan and Mentall (1974)
165.7	CH_4	C I	200	0.348	Pang et al. (1987)
165.7	CH_4	C I	156	0.18	Sroka (1969b)
165.7	C_2H_2	C I	200	0.738	Pang et al. (1987)
165.7	CO_2	C I	100	1.32	Ajello (1971c)
165.7	CO_2	C I	100	1.45	Mumma et al. (1972)
166.7	CS_2	S I	100	1.92	Ajello and Shemansky (1981)
166.7	SF_6	S I	200	0.155	Forand et al. (1986)
168.8	CS_2	S I	100	0.15	Ajello and Shemansky (1981)
174.3	N	N I	17	13.	Stone and Zipf (1973)
174.3	N_2	N I	300	0.46	Aarts and de Heer (1971a)
174.4	N_2	N I	100	2.1	Ajello (1970)
174.4	N_2	N I	200	0.506	Ajello and Shemansky (1985)
174.4	N_2	N I	100	0.91	Mumma and Zipf (1971b)
174.4	NH_3	N I	100	0.14	Morgan and Mentall (1974)
174.5	NO	N I	100	0.87	Mentall and Morgan (1972)
175.2	CS_2	C I	100	0.08	Ajello and Shemansky (1981)
175.2	C_2H_2	C I	200	0.016	Pang et al. (1987)
180.7	CS_2	S I	100	1.15	Ajello and Shemansky (1981)
180.7	SF_6	S I	200	0.17	Forand et al. (1986)
182.0	CS_2	S I	100	0.84	Ajello and Shemansky (1981)
182.3	SF_6	S I	200	0.11	Forand et al. (1986)
190.0	CS_2	S I	100	0.65	Ajello and Shemansky (1981)
191.5	CS_2	S I	100	0.13	Ajello and Shemansky (1981)
192.7 – 193.1	CH_4	C I & C II	200	0.160	Pang et al. (1987)
192.7 – 193.1	C_2H_2	C II	200	0.296	Pang et al. (1987)
193.1	C_2H_2	C I	300	0.504	Boonakker and de Heer (1974)
193.1	CH_4	C I	100	0.03	Morgan and Mentall (1974)
193.1	CH_4	C I	300	0.107	Pang et al. (1987)
193.1	CO_2	C I	100	0.354	Ajello (1971c)